# Stability Studies of Sasol Synfuels Transmission and Distribution Network under Fault Conditions and N-1 Supply Contingency


## University of Cape Town

## Department of Electrical Engineering

**Supervisor:**
Associate Professor S.P. Chowdhury
Department of Electrical Engineering
University of Cape Town

**Co-Supervisor:**
Dr S Chowdhury
Department of Electrical Engineering
University of Cape Town

**Prepared By:**
Patrick O'Donoghue
Department of Electrical Engineering
University of Cape Town

**September 2011**

This thesis is submitted to the University of Cape Town in fulfilment of the requirements for the degree of Master of Science in Electrical Engineering

**Abstract**

The aim of the work is to perform a transient stability analysis of the Sasol Synfuels Transmission and Distribution network when the power system is subjected to fault conditions and N-1 supply contingency conditions.

The work provides an overview of the problem of power system stability as well as discussing issues related to the problem of power system stability; which include power system control and power system modelling.

The literature review comprises a study of the problem of transient stability and the analysis of this phenomenon. Topics that are investigated include power system loads, power system controls and the response of AC elements to transient conditions.

The synchronous machines included in the scope include the ST-driven generators as well as the GT-driven generators. The large synchronous motors used on the plant to drive compressors for various functions are included.

The primary aim of the work is to determine Critical Clearing Times for all synchronous machines connected to the power system for all feasible operating conditions. These operating conditions include N-1 supply contingency as well as operation under fault and disturbed supply conditions. Specific attention is paid to the transmission development plans of Eskom and Sasol to provide a realistic projection of Critical Clearing Times until completion of the planned infrastructure development.

In order to fully appreciate the studies of the Sasol Synfuels power system several general case studies are undertaken for a single generator a two-motor system. These studies provide the background for the more complex stability analysis of the Sasol Synfuels power system.

The methodology applied is developed with the aim of being applicable to industrial power systems in general. The method developed in the work should be practicable and easily transferable, provided that the appropriate modelling software and equipment data is available.

The response of the transmission network will be evaluated in terms of load-shedding and islanding. The schemes used for the most recently commissioned switch-plant are modelled and analysed when the system is subjected to various conditions.

Methods of improving power system stability are investigated and simulated on the Sasol Synfuels Transmission and Distribution Network where appropriate. These methods include Flexible AC Transmission System devices, the Power System Stabiliser and Static VAr Compensator.

The improvement of power system stability is investigated with the aim of recommending feasible solutions for the Sasol Synfuels Transmission and Distribution network.

The work forms a comprehensive transient stability study which records the Critical Clearing Times for all synchronous machines in a readable and presentable format. The charts developed are able to be read in isolation and may form the baseline for future investigations.

**Declaration**

I, Patrick O'Donoghue, submit this thesis in fulfilment of the requirements for the degree of Master of Science in Electrical Engineering.

I certify that all ideas, designs, experimental work and conclusions are my own work. I certify that all material reproduced has been appropriately referenced.

This thesis has not been submitted to this, or any other university, for degree purposes.



**Patrick O'Donoghue**

**Student Number: ODNPAT003**

Signature: _____

Date: _____

**Acknowledgements**

*I would like to acknowledge:*

Sasol Technology for the use of facilities including the ETAP software that proved essential for the execution of the bulk of the simulation work.

The University of Cape Town (UCT) for facilitating the work and providing access to resources necessary for the execution of the work.

Mr Jozef Piorkowski (Sasol Technology) for valuable technical assistance and guidance during the execution of the work.

Dr Frieder Endrejat (Sasol Technology) for valuable technical input during the execution of the work.

Prof S.P. Chowdhury (University of Cape Town) for valuable technical and administrative assistance throughout the execution of the work.

Dr S. Chowdhury (University of Cape Town) for valuable technical and administrative assistance throughout the execution of the work.

Prof J. de Kock (University of Stellenbosch) for valuable technical input in the formative stages of the work.

**Terms of Reference**

The specific deliverables and outcomes are as follows:

- *Conduct a critical literature review.*

A literature review is conducted with the aim of providing an overview of the current state of knowledge on the topic of power system stability.

The emphasis is on transient stability analysis of a network containing both synchronous generators and large synchronous motors. Specific attention is paid to industrial power systems and the impact of transient stability on an industrial power system.

- *Model the Sasol Synfuels network using ETAP.*

The existing model of the Sasol Synfuels network will be updated to include projected loads and generation as well as planned transmission and distribution infrastructure developments.

The model accurately simulates the load-shedding and islanding schemes implemented at the 132 kV switch-plant (2H4-SP-02).

- *Perform transient stability case studies.*

Case studies are undertaken to determine the response of the power system to incomer line faults and supply contingency.

The case studies include the calculation of the critical clearing angles and transient stability margin for generators and large synchronous motors.

The response of the load-shedding and controlled separation (islanding) scheme will be evaluated in the event of various disturbances.

- *Study and evaluate methods of improving transient stability for the Sasol Synfuels network.*

Methods of improving power system stability are investigated and the possibility of application of these technologies to the Synfuels network is assessed.

An assessment is made on suitable candidate technologies for the improvement of power system transient stability improvement in the context of the Synfuels network.

- *Submit thesis in September 2011 for graduation in December 2011.*

***List of Figures***

***List of Tables***

***Abbreviations and Acronyms***

| | |
|---|---|
| **AC** | Alternating Current |
| **AGC** | Automatic Generation Control |
| **AVR** | Automatic Voltage Regulator |
| **BAC** | Booster Air Compressor |
| **CCGT** | Closed Cycle Gas Turbine |
| **CCT** | Critical Clearing Time |
| **CLR** | Current Limiting Reactor |
| **CT** | Current Transformer |
| **DC** | Direct Current |
| **DSE** | Discontinuous Supplementary Excitation |
| **ETAP** | Electric Transient Analysis Program |
| **FACTS** | Flexible AC Transmission System |
| **GIS** | Gas Insulated Switchgear |
| **GT** | Gas Turbine |
| **HV** | High Voltage |
| **HVDC** | High Voltage Direct Current |
| **IEEE** | Institute of Electrical and Electronic Engineers |
| **kV** | Kilo Volt |
| **kW** | Kilo Watt |
| **LOE** | Loss of Excitation |
| **LTC** | Linear Tap-Changer |
| **LV** | Low Voltage |
| **MAC** | Main Air Compressor |
| **MV** | Medium Voltage |
| **MVA** | Mega Volt Ampere |
| **MW** | Mega Watt |
| **NERC** | North American Electrical Reliability Council |
| **OCGT** | Open Cycle Gas Turbine |
| **OLTC** | On Load Tap Changer |
| **OOS** | Out-Of-Step |
| **PF** | Power Factor |
| **PSS** | Power System Stabiliser |
| **QoS** | Quality of Supply |
| **RCB** | Running Circuit Breaker |
| **SAPP** | Southern African Power Pool |
| **SCADA** | Supervisory Control and Data Acquisition |
| **SVC** | Static VAr Compensator |
| **SVS** | Static VAr System |
| **TDP** | Transmission Development Plan |
| **TSEC** | Transient Stability Excitation Control |
| **UFLS** | Under-Frequency Load-Shedding |
| **V** | Volt |
| **VSC** | Voltage Source Converter |
| **VT** | Voltage Transformer |

# 1 Table of Contents

# 1 Introduction

## 1.1 Background

A need for a transient stability study of the Sasol Synfuels Transmission and Distribution system was identified. Several transient stability studies have been conducted of the power system, the most recent of which was conducted in 2008.

Significant changes to the power system infrastructure, including additional generation, have been implemented since the most recent transient stability study of the system. Significant work on the transient stability of the network was completed in 1987 which provided a base for this investigation [10].

***The specific circumstances that warrant a transient stability analysis include:***

1. Addition of new generators and large synchronous motors
    - New Gas-Turbine (GT) generators
    - New large synchronous motors
2. Addition of new GIS switch-plant (2H4-SP-02) and interconnection with 2H4-SP-01 (existing)
3. Addition of new Eskom lines
    - East Shaft interconnection
    - West Shaft interconnection
4. New Eskom SOL B MTS
    - New transmission substation as part of Eskom TDP

In the event of a severe disturbance Out-of-Step (OOS) conditions may result and this may have adverse consequences. These adverse consequences include potential loss of production and potential equipment damage.

The large synchronous machines in the power system include Steam-Turbine (ST) generator sets, GT-driven generators and synchronous motors.

The second driving factor behind this investigation is the construction of a new 132 kV switch-plant that was completed in 2010. This opened scope for an investigation of the system response to an overloading condition.

The system is evaluated in terms of its islanding and load-shedding response. The currently installed infrastructure is modelled as well as the planned future load and generation.

***The specific deliverables that are required include:***

- CCTs of all synchronous machines in all development phases
- CCTs of all synchronous machines in N-1 supply contingency conditions
- Identification of potential transient stability problems

## 1.2 Objectives of Research

The objectives of the research follow:

**i) Calculate CCTs for all Synchronous Machines:**

The CCTs for the large synchronous machines will be calculated under normal operating conditions. The CCT will allow the stability margin to be determined for each machine. The CCTs will be calculated for symmetrical fault conditions.

The CCTs for the large synchronous machines will be calculated under N-1 supply contingency conditions.

The CCTs will be classified according to machine type and function. The GT-driven generators are the primary concern when considering transient stability; however, consideration is also given to the synchronous motors.

**ii) Supply Contingency Conditions**

The machines inherently fall into three subsystems. The western and eastern networks as well as the network supplied by the newest switch-plant form the three subsystems. Each of these three sub-systems will be subjected to N-1 supply contingency following a disturbance to determine the response.

The aim of this section is to determine the effect of N-1 supply contingency on the transient stability limits of the power system.

The impact of Current Limiting Reactors (CLRs), which may be installed to reduce the system fault-level, on the transient stability limits of the system will be analysed.

**iii) Stability Improvement**

Methods to improve power system transient stability will be investigated in the final section with the intention of finding a practical means to improve the transient stability limits of the power system.

There is a large body of work on the improvement of power system stability using various techniques and technologies. The work aims to identify key technologies and methods which are workable in the context of the Sasol Synfuels power system.

**iv) Conclusions and Recommendations**

The aim of the work is to assess the stability of the Sasol Synfuels power system. The stability margin of each machine is evaluated.

Methods to improve the overall system stability are investigated and recommendations as to the most suitable methods are given in the final section.

## 1.3 Research Methodology

The research methodology that is followed is described in this section with the aim of ensuring that the intent and methods are clear and repeatable.

### i. Literature Review

The aim of the literature review is to conduct a survey of the current state of knowledge in the area of power system transient and frequency stability. The intention is to draw from a wide range of sources while relying substantially on the current widely recognised reference works on the topic. The use of academic papers will be used to supplement the theory where deemed appropriate or where contemporary work is being conducted.

The first aim of the literature review is to conduct a study of conventional power system considerations which affect the stability phenomena. Recognised treatises on the areas of power system structure, power system controls, and the fundamental problem of power system stability as well as the classification of stability phenomena are considered.

The theoretical aspects of transient and frequency stability are addressed in preparation for the case studies which follow. Where possible the observations made are related to industrial power systems, and specifically to the Sasol Synfuels industrial power system.

### ii. Practical Work

The body of work that forms the core investigation will comprise a number of case studies. The primary case studies are the responses of the new 132 kV system to various disturbances. The system in the scope of study forms three distinct subsystems which are treated as such in the case studies.

The supplementary case studies are executed to cover certain topics that are deemed to require further investigation. These topics include the investigation of governor and excitation system response to disturbances as well as the improvement of power system stability.

The packages that will be used for the sections requiring simulation will be ETAP Version 7.5.5, for which Sasol Technology has a corporate license. The bulk of the work is implemented using ETAP for which the network model is developed. MATLAB SIMULINK is used to explore certain specific concepts.

The scope of this investigation does not involve live measurement of equipment transient or dynamic response. The measurement of live plant response is not practical. Actual machine responses were used to verify the accuracy of the model in terms of run-down response.

The aim of the practical work is to expand on the literature review and to apply theoretical considerations to a practical power system. The practical work is used to draw conclusions and recommendations which are described in the final section.

## 1.4 Chapter Outline

**Chapter 1** introduces the topic and outlines the research methodology to be followed. The objectives of the research are clearly stated and defined.

**Chapter 2** presents an introduction to the theory of power system stability, which includes sections on power system structure, power system controls, an introduction to the stability problem and notes on the classification of power system stability.

The key power system components covered in this section include:

- Synchronous generator governors
- Generator Excitation control

The section on transient stability is concerned with the deviation of rotor angle of specific synchronous machines when the system is subjected to a disturbance. This section explores the theory of transient stability as well as factors affecting transient stability. Protective relaying for OOS conditions is also addressed.

The section on frequency stability is concerned with the effect that a power imbalance may have on the system frequency.

This section provides the basis for the islanding and load-shedding schemes which are analysed in Chapter 5.

**Chapter 3** outlines the study methodology which is implemented for the simulation case studies. The methodology is developed with the intention of being repeatable and transferable.

**Chapter 4** covers general case studies which illustrate the problem of power system transient stability in the context of single-generator and two-machine systems.

**Chapter 5,** which forms the bulk of the practical work, covers the practical implications of power system stability to the Synfuels power system.

A qualitative and quantitative analysis of the problem of power system transient stability is addressed with reference to a series of simulated waveforms.

This section explores the results of extensive ETAP simulations. The main outcomes of this section are the CCTs for various different network configurations.

**Chapter 6** explores methods of improving power system stability.

The intention is to explore possible methods of power system stability improvement and to evaluate each method in terms of its practical application to the Synfuels Network.

**Chapter 7** presents the conclusions and recommendations based on the work. Conclusions are made on the overall stability of the system as well as specific stability aspects that were identified.

Recommendations regarding the improvement are presented and practical aspects of system stability improvement are discussed.

# 2 Literature Review

## 2.1 Evolution of Electric Power Systems

The timeline illustrated in figure 2.1 below shows how power systems have evolved from the late 1870s until the present day [2].

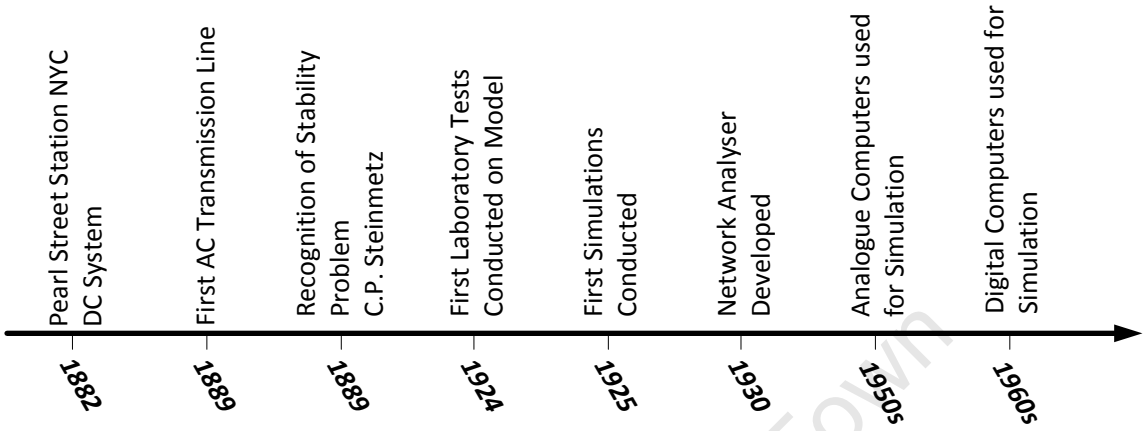


**Figure 2.1:** *Historical Timeline of Transient Stability Analysis*

The problem of power system stability was first recognised in 1920 in a paper by C.P. Steinmetz[1]. The first laboratory simulations regarding power system stability were conducted in 1924, and the first practical tests were done in 1925 [2].

The problem of high system fault levels had been identified as linked to the problem of power system stability. Steinmetz identifies several methods of improving the system fault levels including generator reactors, busbar reactors and feeder reactors [13].

Steinmetz performed a mathematical investigation into the parallel operation of two synchronous generators. Concepts such as slip, synchronising torque and power oscillations were investigated. It was from this point that the two-machine model used for transient stability studies was developed [13].

Early methods of analysis were determined by the available tools at the time. These tools included graphical aids such as the equal-area criterion. Only greatly simplified models of actual systems were able to be analysed in terms of transient stability due to the computation limits at the time [2].

The network analyser, which is effectively a scaled model of a power system, was developed in 1930 and allowed considerably more complex phenomena to be analysed for load-flow. Stability calculations still had to be done by hand [2].

In the 1950s analogue computers were used for the modelling of power system elements, such as governors and exciters, which allowed the effects of equipment characteristics to be investigated.

[1] Charles Proteus Steinmetz (1865 - 1923) was an electrical engineer and scientist credited with first identifying the problem of power system stability.

In 1956 the first digital computer program was developed for the transient stability analysis of power systems [2].

The study of power system stability since 1960 has been dominated by the study of power system transient stability. The increase in computing ability, driven by a multitude of factors, has allowed increasingly complex systems to be modelled. As the complexity of the models increases so does the demands on the simulator processing capability. As technology advances further it will likely become possible to accurately simulate any power system condition provided that certain parameters are known.

## 2.2 Power System Structure

Electric power systems have three basic characteristics in common, although exceptions do exist, which are listed below:

1. They are three phase systems that operate essentially at constant voltage and frequency.
2. They use synchronous machines for generation of electricity.
3. They transmit power over significant distances and large areas.

The power system is typically divided into generation, transmission and distribution sub-systems. These sub-systems may be independently owned and operated but regulated by a central authority or they may be controlled by a single utility company.

### 2.2.1 Generating Unit General Arrangement

The block diagram of a generating unit is show below in figure 2.2. The synchronous generator is driven by the prime-mover (ST) which is controlled by the ST-governor. The field current is provided by the exciter and is controlled by the Automatic Voltage Regulator (AVR) [3].

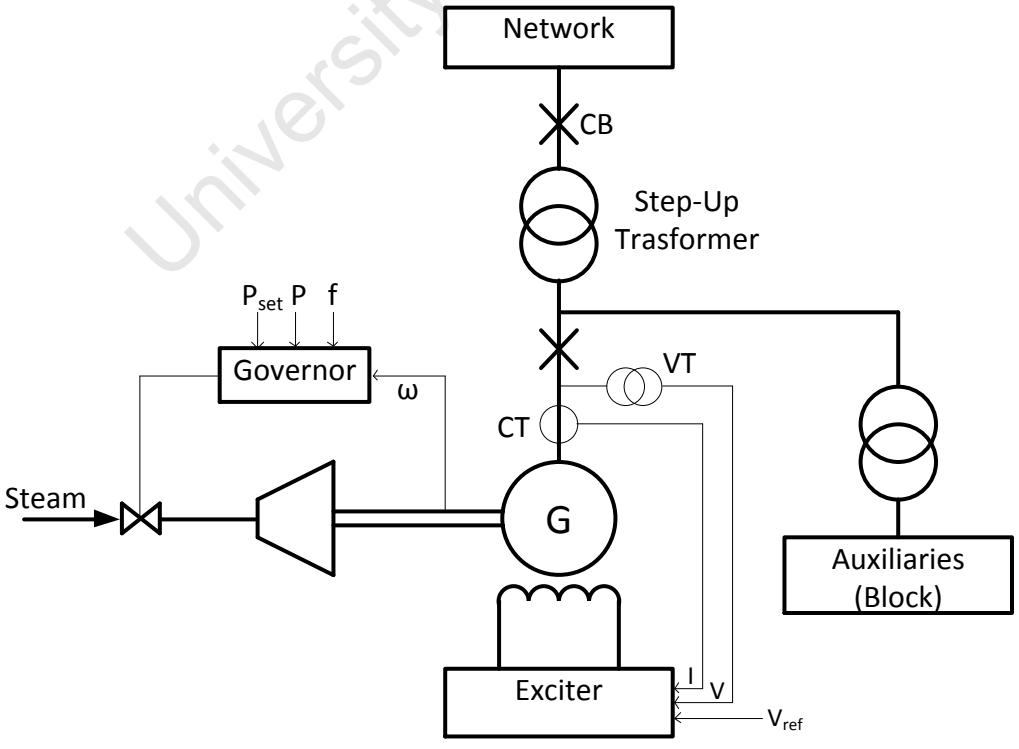


**Figure 2.2:** *Typical Power Generation Unit Arrangement*

The generator is typically connected to the network via a step-up transformer and to its auxiliaries via a separate transformer [2].

### 2.2.2 Excitation Systems

The excitation system comprises an exciter and an AVR. The power rating of the exciter is typically 0.2% to 0.8% of the generator's power rating. The voltage rating of the exciter is limited by the field winding insulation and is conventionally limited to 1000 V [3].

Exciters can be classified as rotating or static devices. The excitation current in a rotating exciter may be supplied by cascaded DC generators or an AC generator with a rectifier. A popular excitation system design uses a synchronous exciter with the field winding on the stator and armature winding on the rotor. The armature current is rectified on the rotor by rotating diodes and fed directly to the generator field winding. The excitation current can only be controlled by adjusting the exciter field current which introduces a response time lag. A possible solution is to use thyristors instead of diodes, and to control the firing angle, which improves the response time.

### 2.2.3 AC Rotating Exciter

A three-phase rotating rectifier typically comprises six diodes arranged as shown in figure 2.3. The input is a three-phase AC voltage source and the output is a DC voltage. In this arrangement the whole assembly will be rotating synchronously with the generator shaft [4].

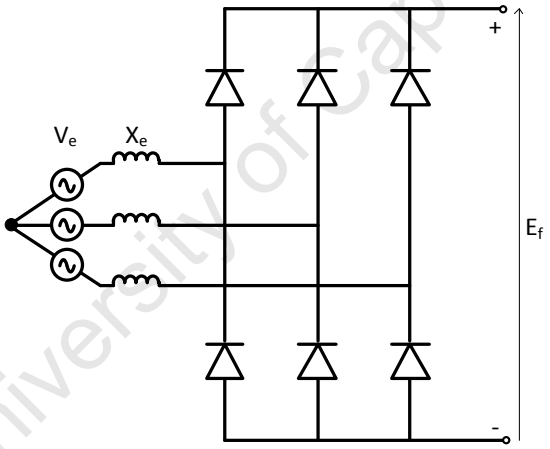


**Figure 2.3:** *Rotating Rectifier Arrangement*

### 2.2.4 Generator Capability Limits

An understanding of synchronous generator reactive power capability limits is necessary for voltage stability and long-term stability studies. Capability curves are useful graphical tools for representing these limits [2].

The active power of a synchronous generator is limited by the prime mover to points within the apparent power capability curve. The reactive power output is limited by the armature current limit, the field current limit and the end-region heating limit [2].

The energy loss associated with the armature current must not exceed the heating limitation of the winding. The armature current limit is, therefore, an arc centred at the origin with the generator MVA rating being the radius [2].

The energy loss associated with the current in the field winding imposes a second limit on the generator capability. In most designs the field current limit and armature current limit should coincide at rated MVA and PF [2].

Localised heating in the underexcited state imposes a third limit on the generator capability curve. The localised heating is caused by eddy currents in the end-region laminations due to the leakage flux [2].

The reactive power capability curve for generator 4 west is shown below in figure 2.4. This curve is generated from the ETAP model of the generator. The end-region heating limit is linear in this diagram. $Q_b$ represents rated MVA and PF and is the intersection of the armature current limit and the field current limit. It can be seen that the capability curve effectively comprises four sections.

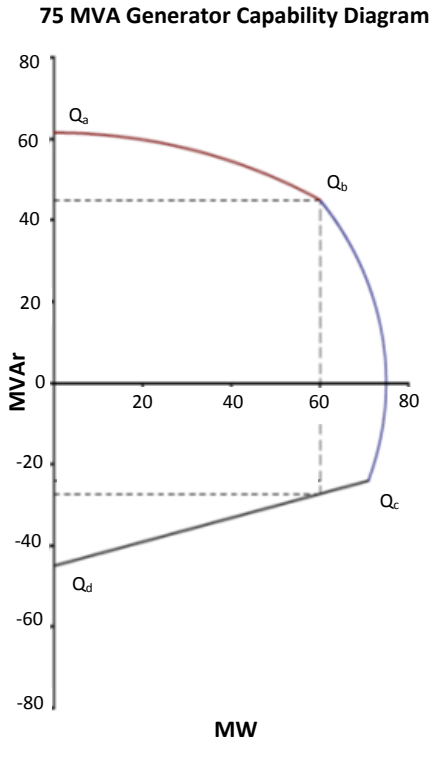


**Figure 2.4:** *Sasol 75 MVA Generator 4 Capability Diagram*[2]

The generator capability diagram can effectively be captured by four parameters, which are tabulated below in table 2.1.

| Parameter | Parameter Name | Value |
|---|---|---|
| $Q_a$ | Maximum Reactive Power | +61.5 MVAr |
| $Q_b$ | Rated Reactive Power | +45 MVAr |
| $Q_c$ | Lower Limit Intersection | -24 MVAr |
| $Q_d$ | Minimum Reactive Power | -45 MVAr |
| $P_{min}$ | Minimum Power | 0 MW |

**Table 2.1:** *Generator 4 Capability Limits*

[2] The generator capability diagram was adapted from the ETAP model of the 118 MW GT-driven generators.

## 2.3 Power System Control

The purpose of an electric power system is to convert energy from a naturally available form and to convert it to electric power which is distributed to the points of consumption.

**Fundamental Requirements:**

1. System must meet changing load demand for active and reactive power
2. The system should supply energy at minimum cost and environmental impact
3. Quality of Supply (QoS) must meet minimum standards
    a. Regulated voltage levels with fluctuations within limits
    b. Regulated frequency with fluctuations within limits
    c. Limits on harmonic content

Under normal conditions, the control objective is to operate as efficiently as possible with voltage and frequency as close as possible to nominal values. The control objective may need to change in abnormal conditions.

**System Operating Conditions:**

1. Normal
2. Alert
3. Emergency
4. *In Extremis*
5. Restorative

The power system typically moves between states as illustrated in figure 2.5 shown below. The power system and power system controls should be designed to avoid direct transition from Normal to Emergency or *In Extremis* states.

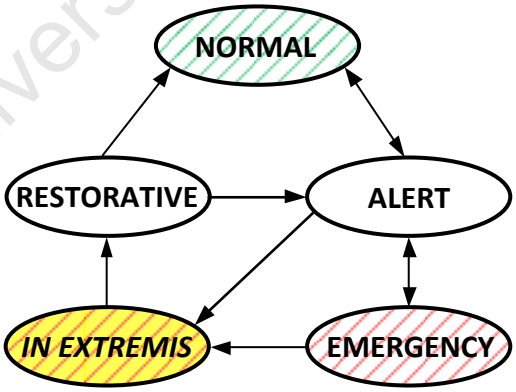


**Figure 2.5:** *Power System States*

## 2.4 Design for Stability

A power system must be able to withstand a wide variety of disturbances and remain intact to ensure reliable delivery. The 1965 Blackout in Northeast USA led to the formation of the NERC and a rethinking of conventional wisdom on power system stability. The use of criteria in design ensures that under a typical disturbance the power system will only shift from the normal to alert state and should never enter the emergency state directly [3].

Stability analysis is an important subset of system security and reliability assessment. System stability and security are time-varying indicators; while system reliability is an average performance attribute [11].

System reliability is defined by the North American Electrical Reliability Council (NERC) as follows [11]:

*"Reliability, in a bulk power electric system, is the degree to which the performance of the elements of that system results in power being delivered to consumers within accepted standards and in the amount desired. The degree of reliability may be measured by the frequency, duration, and magnitude of adverse effects on consumer service."*

**Normal Design Contingencies:**

1. Three Phase Faults with normal clearing
2. Phase to Ground Faults with normal clearing
3. Loss of Element

## 2.5 The Stability Problem

Stability may be defined as the property of a system to return to the pre-disturbance equilibrium point or an acceptable equilibrium point in a reasonable time period following a system disturbance. There are different categories into which the stability problem can be subdivided. The classification of power system stability is covered in section 2.6.

The definition proposed by the IEEE/CIGRE Joint Task Force on Stability Terms and Definitions [11] follows:

*"Power system stability is the ability of an electric power system, for a given initial operating condition, to regain a state of operating equilibrium after being subjected to a physical disturbance, with most system variables bounded so that practically the entire system remains intact."*

This definition applies to a power system as a whole and the physical disturbance may be a range of events. A single generator may lose synchronism without causing cascading instability of the system as a whole. Power system stability is, therefore, a property of the motion of the system operating point around an equilibrium set [11].

### 2.5.1 **Rotor Angle Stability**

Rotor angle stability refers to the ability of the interconnected synchronous machines in a power system to remain in synchronism. A sample two-machine system is defined by model illustrated in figure 2.6 [2].

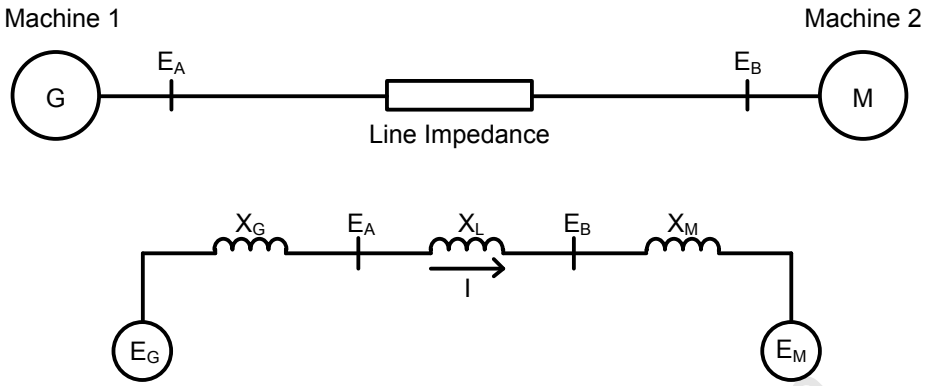


**Figure 2.6:** *Simplified Two-Machine System*

$$P = \frac{E_G \cdot E_M}{X_T} \cdot \sin\delta \quad \ldots \quad (2.1)$$

$$X_T = X_G + X_L + X_M \quad \ldots \quad (2.2)$$

The power relationship defined in equation 2.1 is highly non-linear. This relationship is displayed graphically in figure 2.7 shown below.

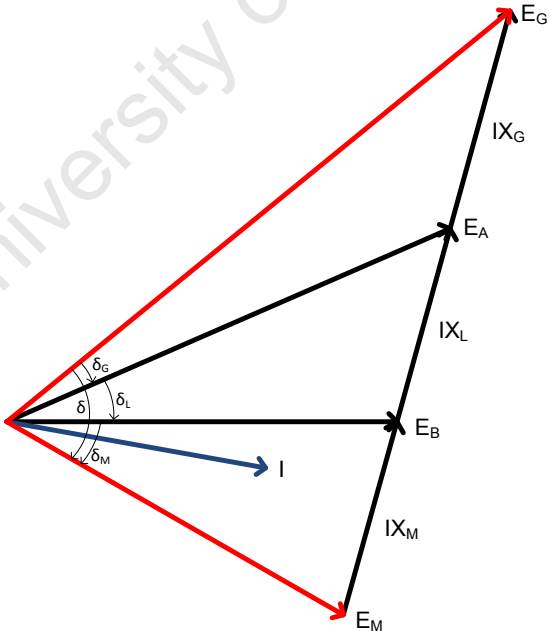


**Figure 2.7:** *Two-Machine Vector Diagram*

$$\delta = \delta_G + \delta_L + \delta_M \quad \ldots \quad (2.3)$$

$$E_G = E_M + I \cdot X_M + I \cdot X_L + I \cdot X_G \quad \ldots \quad (2.4)$$

The vector diagram shown in figure 2.7 illustrates that the power angle that determines the real power transfer comprises three components as described in equation 2.3.

The vectors of interest are the generator voltage and the motor voltage which are defined by equation 2.4. The angle between these vectors determines the real power transfer.

The change in electrical torque following a disturbance can be resolved into the synchronizing torque and the damping torque as shown in equation 2.5.

$$\Delta T_e = T_s \cdot \Delta\delta + T_D \cdot \Delta\omega \quad \ldots \quad (2.5)$$

This resultant torque is necessary to ensure rotor angle stability. Insufficient synchronizing torque may result in aperiodic drift of the rotor angle while insufficient damping torque may result in oscillatory instability [2].

Rotor angle stability can be subdivided into the categories of small-signal stability and transient stability. Small signal stability covers the relatively small changes in load and generation. In the small-signal stability region linearization of the system equations is reasonable.

Small signal instability may be of two forms; steady rotor angle increase due to insufficient synchronizing torque or oscillatory instability due to insufficient damping torque [2].

**Oscillation Modes:**

1. Local Modes
2. Inter-Area Modes
3. Control Modes
4. Torsional Modes

Transient stability involves large disturbances and is influenced by the non-linear power angle relationship. Stability depends on both the initial operating state and the severity of the disturbance [2].

The frequency of oscillation of the rotor angle is inherently significantly lower than the nominal power system frequency. This is due to a number of factors, the most significant of which is the inertia of the rotor. A fast change in rotor angle is not physically possible.

The frequency of oscillation is typically in the region of 1 Hertz which corresponds to a period of 1 second.

## 2.6 Classification of Stability

The problem of classification of power system stability has been investigated by several IEEE and CIGRE reports. The investigation done by the IEEE/CIGRE Joint Task Force on Stability Terms and Definitions published in May, 2004, is used as the basis for stability classification [11].

Transient stability is the focus of this investigation. It is, however, important to contextualise the transient stability phenomena. This section aims to provide an overview of power system stability classification.

Transient stability, which is large-signal rotor angle stability, has historically dominated power system stability studies. As power systems have grown larger, more complex and are operated closer to their limits other forms of instability have emerged. Voltage stability, frequency stability and inter-area oscillations have emerged as areas of concern [11].

Stability is essentially a condition in which two or more forces are in equilibrium. Depending on the initial operating conditions and disturbance type different sets of unbalanced forces may lead to different forms of instability. Although power system stability is essentially a single problem, the rigorous classification of power system stability is necessary [11].

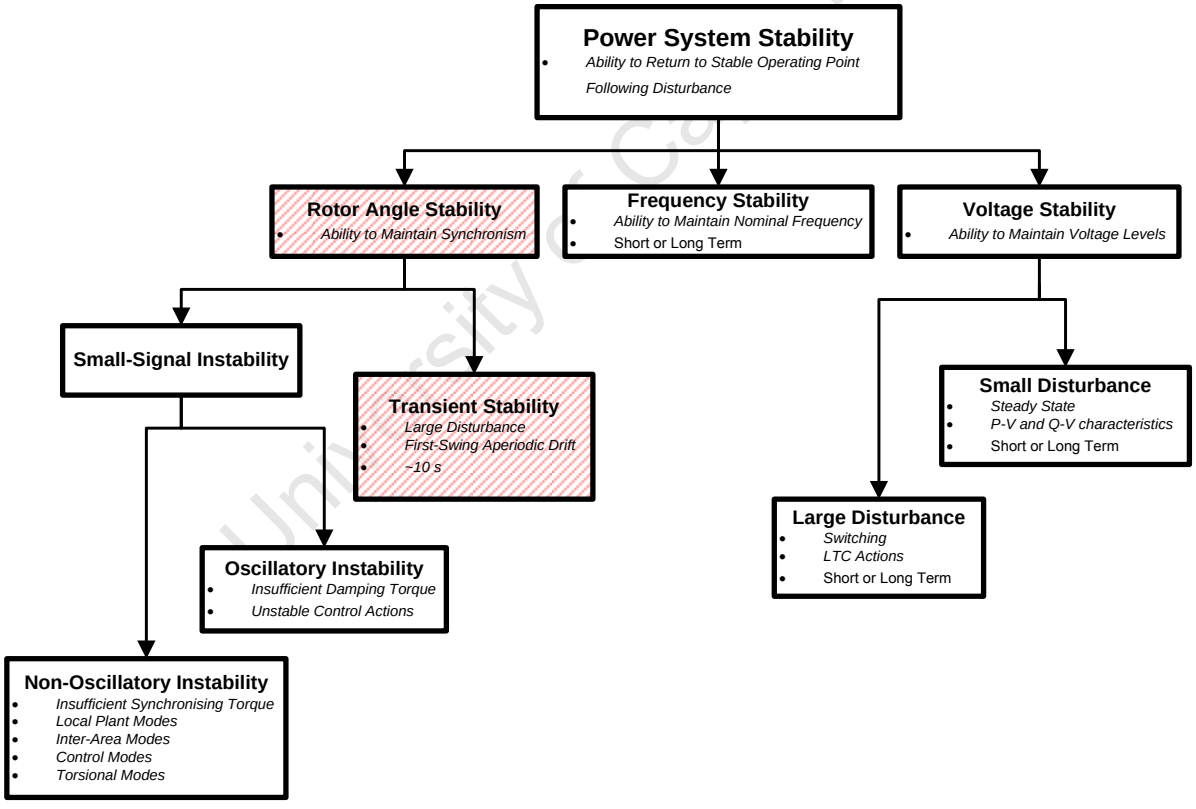


**Figure 2.8:** *Classification of Power System Stability*

The diagram shown above in figure 2.8 illustrates the different classifications of stability. The distinction between mid-term and long-term stability is not clearly defined [3].

A power system is an interconnected system comprising elements of different characteristics which create a large, dynamic and complex system. The dynamic response may vary from local effects to system-wide effects [3].

The primary concern of power system stability is how a power system will respond to both changes in demand and system supply or configuration disturbances [3].

Based on their physical characteristics and time frame, power system dynamics can be divided into wave, electromagnetic, electromechanical and thermodynamic phenomena. The grouping of dynamics is illustrated below in figure 2.9. There are considerable overlaps of the time windows of the different dynamics [3].

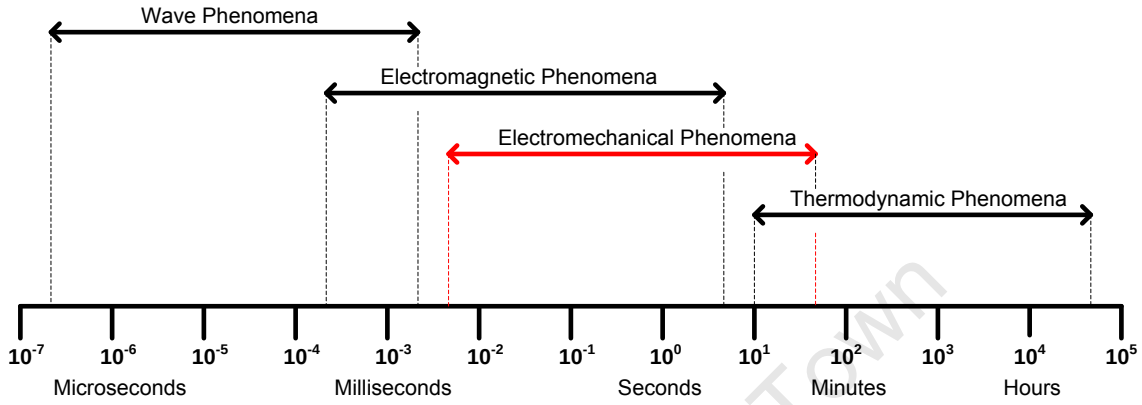


**Figure 2.9:** *Time Frame of Power System Dynamic Phenomena*

The fastest dynamic effects are wave phenomena, which correspond to surges in HV transmission lines caused by lightning or switching operations. These fast wave phenomena do not propagate beyond the transformer windings. The electromagnetic phenomena are due to the interaction of the changing winding currents as well as protection operations. The electromechanical phenomena include the rotor oscillations that occur subsequent to a disturbance. Transient stability events, which are the subject of this investigation, occur in the electromechanical time window. The slowest dynamics are due to boiler controls and automatic generation controls [3].

## 2.7 Synchronous Motor Behaviour through Disturbances

Industrial complexes typically implement switching schemes to ensure continuous power to large induction and synchronous motors. These large motors typically fulfil important roles and continuous operation is critical for continued production. A loss of power would typically result in significant production losses [6].

For analytical purposes small induction motors are generally lumped into an equivalent load having the characteristics of the average motor in the group [6]. Larger induction motors are generally kept separate from the lumped load in the interest of model accuracy.

It has been determined by Bottrell, *et al*, that the stability of synchronous machines is sensitive to the type and size of parallel operating loads. For this reason it is necessary to model parallel operating induction motors accurately [6]. It has been hypothesized by Bottrell that the ride-through characteristics of induction motors aggravates transient stability concerns for the parallel synchronous motor. Alternatives to ride-through are to allow the induction motor to trip relatively quickly in the event of a disturbance or to implement a fast-transfer scheme [6].

An alternative to the slow transfer scheme, where the motors are tripped and re-accelerated onto a new power source, is to use a fast transfer scheme which ensures continuity of supply. The primary concern regarding this scheme is damaging transients at the moment of transfer. The investigation of bus transfer schemes is out of the scope of this work. The basic problem being that the transfer is not instantaneous and during the time delay there is voltage, frequency and phase drift between load and standby supply.

### *2.7.1.1 Timed Voltage Dip*

The power angle of a synchronous motor is sensitive to impact disturbances. The response of a 36 MW synchronous motor to a 10 percent voltage dip which was ramped down over 10 ms is illustrated below in figure 2.10. The voltage dip was simulated for 300 ms.

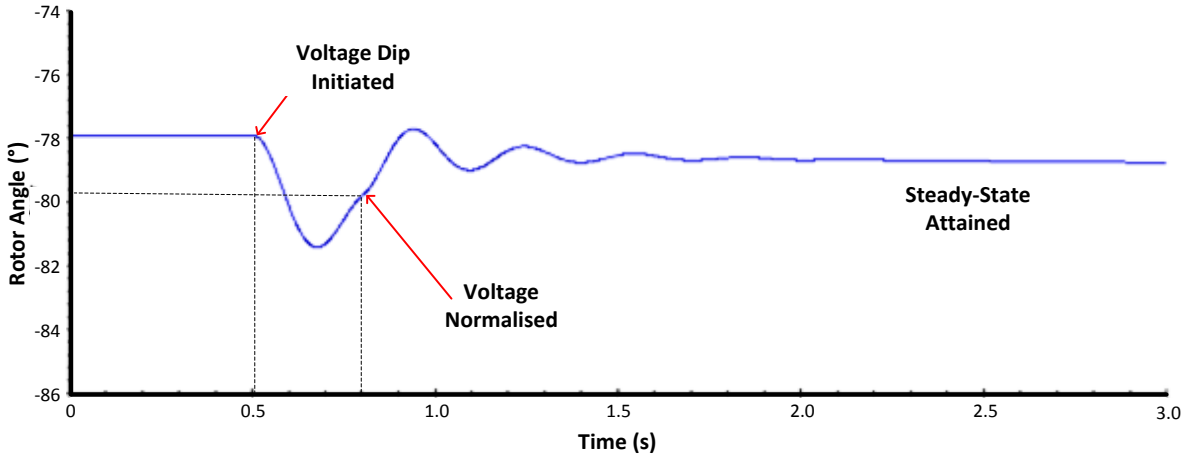


**Figure 2.10:** *Power Angle Response to 300 ms Voltage Dip*

The oscillation is significantly reduced if the rate of change in voltage is relatively slow. The power angle response to a prolonged -10 % voltage dip when the voltage is ramped down over 1 second is shown below in figure 2.11. The oscillations in this case result when the impact occurs to return the voltage to the nominal level.

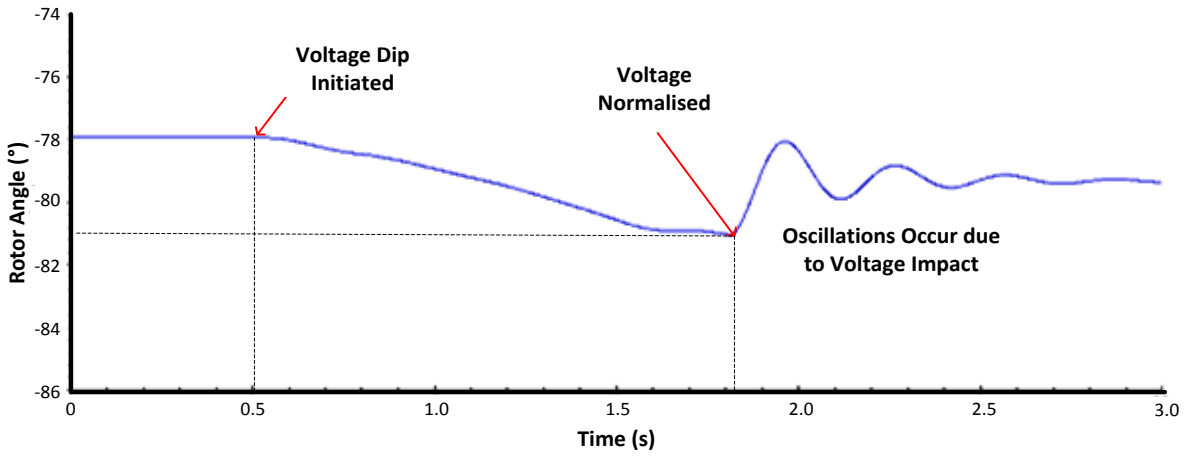


**Figure 2.11:** *Power Angle Response to Slowly-Ramped Voltage Dip*

### *2.7.1.2 Permanent Voltage Dip*

This example is of the system response to a 5 % permanent voltage dip which is initiated at 0.5 s. The total simulation time is 5 seconds to allow all transients to settle. A 5% voltage dip is within rated limits of most electrical equipment and the plant should continue to run without tripping.

The machine terminal voltage is visible below in figure 2.12 which is the utility source voltage in this case. The voltage ramps down to 95 % of nominal voltage and remains at that level.

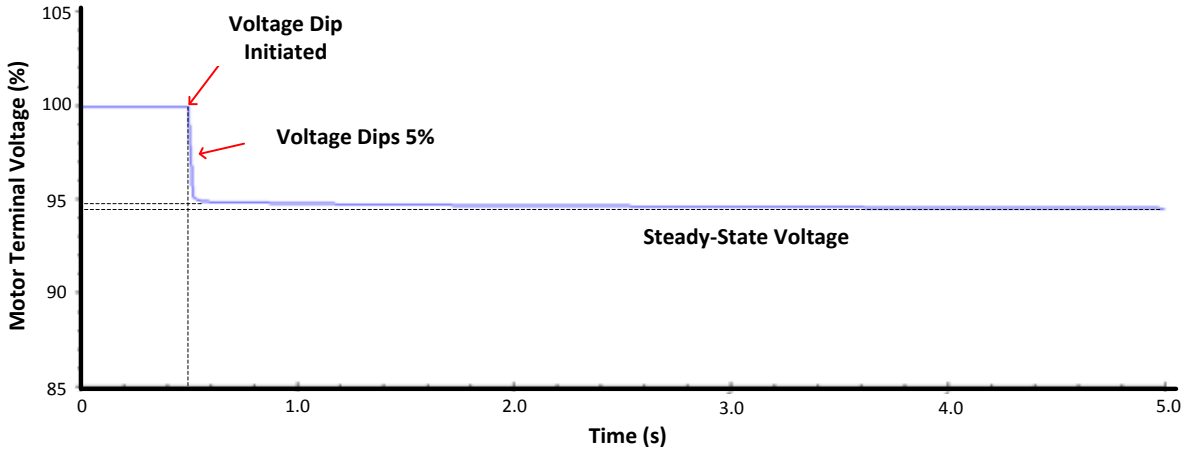


**Figure 2.12:** *Machine Terminal Voltage Response to 5 % Voltage Dip*

The motor electrical power is visible below in figure 2.13. The initial waveform displays oscillations which stabilize and the motor returns to nominal power. The magnitude of the power oscillations is proportional to the depth of the voltage dip and the inertia of the system.

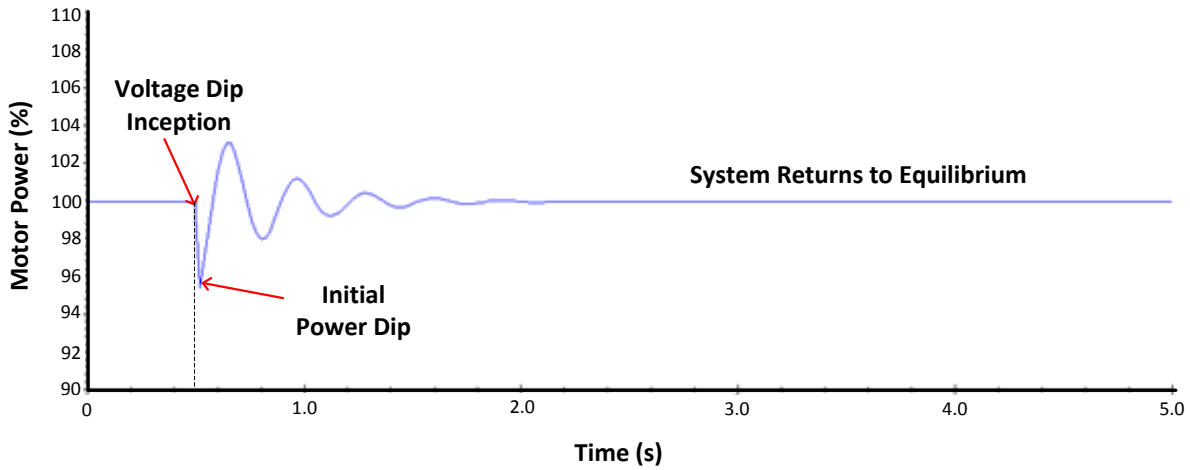


**Figure 2.13:** *Motor Electrical Power Response to 5% Voltage Dip*

It is possible for the motor to lose synchronism if the voltage dip is deep and long enough. The ride-through probability is inversely proportional to the depth and duration of the voltage dip.

## 2.8 Power System Controls

Active and reactive power flows in a transmission system are relatively independent of each other. Active power balance is closely linked to frequency control while reactive power balance is closely linked to voltage control [2].

### 2.8.1 Active Power and Frequency Control

For satisfactory system performance the power system frequency should remain as constant as practically possible. This will ensure the running of induction and synchronous machines at constant speed [2].

The frequency of a power system is dependent on the active power balance. A speed governor on each generating unit provides the primary speed control function while a supplementary control unit at the central control station allocates generation. The control of generation and frequency is commonly known as Load-Frequency Control (LFC) [2].

### 2.8.2 Generator Voltage Control

A ST-driven generator typically has voltage and turbine-governor controls. The AVR modulates the excitation current in order to control the generator terminal voltage [1].

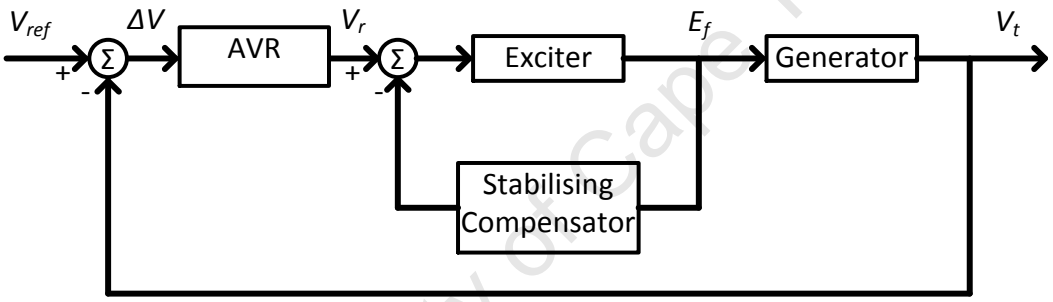


**Figure 2.14:** *Generating-Unit Voltage Control Block Diagram*

A simplified generator control system is illustrated above in figure 2.14. The voltage reference is compared to the terminal voltage and the difference is applied to the AVR. The AVR introduces an inherent time-delay. The output is applied to the exciter block which outputs the field voltage to the generator.

The stabilising compensator is used to improve transient response by reducing overshoot and the resulting oscillations [1].

An alternative method of voltage regulation is to use the tap-changer of the generator transformer to regulate the terminal voltage. This allows the AVR to be set in a different control mode such as PF or reactive power control.

### *2.8.2.1 Generator Speed Control*

The turbine speed-governor adjusts the main steam-valve in order to control the mechanical output power of the turbine. The governor also monitors the rotor speed to maintain the frequency at the nominal value of 50 Hz if the generator is running in an islanded condition where the utility does not determine the frequency [1].

In the event that there is a load increase, the generating unit will respond by effectively releasing kinetic energy to supply the load deficit. The electrical torque will initially increase while the mechanical torque initially remains constant. The acceleration on the turbine-generator set is, therefore, initially negative and the unit will begin to decelerate. This will result in a falling system frequency [1].

The changing speed, and frequency, can, therefore, be used as an indication of an imbalance between electrical torque and mechanical torque. The steady-state frequency-power equation for turbine-governor control is given by equation 2.6, where *R* is the regulation constant.

$$\Delta P_m = \Delta P_{ref} - \frac{1}{R} \cdot \Delta f \quad \ldots \quad (2.6)$$

A simplified block diagram of a speed governing system is illustrated in figure 2.15 below. This model is of an isolated generating unit supplying a single load [2].

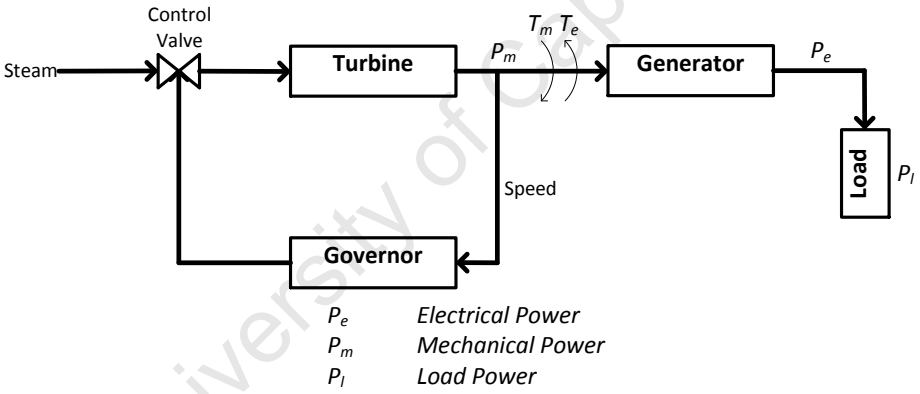


**Figure 2.15:** *Generating Unit Supplying Isolated Load*

The transfer function illustrated below in figure 2.16 is used to explain the effect of a load change. The load change results in an instantaneous torque imbalance which results in a rotor speed deviation. The magnitude of the speed deviation is inversely proportional to the inertia constant, *H*, which has units of $\frac{MW.s}{MVA}$ [2].

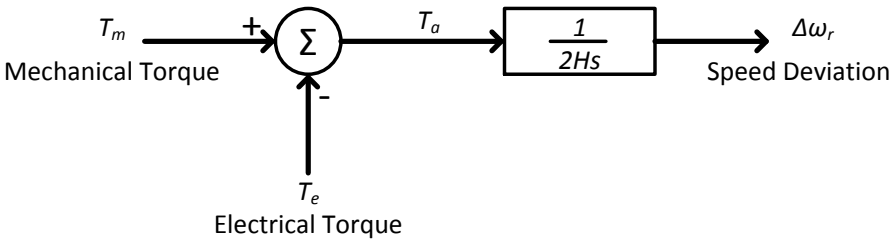


**Figure 2.16:** *System Transfer Function relating Speed and Torque Balance*

The frequency-dependent characteristic of a composite load can be represented by equation 2.7. The damping constant, *D*, is expressed as a percentage change in frequency for 1 % load change [2]. The equation comprises the non-frequency-sensitive load change ($\Delta P_L$) and the frequency-sensitive load change ($D\Delta\omega_r$).

$$\Delta P_e = \Delta P_L + D \cdot \Delta\omega_r \quad \ldots \quad (2.7)$$

The system block diagram relating mechanical and load power to speed deviation is shown below in figure 2.17. In the absence of a governor the system response is determined by the inertia constant and load constant [2].

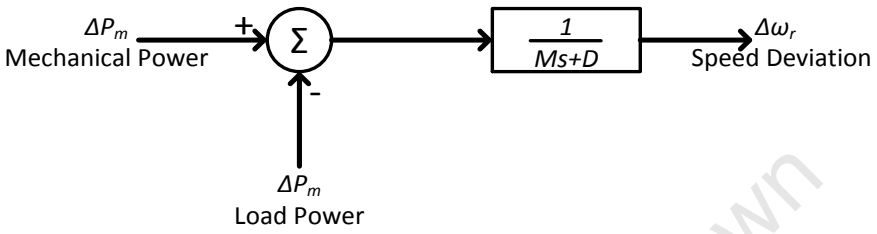


**Figure 2.17:** *System Transfer Function Relating Speed and Powers*

#### 2.8.2.1.1 Droop Characteristic

The governor needs to be set with a speed-droop characteristic when the system comprises multiple generating units. The droop characteristic reduces the reference speed as the load increases. The generator is connected to a practically infinite bus. This means that adjusting the speed reference effectively adjusts the generator load. This is used for load division among parallel generators [2].

This method requires a steady-state feed-forward loop to be installed around the integrator. The adjusted block diagram is illustrated below in figure 2.18 [2].

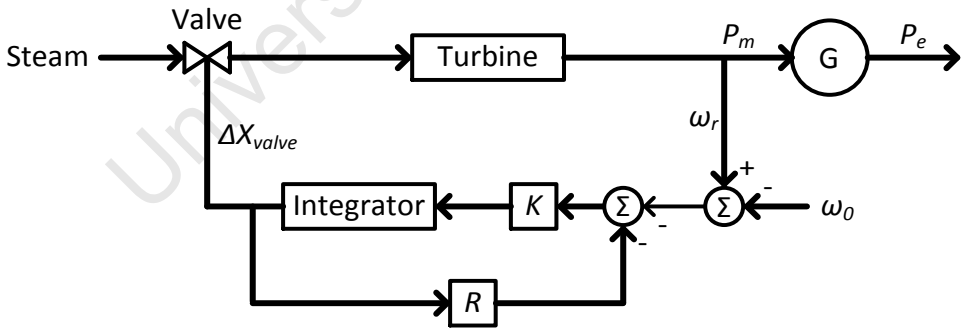


**Figure 2.18:** *Governor with Droop Characteristic*

The reduced block diagram is shown below in figure 2.19. The block diagram has been reduced to a proportional controller. The gain is $\frac{1}{R}$ and the governor time constant, $T_G$, is defined as $\frac{1}{KR}$.

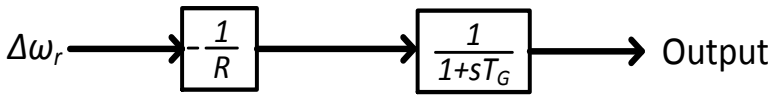


**Figure 2.19:** *Simplified Governor Block Diagram*

#### 2.8.2.1.2 Percent Speed Regulation

The droop is defined in equation 2.8. The droop, *R*, represents the ratio of speed deviation to the corresponding change in power output. The speed deviation is synonymous to a frequency deviation [2].

$$R = \left(\frac{\omega_{NL} - \omega_{FL}}{\omega_0}\right) \cdot 100 \quad \ldots \quad (2.8)$$

The concept of droop-speed, or percent-speed, regulation is illustrated below in figure 2.20. The droop characteristic will determine the ratio of the load increase that each generating unit will assume. For two equal rating units the droop should be equal. The gradient of the characteristic is the droop or percent-speed regulation. [2].

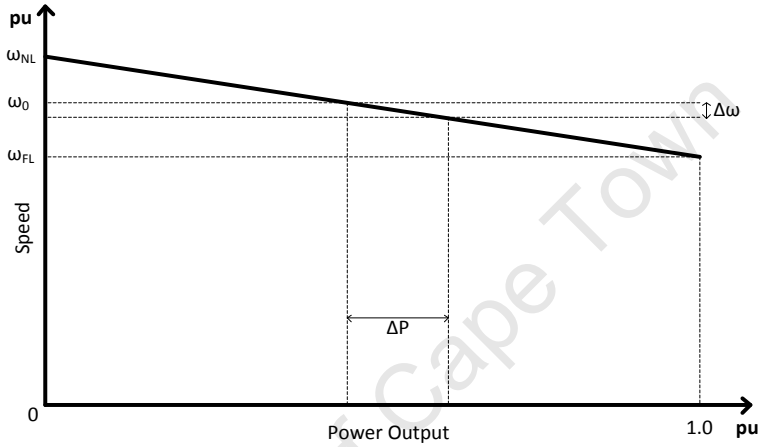


**Figure 2.20:** *Ideal Steady-State Speed Droop Governor Characteristic*

A generating unit equipped a droop-speed governor will have a steady state error associated with any change in load. This is due to the change in speed reference associated with a change in load power. This principle is illustrated below in figure 2.21 [2].

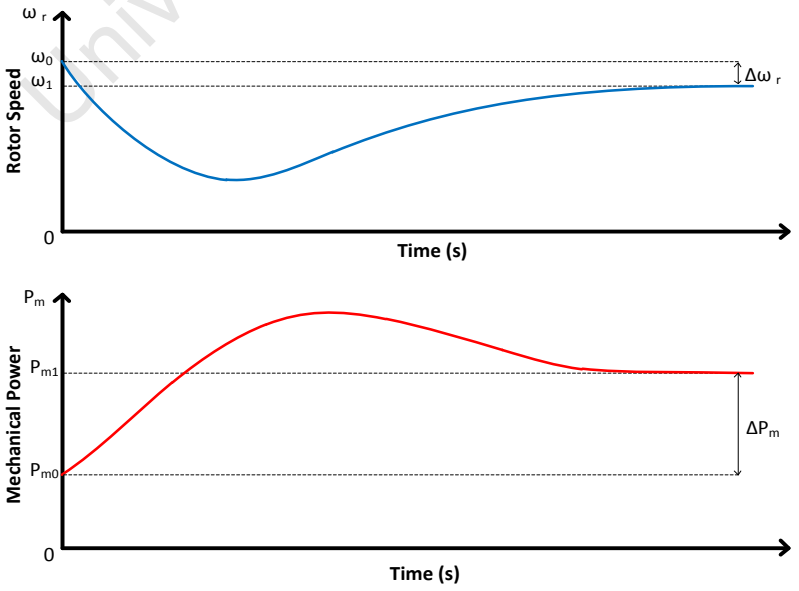


**Figure 2.21:** *Response of Generating Unit with Droop-Speed Governor to Load Change*

#### 2.8.2.1.3 Governor Transient Response

The 118 MW generating unit is used as a case study to illustrate the effect of a droop-speed governor on the unit's transient response. The generator bus was subjected to a 100 ms symmetrical fault. No limitations were programmed into the simulation. This was done in order to demonstrate the unconstrained response.

The generator electrical power is visible in figure 2.22 below for two cases. Case 1 uses a droop governor with the typical parameters (deliberately unsuitable). Case 2 does not implement a governor. The fault condition is clearly visible as the time during which the electrical power is zero.

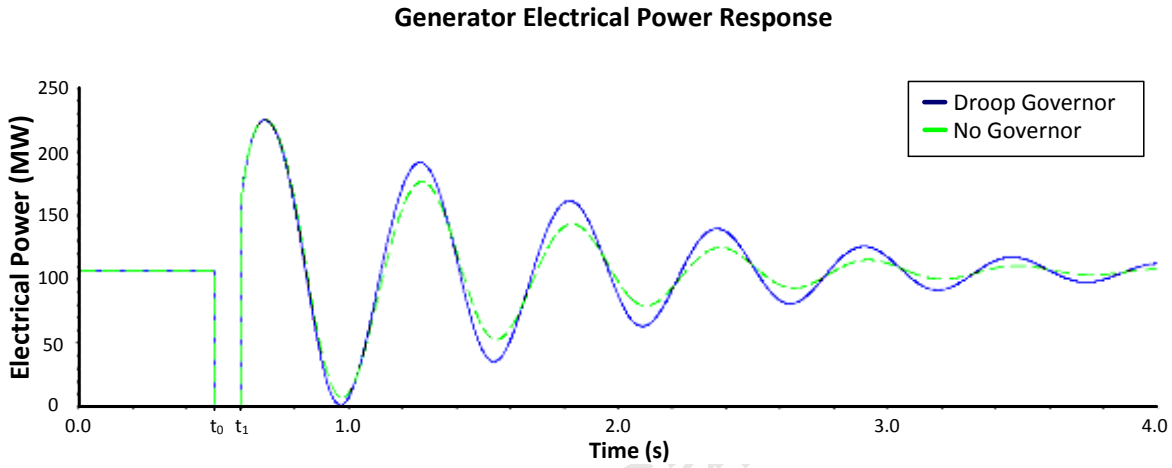


**Figure 2.22:** *118 MW Unit Electrical Power Responses with and without Droop Governor*

It is clear that the response of the governor exacerbates the swinging of the rotor in case 1. It is important to consider rotor angle transient and dynamic responses to disturbances when designing a governing system.

The turbine mechanical power response and the generator electrical power can be analysed qualitatively to explore their transient relationship. The first swing of the generator electrical power response begins at a value higher than the pre-fault condition. The power then increases until a peak value is reached and then declines. Several oscillations ensue until the electrical power stabilises.

The turbine post-fault response is to decrease mechanical power due to the governor response. The turbine mechanical power will also oscillate until it stabilises at the pre-fault value.

The turbine post-fault mechanical power and the generator post-fault power should oscillate at the same frequency but 180° out of phase. This would, everything else equal, result in the optimally damped response.

## 2.9 Transient Stability

Transient stability will be the focus of the work. Transient stability is defined as the ability of an electric power system to maintain synchronism when subjected to a severe transient disturbance. The severe transient event may be a fault on a transmission line, loss of generation or a loss of a large load.

According to Crappe, *et al*, the time-domain transient analysis approach is not suitable for real-time analysis and definitely not for preventative or corrective actions [5]. Two categories of non-conventional analysis methods exist, namely the direct methods and the automatic learning methods [4].

The range of transient stability phenomena fall into the dynamic-phenomena division of power system security analysis. Dynamic phenomena include transient or rotor angle stability, voltage stability and frequency stability.

### 2.9.1 Simplified Model

A simplified model of a power system can be used to explain the fundamental concepts of transient stability analyses. The model is illustrated in figure 2.23 shown below. The model comprises a generator, a transformer and two parallel transmission lines connecting the system to an infinite bus. The sub-transient period is very short compared to the rotor power swings and the sub-transient electromechanical dynamics can be neglected [3]

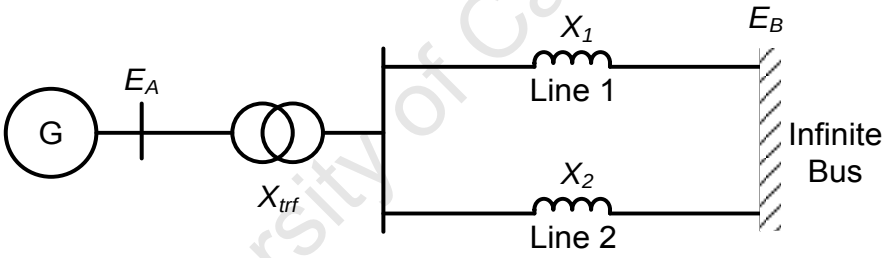


**Figure 2.23:** *Single Machine connected to Infinite Bus*

The arrangement in figure 2.23 can be simplified by grouping reactances to yield figure 2.24. The generator direct-axis reactance will vary based on the investigation time-frame. The equivalent reactance will vary if one of the lines is removed.

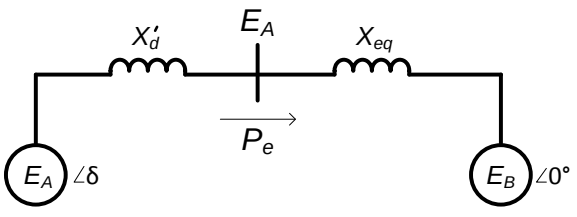


**Figure 2.24:** *Single Machine Equivalent Circuit*

The electrical power equation for this simplified system is given below in equation 2.9. The equation is non-linear and is dependent on the power angle and the system reactance.

$$P_e = \frac{E_A \cdot E_B}{X_{eq}} \cdot \sin\delta = P_{max} \cdot \sin\delta \quad \ldots \quad (2.9)$$

A change in the system reactance will result in a change in the shape of the power curve, provided all other conditions remain constant. The new power curve will require a new power angle to provide the same power as before the disturbance.

$$\frac{2H}{\omega_0} \cdot \frac{d^2\delta}{dt^2} = P_m - P_{max} \cdot \sin\delta \quad \ldots \quad (2.10)$$

The swing equation is shown above in equation 2.10. This equation can be used to analyse the swinging behaviour of a synchronous machine following a disturbance [2]

There are typically three states that need to be assessed to determine the transient stability of the system. The pre-fault state is the normal operating arrangement of the power system. The fault state is the state of the system during the fault and the post-fault state is the condition of the system following fault clearance. It is necessary to evaluate the power curve for each of the reactances corresponding to the three states [3].

The equivalent circuit allows the equivalent reactance to be determined. The fault impedance is determined by the type of fault as defined by table 2.2. The fault impedance can be connected between the fault point and the neutral in the circuit. The use of sequence components allows any type of fault to be represented [3].

| Fault Type | 3-ϕ L-G | L-L-G | L-L | L-G |
|---|---|---|---|---|
| **Shunt Reactance** | 0 | $\frac{X_2 X_0}{X_2 + X_{02}}$ | $X_2$ | $X_1 + X_2$ |

**Table 2.2:** *Shunt Reactances for Different Fault Types [3]*

The most severe class of fault is a three-phase bolted fault. In this state all the phases are connected to each other and directly to ground. The fault impedance is effectively zero and there can only be positive sequence current since the fault is symmetrical. This means that a three-phase fault blocks power transfer and results in a purely inductive fault current [3].

Unless a three-phase fault is cleared before the critical clearing angle the system will become unstable, provided no other protection is in operation. The power angle will follow a parabolic curve until the fault is cleared as shown in figure 2.25. This diagram illustrates both a stable and an unstable condition [3].

In the unstable case illustrated in figure 2.25 the rotor angle will increase due to a net accelerating torque after point 8 is reached. The rotor makes an asynchronous rotation and will lose synchronism with the system [3].

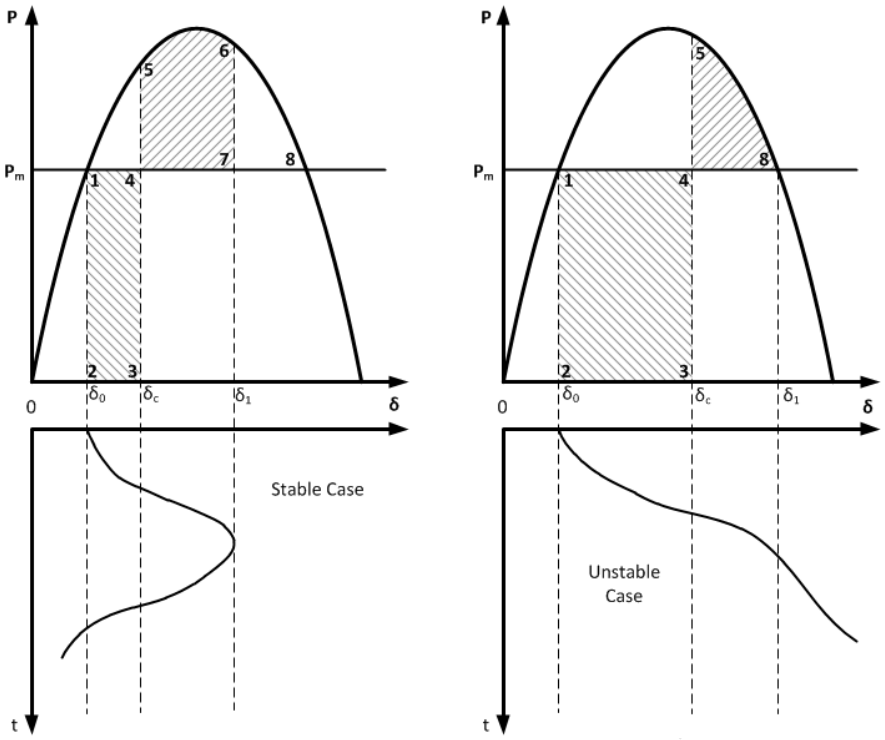


**Figure 2.25:** *Equal Area Criterion for Symmetrical Fault*

The transient stability margin can be defined as the ratio of area 6-7-8 to ratio 4-5-8 as defined in equation 2.11.

$$K_{area} = \frac{Area\ 6-7-8}{Area\ 4-5-8} \quad \ldots \quad (2.11)$$

The transient stability margin can also be determined from the critical and actual clearing times as defined in equation 2.12.

$$K_{time} = \frac{t_{cr} - t_f}{t_{cr}} \quad \ldots \quad (2.12)$$

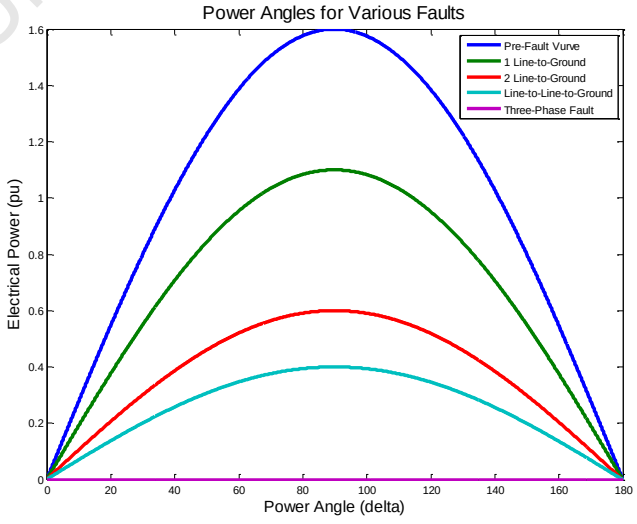


**Figure 2.26:** *Power Angles for 4 Different Fault Types*

The power-angle characteristics of different fault types are illustrated above in figure 2.26. The pre-fault load is an important factor to consider. A general rule is that the higher the pre-fault load the shorter the CCT [2].

The CCT is generally the metric of choice in Europe while the USA refers to the critical power. The CCT is a simple calculation and can be used to rank contingencies.

### 2.9.2 Response to Step Change in Mechanical Power

The response of the model to a step change in mechanical power is shown in figure 2.27. The increase in mechanical power causes the power angle to increase and overshoot the new equilibrium point due to the system inertia. In the simplified model the power angle will oscillate with constant magnitude.

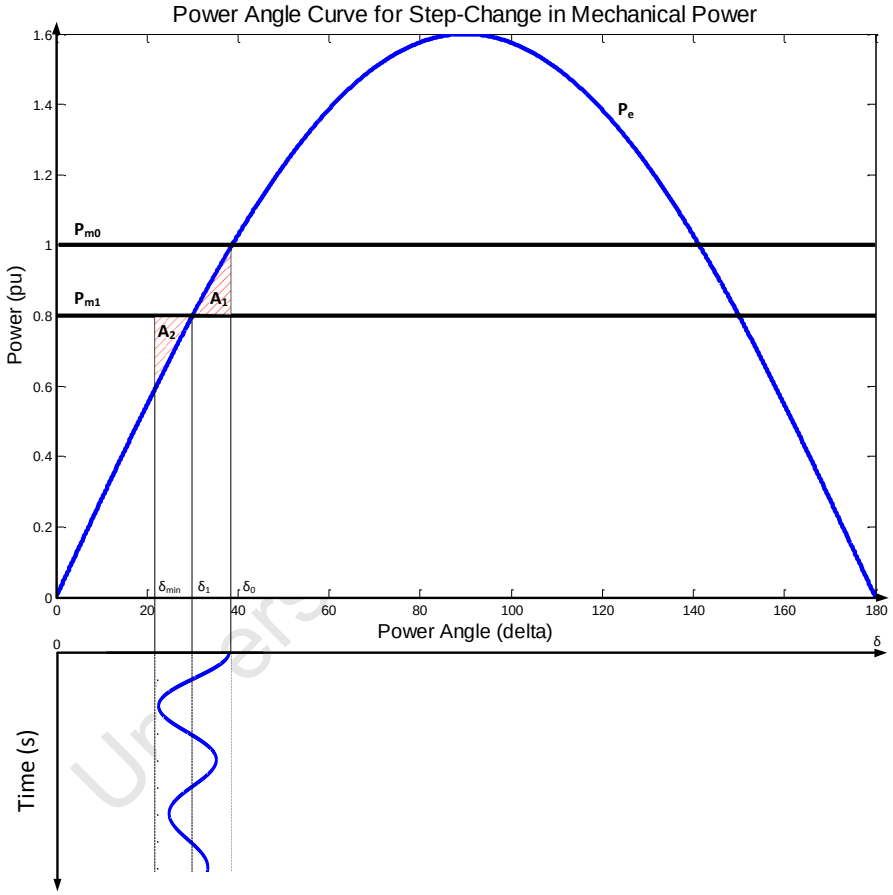


**Figure 2.27:** *Simplified Response to Step-Change in Mechanical Power*

The difference at any point between the mechanical and electrical power represents the accelerating power. At the moment of the mechanical power step-change there is a deficit of mechanical power of 0.2 pu. The deficit of mechanical power, in the case of a generator, results in the power angle decreasing, and shifting to the left along the power-angle curve [3].

The power angle will move, from $\delta_0$, to a new steady state power angle at $\delta_1$. Due to the inertia of the system the power angle will overshoot the new steady-state power angle for several oscillations. The power angle will reach a minimum angle of $\delta_{min}$ [3].

The principle of the equal-area criterion is demonstrated by the fact that area $A_1$ equals area $A_2$ in figure 2.27.

### 2.9.3 **Equal-Area Criterion**

For a system to be stable the power angle needs to increase to a maximum and then decrease. It needs to be bounded by well-defined upper and lower power angle limits. The area under the $P_m$ - $P_e$ curve needs to be zero for the system to be stable. This can be represented as an integral as shown in equation 2.13.

$$\int_{\delta_0}^{\delta_m} \frac{\omega_0}{H}(P_m - P_e)d\delta = 0 \quad \ldots \quad (2.13)$$

This equation allows the critical clearing angle to be calculated given the power curve and the system parameters.

The equal-area criterion can be used to assess system stability subsequent to a disturbance based on the clearing time and the consequent clearing angle. The cases of a stable and unstable system are illustrated in figure 2.28 shown below.

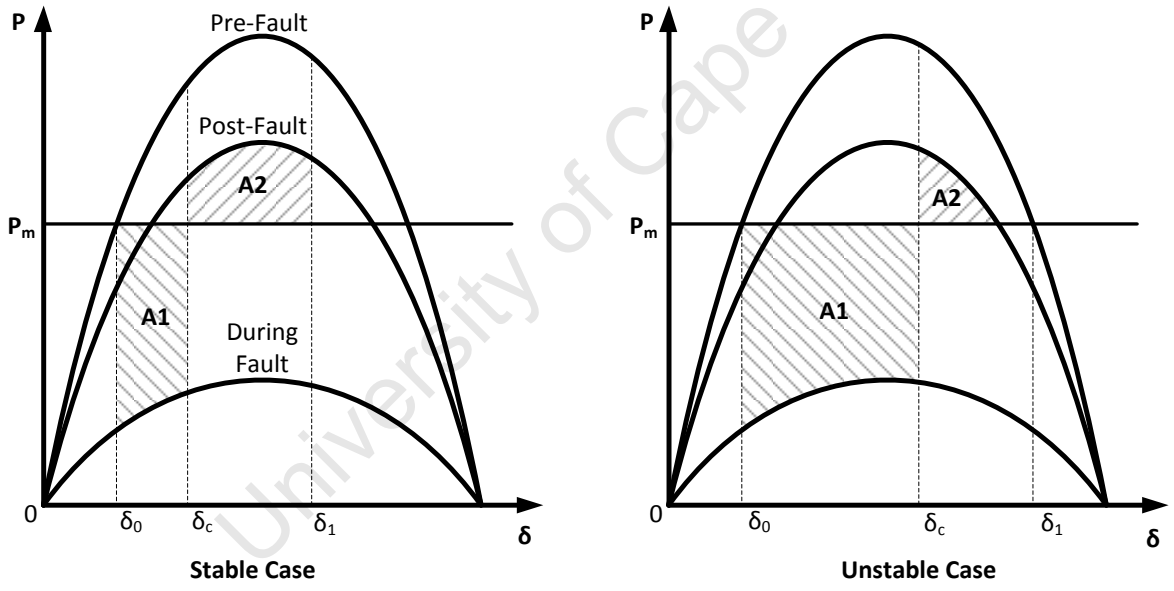


**Figure 2.28:** *Equal-Area Criterion Application*

The simplified application of the equal-area criterion presented above neglects damping and synchronising torques. It has been proposed by Willems (1969) that the synchronising torque, which is proportional to the rate of change of the rotor angle, can be plotted graphically as shown in figure 2.29 below [8].

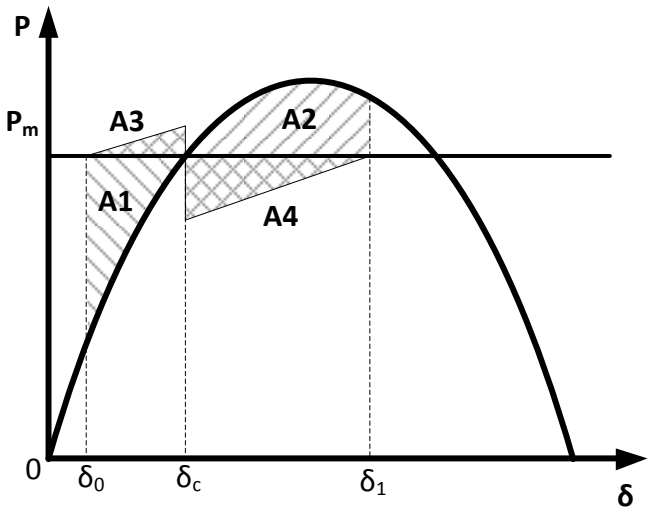


**Figure 2.29:** *Extended Equal-Area Criterion*

The damping torque is represented by the additional inclined characteristics. The addition of the damping torque curve implies a subtle change to the equal-area criterion. The area enclosed by contour A1 + A3 must not exceed the area enclosed by contour A2 + A4. The extension of the equal-area criterion is summarised in equation 2.14 which specifies the conditions for stability to be ensured [8].

$$\frac{pk^2}{2J}(\delta_1 - \delta_0)^2 + \int_{\delta_0}^{\delta_1} \{T_s(\delta_1) - T_s(\delta)\}\, d\delta \leq \frac{pk^2}{2J}(\delta_2 - \delta_1)^2 + \int_{\delta_1}^{\delta_2} \{T_s(\delta) - T_s(\delta_1)\}\, d\delta \quad \ldots \quad (2.14)$$

It is important to note that the damping torque is more accurately given by equation 2.15. The damping factor is not constant as presented above but is dependent on the rotor angle [8].

$$T_d = k(\delta)\frac{d\delta}{dt} \quad \ldots \quad (2.15)$$

### 2.9.4 Factors Affecting Transient Stability

Common factors affecting transient stability include:

1. Generator pre-fault loading
2. Faulted generator output power
3. Fault-clearing time
4. Post-fault transmission reactance
5. Generator sub-transient reactance
6. Generator and turbine inertia
7. Generator internal voltage magnitude
8. Infinite bus voltage magnitude

The graphical tool is useful for illustration of transient stability principles but its practical use is limited since it does not provide accurate time domain representations of the power angle. The most practical method of transient stability analysis is time-domain simulation in which the non-linear differential equations are solved using iterative numerical integration techniques.

## 2.10 Structure of the Power System

The structure of the model that will be used for transient stability studies of the power system is shown below in figure 2.30 [2].

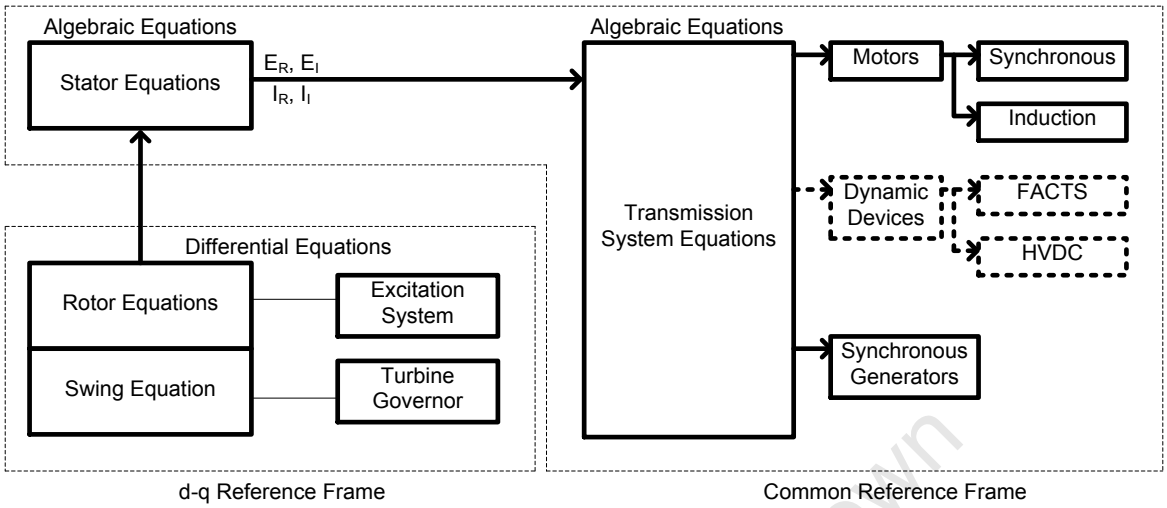


**Figure 2.30:** *Power System Structure*

The model comprises several subsystems such as generators and transmission lines which need to be accurately modelled.

The model incorporates non-linear differential equations and must be capable of handling the large discontinuities due to severe disturbances [2].

## 2.11 Protective Relaying

Protective relays detect abnormal operating conditions and initiate breaker operations in order to remove faulted equipment from service and maintain operation when possible. A protective relay needs to distinguish between fault conditions, stable power swings and OOS conditions [3].

Protective actions may weaken the power system and exacerbate already unstable conditions. The controlled separation of the system is determined by protective relays. It is, therefore, important to study the protection principles relevant to transient stability [1].

### 2.11.1 Transmission Line Protection

There are a multitude of line protection schemes in installed in heavy industry and the utility. The three basic types of relaying schemes used for line protection are overcurrent protection, distance protection and pilot relaying.

Overcurrent relaying is the simplest and most widely used form of line protection. Overcurrent protection may be timed or instantaneous. It is important to choose the correct operating times for the relays in the system to ensure grading [1].

A distance relay is triggered by the ratio of voltage to current being less than a specified value. The impedance is an indication of distance along the line and a fault will result in lower impedance which may trigger the relay [2].

**Basic Types of Distance Protection Relays:**

1. Impedance Relay
2. Reactance Relay
3. Mho Relay
4. Modified Mho and Impedance Relays

### 2.11.2 Fault Clearing Times

The removal of a faulted element requires the relay to detect the fault condition and to initiate a trip to the appropriate circuit breaker. The fault clearing time is, therefore, made up of the relay time and the breaker-interrupting time. On HV systems relay times typically range from 15 ms to 30 ms while breaker-interrupting times typically range from 30 ms to 70 ms.

It is critical to minimise the fault clearing time in order to minimise power swings. A short fault clearing time reduces the kinetic energy transferred to the rotor during fault conditions.

### 2.11.3 Relaying Quantities during Power Swings

The performance of relays during electromechanical oscillations (power swings) can be illustrated using the two-machine system illustrated below in figure 2.31.

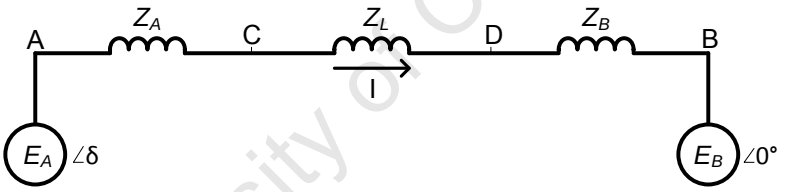


**Figure 2.31:** *Line Model for Relaying Quantities during Power Swings*

$$Z_T = Z_A + Z_L + Z_B \quad \ldots \quad (4.x)$$

The apparent impedance measured by the relay at C protecting line CD is given by equation 2.16, which is expanded to yield equation 2.17 with the voltage sources normalised.

$$Z_C = \frac{E_C}{I} = \frac{E_A - Z_A I}{I} \quad \ldots \quad (2.16)$$

$$Z_C = \left(\frac{Z_T}{2} - Z_A\right) - j\left(\frac{Z_T}{2}\cot\frac{\delta}{2}\right) \quad \ldots \quad (2.17)$$

During a swing the angle $\delta$ changes which results in a varying apparent impedance. Figure 2.32 below plots the locus of $Z_c$ on the complex plane as the power angle varies. The origin is assumed to be at the relay location. The impedance locus as seen at bus C is described in figure 2.32 and applies when the voltage sources are equal in magnitude.

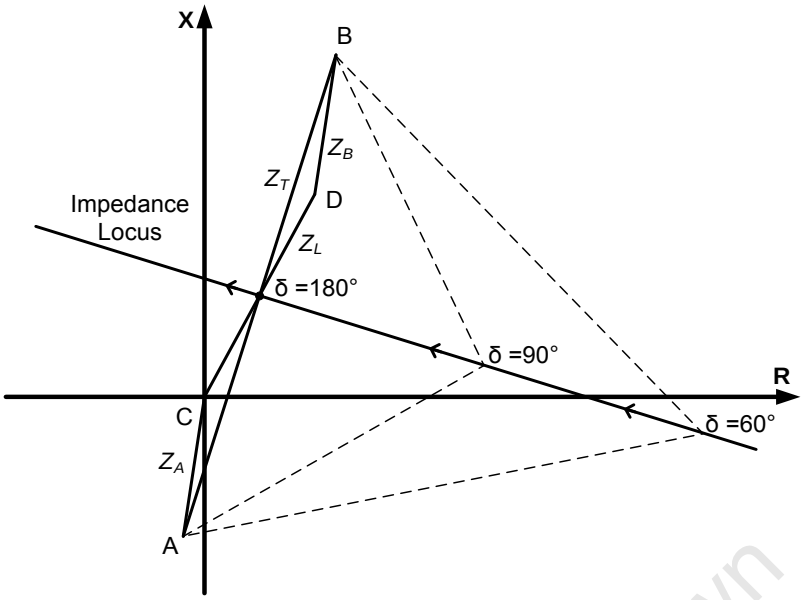


**Figure 2.32:** *Impedance Locus and Power Angle Relationship*

In the case that the voltage-sources are not equal the impedance locus will be non-linear as illustrated in figure 2.33. In the event that the power angle is 180° the electrical centre and impedance centre will coincide.

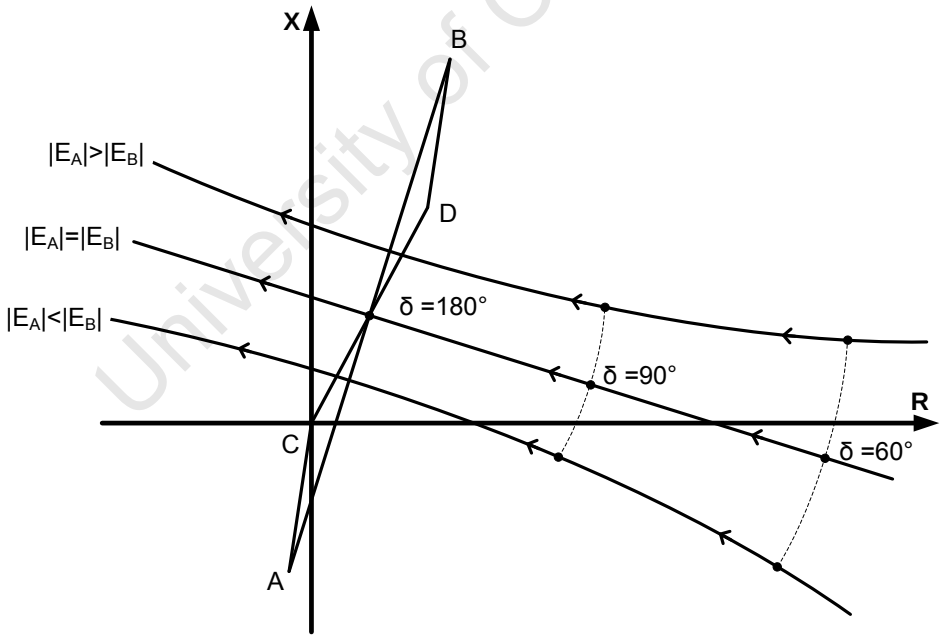


**Figure 2.33:** *Impedance Loci for Varying Source Voltages*

The electrical centre is not a fixed point and will vary during dynamic conditions when the dynamic reactances and voltage magnitudes vary.

If the power angle increases to 180° this means that the voltage sources are 180° out of phase. In the event that the voltage sources are representing synchronous machines; a pole has slipped when this situation occurs.

### 2.11.4 **Out-of-Step Relaying (OOS)**

The principle of OOS relaying is to, firstly, avoid tripping of any power system element during stable power swings and, secondly, to protect the system during unstable or OOS conditions. The functions of OOS relaying can, therefore, be separated in OOS tripping and OOS blocking [7].

It may be required to force separation at a point other than the natural separation point. This may be done to balance generation and load or to ensure continuity of critical supply. It follows that an unstable power swing may result in islanding of the power system [2].

The movement of apparent impedance during OOS conditions is slow compared to the movement during a line fault. A transient swing condition can be differentiated from a line fault using two vertical or circular relay characteristics. If the impedance locus remains between the two characteristics for longer than a specified time the protection function is initiated [2]. The fundamental discriminating factor between faults and power swings is the difference in rate of change of apparent impedance [7].

The principle of OOS protection is illustrated below using four vertical characteristics. In the case illustrated in figure 2.34 four vertical blinders are used. It is possible to use different blinder schemes such as concentric circular blinders or rectangular blinders [7].

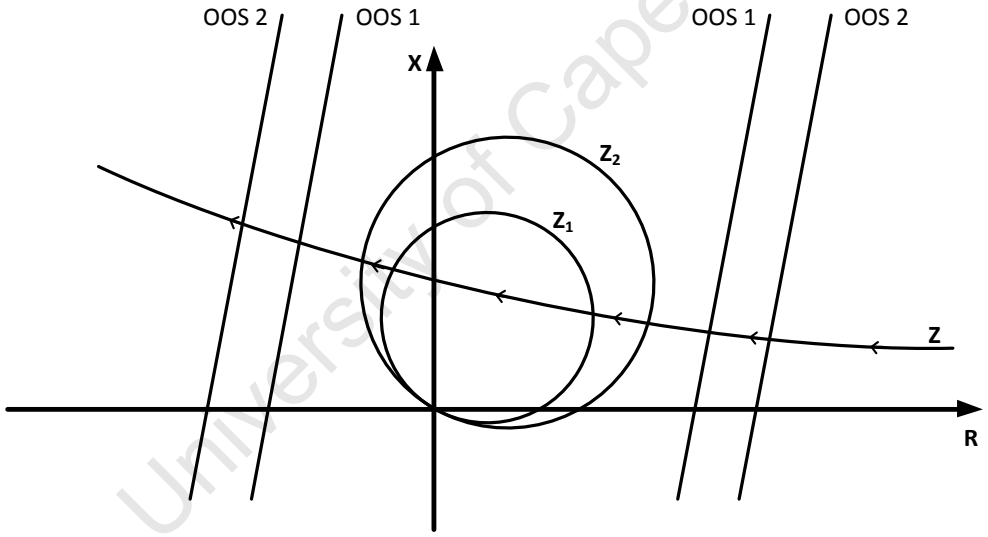


**Figure 2.34:** *Out-of-Step Relay Characteristic*

It is important to ensure that the OOS protection is enabled in the relay settings to operate before the line protection operates [2].

An important consideration when designing an OOS scheme is the loss-of-synchronism characteristic of the machine under investigation. It is also necessary to identify critical machines and groups of critical machines.

Consideration of these factors and a transient stability study will enable optimal separation points to be determined [7].

### 2.11.5 Generator Out-of-Step Protection

In modern power systems the trend is for the generator and step-up transformer impedance to increase and for the system impedance to decrease. This results in the electrical centre moving into the step-up transformer or the generator itself [15].

If the electrical centre is located between the HV terminals of the step-up transformer and the generator winding then separate generate OOS protection should be used [15].

During OOS conditions there are large variations in current and voltage with the frequency being a function of the rate of pole-slipping [7].

The resulting high peak currents and off-frequency operation may cause pulsating torques, mechanical resonances and mechanical stress on the generator windings [15].

In order to avoid the adverse effects that arise from generator OOS conditions it is necessary for a protective relay to initiate separation of the generator from the system. The generator auxiliaries may remain in service until the generator is resynchronised and returned to service [7].

The conventional method of detecting an OOS condition is to monitor the apparent impedance from the generator terminals which will change due to the varying voltages and power angle. A graphical approach is then used to determine the optimal point of the impedance locus at which the generator should be tripped [15].

The generator apparent impedance locus loops in an anticlockwise direction forming a full ellipse for one swing cycle. The loop is completed 300 ms after the fault is cleared and the impedance is practically the same as the moment of fault clearance.

The fact that the impedance returns to the value it had at the moment of fault clearance is intuitive when the power angle is referred to. The symmetry of the swing characteristic means that the power angle is periodic every 300 ms (for the first cycle at least).

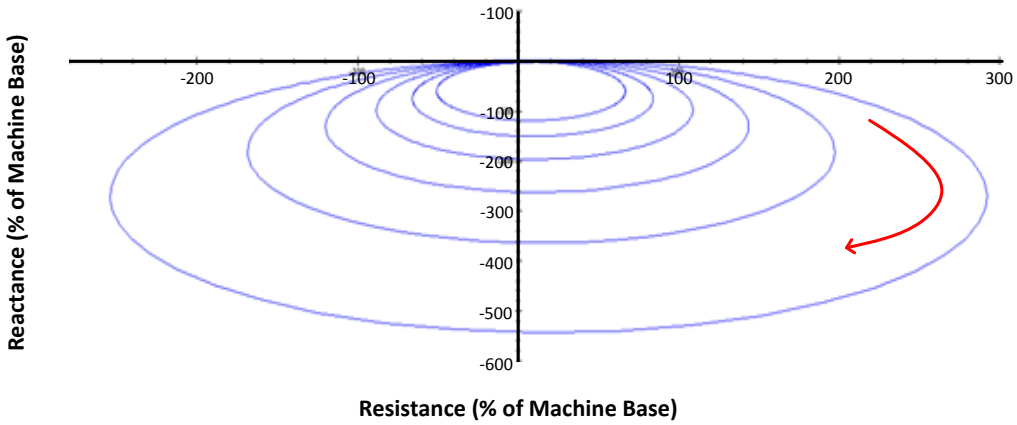


**Figure 2.35:** *Impedance Characteristic Trends for a Symmetrical Fault*

### 2.11.6 **Loss-of-Excitation Protection**

A loss-of-excitation (LOE) condition may arise from a number of field winding disturbances which may effectively leave the field winding short-circuited or open-circuited. In the event of LOE the synchronous machine will function as an induction generator running above synchronous speed. The excitation is drawn in the form of reactive power from the power system. Severe voltage dips may result from this condition [2].

Prolonged operation of the synchronous generator as an induction generator will result in thermal overload and eventually damage to windings and insulation. Widespread voltage instability may also result from this condition. A quick-acting relay is required to trip the main and field breakers in the event of a LOE condition [3].

The first types of relay used for LOE protection detected undercurrent in the field winding. Modern types use the principle of a directional distance relay connected at the generator terminals [2].

The most widely accepted tripping characteristic for generator LOE protection is the offset Mho relay. This characteristic is able to detect a variety of excitation failures and is able to distinguish these failures from other system faults. This type of characteristic was first used in 1949 for LOE protection [16].

The machine response following a LOE condition depends on the initial loading. A LOE characteristic is illustrated below in figure 2.36. The curve begins at the initial power angle and end at 180° before a pole is slipped.

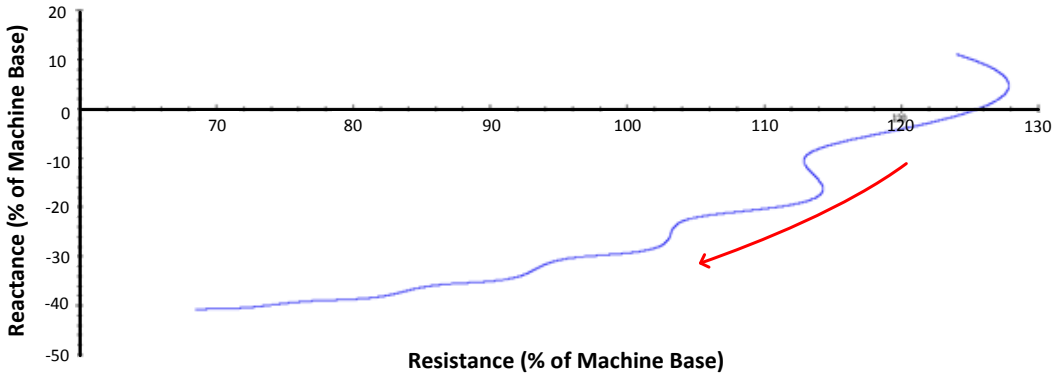


**Figure 2.36:** *LOE Characteristic*

The locus of the end-points of the LOE characteristics for different loading conditions must be enclosed by the relay characteristic. A generator with a high initial load will reach the pole-slipping limit quicker than a generator with a low initial load. This scheme will avoid pole-slipping which may have far-reaching adverse effects.

## 2.12 Frequency Stability

### 2.12.1 The Problem of Frequency Stability

The response of a synchronous machine to a momentary imbalance in the power generated and consumed in a power system is covered by transient stability. The problem of transient stability is primarily the concern of rotor angle and loss-of-synchronism [3].

If a disturbance results in a sustained power imbalance it is necessary to consider the system response in a longer time-frame. Provided that transient stability is maintained it is necessary to consider the problem of frequency stability [3].

An understanding of AGC is necessary for an analysis of the frequency response of a power system to a prolonged power imbalance.

This section on medium-term to long-term stability focuses on the *in extremis* state. A more detailed illustration of how and why the system moves between states is shown below.

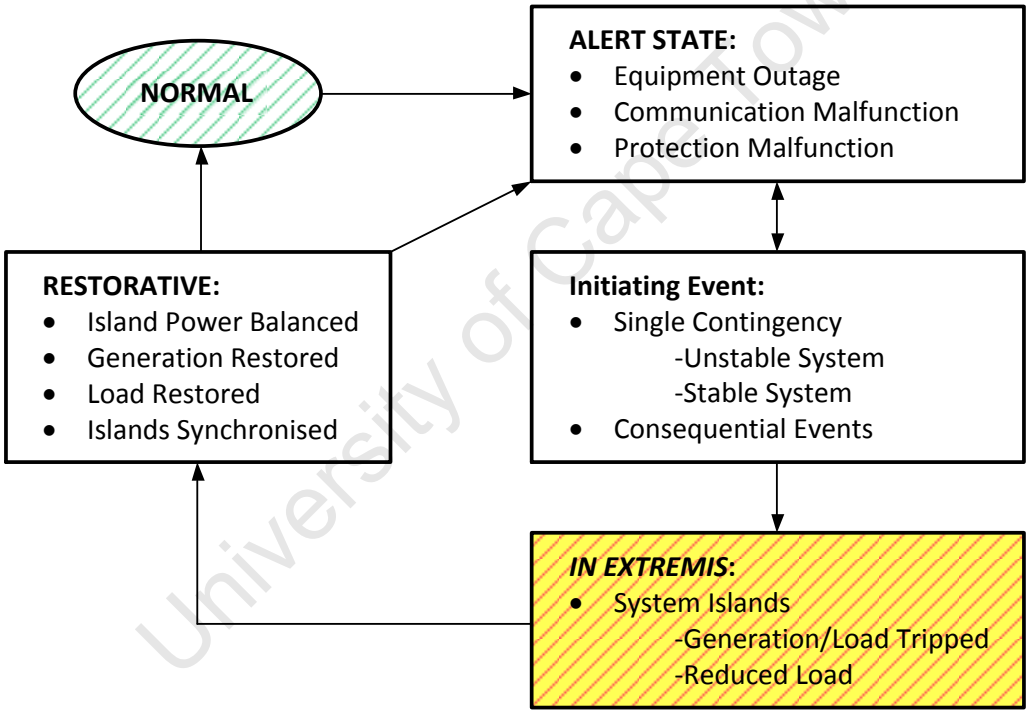


**Figure 2.37:** *Power System State Transition*

The primary control action is the system response due to the load and generation characteristics. The secondary control action is due to the turbine-governor system and any supplementary control systems connected to the governor. Tertiary control, which is typically the slowest acting, is set by the power system controller and is generally based on optimal power flow considerations [3].

The combined effect of these three control modes is to regulate the system frequency to within defined limits around nominal frequency.

### 2.12.2 System Frequency Response to Power Imbalance

Having described the operation of AGC it is possible to examine the response of a power system to an imbalance caused by a disturbance. The operation of AGC is typically limited to within 0.2 Hz of the nominal frequency. Operation outside this range will necessitate local controls and protection devices to operate [3].

The response of the power system can be divided into four categories based on the time duration of the stage [3].

#### *2.12.2.1 Stage 1: Rotor Swings in the Generators*

The first response of the system is evident in the form of rotor power angle swings. A sudden imbalance in power will cause large oscillations in the synchronous machines electrically close to the disturbance [3].

Simulation of rotor swings requires the generator transient model to be used. The generator model used in this work uses the machine data at the time of manufacture to generate the transient model [3].

The study of the rotor swings subsequent to a disturbance is the domain of transient stability analysis. The fundamental problem is whether, or not, the synchronous machines being considered will maintain transient stability [3].

The frequency drop, which is the domain of the next stage, is relevant if transient stability and a power imbalance are maintained [3].

#### *2.12.2.2 Stage 2: Frequency Drop*

The first stage of the system response will display oscillations of decreasing magnitude, provided stability is maintained. The persistence of the power imbalance will result in a decaying system frequency. The rate of decay of individual frequencies will coincide with the system frequency rate of decay after several decaying rotor swings [3].

Each generator will contribute to the power in proportion to its inertia and independent of its electrical proximity to the disturbance [3].

#### *2.12.2.3 Stage 3: Primary Control Actions*

The third stage of the frequency response depends on the generation and load characteristic.

Primary control action is defined as the response of the turbine governing unit in this context. In the event that there is insufficient generation the main steam valves will be opened by a specified amount in an attempt to eliminate the imbalance [3].

The system is initially operating at point A which is the intersection of the initial load and generation characteristics. Due to a disturbance the generation characteristic is shifted to the left, from $P_{G0}$, by an amount of $\Delta P_0$, to $P_{G1}$. At the moment of the loss of generation, generation moves to point B, while the load power remains at point A. Due to the imbalance between generated and consumed power the frequency of the system will begin to decline. As frequency drops the generated power increases while load power decreases until the first equilibrium, which is a local minimum for the frequency trajectory [3].

Due to time delays and inertia there is overshoot and the power trajectory lies below the static generation characteristic. The system will settle at the intersection of the static characteristics after several oscillations [3].

The system will reach a new equilibrium point at a lower frequency and power as a result of the primary control actions. It is the response of secondary control actions to restore the frequency and power to the nominal set-points [3].

The implication of insufficient spinning reserve may be that the system enters a state of frequency collapse. This necessitates the implementation of Under Frequency Load Shedding (UFLS) schemes which reject load at defined frequencies on the way down. This is done in an attempt to eliminate the power imbalance [3].

### *2.12.2.4 Stage 4: Secondary Control Actions*

The total control action resulting in system frequency restoration is illustrated below in figure 2.38.

The basic action of AGC is to shift the generation characteristic such that the new equilibrium point will coincide with the nominal system frequency. The load power will follow the generated power to the new equilibrium condition [3].

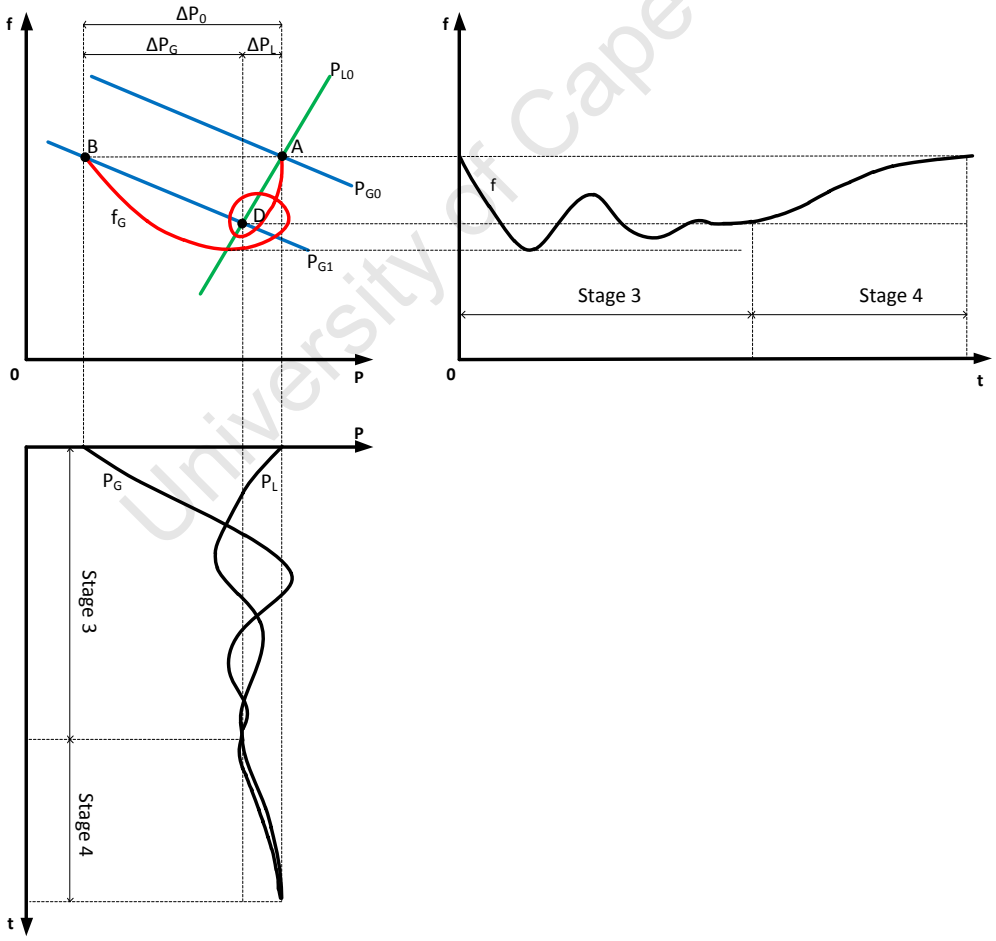


**Figure 2.38:** *Illustration of Secondary Control Actions (AGC)*

### 2.12.3 **Controlled Separation**

An islanded system is electrically isolated from the rest of the power system through a process known as controlled separation. This is typically done to avoid damage to critical equipment or to maintain critical equipment in operation following certain severe system disturbances. Controlled separation can prevent a severe disturbance in a distinct part of the power system from propagating throughout the system and causing extensive tripping [2].

The types of island that may exist are typically small or large islands. A small island comprises only a generator and its auxiliaries (block supply). A large island comprises one or more generators and load. The islanded conditions that may exist are an under-generated island, an over-generated-island and a balanced island. [2].

If the power imbalance is less than the spinning reserve coefficient then the system frequency will return to nominal value due to the actions of primary and secondary control as shown in figure 2.39 [3].

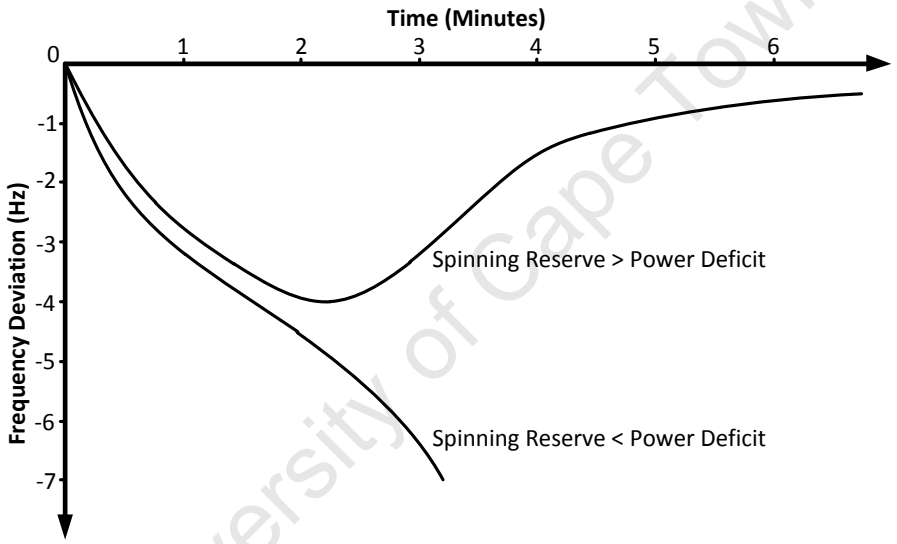


**Figure 2.39:** *Frequency Variation for Different Spinning Reserve Coefficients*

The generating unit auxiliaries are significantly affected by the island voltage and frequency conditions. The auxiliaries are typically driven by induction motors which suffer performance degradation enduring undervoltage and underfrequency conditions. Protection typically exists to trip the generating unit in the event that defined underfrequency and/or undervoltage limits are exceeded [2].

Stability in terms of frequency during an islanded condition is defined below:

"*The long-term frequency stability is defined as the ability of each island to reach an acceptable state of equilibrium, with minimum disruption to services [2].*"

Once the acceptable equilibrium point has been reached it is possible to attempt a restoration to return the system to pre-disturbance configuration. This restoration procedure involves balancing the power in each island, synchronising each island to the system frequency, and closing the appropriate ties between the islands. [2].

### 2.12.4 Underfrequency Load Shedding

Electrical power systems are typically designed such that generation and load are balanced and that the transmission capacity is matched. The normal operating conditions include certain contingencies such as N-1 supply contingency [12].

Severe system disturbances can result in cascading outages and isolation of electrical areas. The resulting electrical islands may experience an active power imbalance, and may experience frequency decline if generation is insufficient. Underfrequency Load Shedding (UFLS) schemes are designed to reduce the load to a level that can be safely supplied by the available generators [2].

The two main concerns of operating a generating unit below nominal frequency are vibratory stresses and reduced operating capacity of auxiliaries [2].

It is important to distinguish between two forms of overloading that may occur. In the event of a deficiency of active power the frequency will begin to decline due to the mismatch between prime-mover torque and the load torque. In the event of a deficiency of reactive power voltage drops may become evident [12].

#### *2.12.4.1 System Frequency Response*

For a simplified analysis of the transient response to a change in load it is feasible to assume constant generation constant load and no oscillations between generators [12].

The rotating mass possesses rotational kinetic energy which is related to speed by equation 2.18 where *J* is the moment of inertia in $kg.m^2$. In the event of a torque mismatch the rotor will either accelerate or decelerate and consequently gain or lose rotational kinetic energy [12].

$$E_k = \frac{1}{2} J\omega^2 \quad \dots \quad (2.18)$$

The inertial constant H of a generator is defined in equation 2.19 as the ratio of the rotor kinetic energy to the generator VA rating.

$$H = \frac{\frac{1}{2} J\omega^2}{VA} \quad \dots \quad (2.19)$$

It may be required to use an averaging method to determine the inertial constant for an N-machine system. Equation 2.20 describes the averaging method to be used which includes the load inertial constant and the generators' inertial constants [12].

$$H_{net} = \frac{H_1 \times MVA_1 + H_2 \times MVA_2 + H_N \times MVA_N}{MVA_1 + MVA_2 + \cdots + MVA_N} \quad \dots \quad (2.20)$$

An equation for relating frequency to time can be derived to yield equation 2.21. The frequency at any point in time[3] can be calculated provided the accelerating power is known. [12].

$$f(t) = f_0 \left[1 + \left(\frac{P_{a,pu}}{2H}\right) t\right] \quad \dots \quad (2.21)$$

[3] This process can be iterative which will allow the accelerating power and the system inertial constant to be recalculated following each step.

### *2.12.4.2 Overload Detection*

The frequency decline that is under investigation is caused by overload conditions. The primary means of detecting overload are through frequency monitoring and voltage monitoring. Alternatives that exist are SCADA monitoring and current/power monitoring [12].

Frequency monitoring is a fast method of detecting an overload condition. It only provides indication, however, that the frequency has passed a threshold and is not pre-emptive in this regard.

A simplified procedure for determining under-frequency settings is presented below:

- Select the minimum allowable frequency.
- Select worst case feasible power imbalance possible.
- Determine number of load shed frequency levels.
- Distribute load shedding over the frequency range above allowable minimum and below first minimum level.

A three-bus system is simulated using MATLAB for illustrative purposes and shown in figure 2.40. The initial power imbalance was set at 10 % generation deficiency. The frequency begins to decline at a rate of -1 Hz.s$^{-1}$. At two seconds the frequency has declined to 48 Hz and 5 % of the load is shed. The system is still overloaded but the frequency declines at a slower rate of - 0.4 Hz/s. After four seconds the frequency has reached 47.25 Hz and a further 8 % of the load is shed. The system no longer has a generation deficit and the frequency begins to improve.

This simulation neglects any governor or exciter actions that may take place in a realistic system in order to counteract a generation deficiency[4].

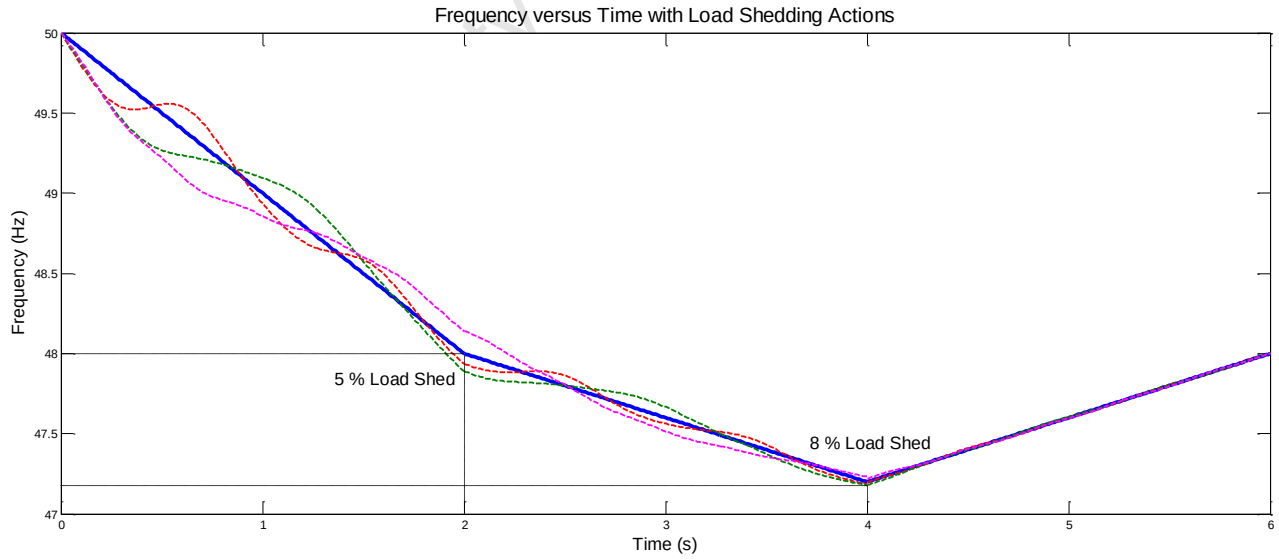


**Figure 2.40:** *Load Shedding Simulation using MATLAB*

[4] This simulation is not based on a transient stability analysis but rather on equations designed to illustrate the principles of load shedding.

# 3 Study Methodology

## 3.1 Stability Analysis Methodology

There are specific circumstances that warrant a stability study being conducted on a power system. These circumstances include any infrastructure changes or setting changes that may influence the voltage, frequency or transient stability of the power system. In this investigation the stability types analysed are transient stability and frequency stability.

***Circumstances warranting a stability study include:***

1. Addition of synchronous machines to the network

   *These may be additional synchronous generators or additional large synchronous motors driving heavy equipment.*

2. Changes in protection philosophy

   *Any changes in protection philosophy that may affect the fault clearing time may have a direct impact on the CCT of a synchronous machine.*

3. Transfer scheme changes

   *The stability associated with a bus fast transfer scheme with connected synchronous machines is highly sensitive to changes in transfer time.*

4. Fault-level changes

   *Fault-level changes may arise due to a number of factors including the addition of inductive (motor) load, connection of additional incomers or a change in the bus-tie configuration.*

5. Changes to power sources

   *A change of power source may effectively increase or decrease the source impedance which will affect the system fault-level.*

6. Changes to network impedance

   *A change to the network impedance may either increase or decrease the through-fault which may affect the fault-level at critical areas.*

7. Changes to synchronous machine normal loading

   *The initial loading condition of a synchronous machine is known to influence the system response to a disturbance.*

***The specific circumstances in this case warranting a study include:***

5. Addition of new generators and large synchronous motors
6. Addition of new GIS switch-plant (2H4-SP-02) and interconnection with 2H4-SP-01 (existing)
7. Addition of new Eskom incoming lines
8. New Eskom SOL B MTS

***Outputs of Stability Studies***:

1. Dynamic response plots:
    a. Rotor angle plots
    b. Electrical power plots
    c. Mechanical power plots
    d. Machine and bus voltage
    e. Machine speed and frequency
    f. Bus frequency
2. CCTs
3. Critical clearing angles
4. Load-shedding response to disturbances
5. Islanding response to disturbances.

***Methodology to be applied:***

1. Identify all synchronous machines (motors and generators)
2. Collect synchronous machine data including:
    a. Steady-state parameters
    b. Transient parameters
    c. Sub-transient parameters
    d. Unit inertia (rotor + coupling + driven mass)
3. Identify control modules applied to unit
    a. AVR
    b. Speed governor (droop characteristic)
    c. Control mode (Voltage, PF, VAr)
4. Identify supplementary control modules
    a. Excitation limiter
    b. Stator current limiter
    c. V/Hz limiter (flux limiter)
    d. Terminal voltage limiter
    e. PSS
5. Identify all large induction motors (> 1 MW)
    a. Collect induction motor data
6. Collect source data ($MVA_{SC}$, X/R and V)
7. Select which buses are to be faulted
8. Identify the swing bus (the swing bus may be a generator)
9. Perform load study and check against reference studies
10. Perform fault-level study and check against reference studies
11. Perform stability study with no disturbance to ensure numerical stability
    a. ETAP requires at least one action so a dummy breaker is opened
12. Generate disturbance sequence
13. Obtain output plots as listed previously
    a. Vary fault type and location
    b. Vary clearing times

***Important Points to Note:***

1. Transient stability is determined by considering mechanical and electromechanical machine characteristics and the impedance of the connected network (The response of the control systems and supplementary control systems are important for dynamic stability considerations, but have limited impact on transient stability)
2. For stability to be maintained there must be no divergence between any machine and the utility load angle. Provided the load angle diverges and converges within acceptable limits stability exists.
3. According to the power flow equation significant impedance needs to exist between generators for instability to occur. Parallel generators, therefore, behave as a composite machine.
4. Forcing the excitation to a higher than nominal level increases the synchronising torque and increases the reactive power output, provided the terminal voltage is constant. Forced excitation may improve transient stability. In a small-islanded system with no bus voltage control increasing the excitation will increase the terminal voltage.

The fault signature voltage shown below in figure 3.1 is typical of a symmetrical fault at the machine terminals. The fault is characterised by an initiating and clearing time followed by a transient recovery period.

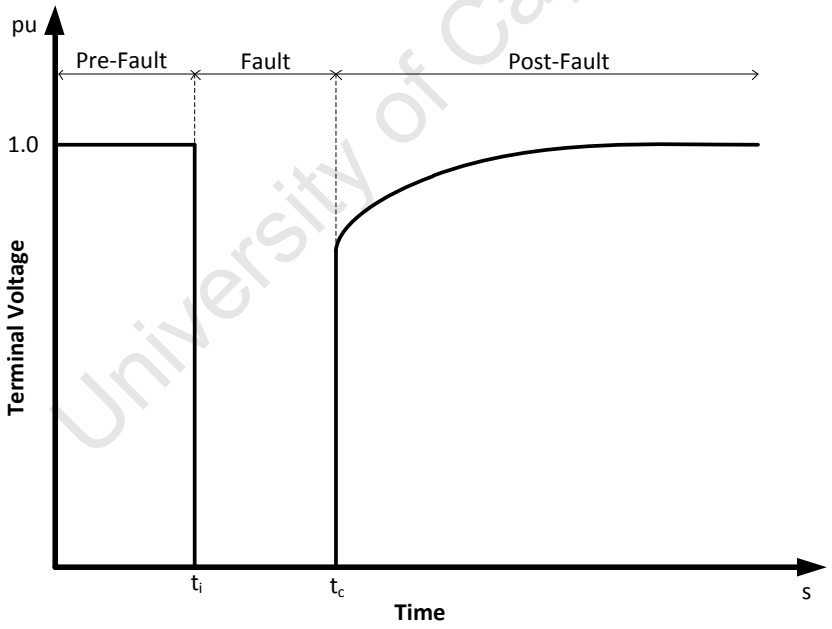


**Figure 3.1:** *Typical Symmetrical Fault Signature*

The voltage during a symmetrical fault is practically zero which means that the power flow is blocked during this condition. The symmetrical fault is the simplest and most severe type of fault that can occur for a single element. Other fault sequences will be a combination of the above signatures in a defined sequence. It is important to note that it is only during a bolted symmetrical fault that power transfer is completely blocked.

# 4 General Case Studies

## 4.1 Single Generator Response to Disturbance

This section investigates the response of a single synchronous generator (GEN 4 E), which was extracted from the overall system model, to defined disturbances. The remaining ten ST-driven generators display similar responses to those documented in this section.

The machine ratings are defined in table 4.1 below. These parameters are specific to GEN 4 E, but the 9 remaining ST-driven generators in the Sasol Synfuels network are of the same type as GEN 4 E.

| Parameter | Value |
|---|---|
| **Active Power** | 60 MW |
| **Apparent Power** | 75 MVA |
| **Rated Voltage** | 11.2 kV |
| **Power Factor** | 0.8 |
| **Efficiency** | 98% |
| **Poles** | 2 |
| **Full Load Current** | 3866 A |
| **Speed** | 3000 rpm |

**Table 4.1:** *Generator Parameters*

The different synchronous generator modes of operation are swing, voltage control, reactive power control and PF control. The generator in this case study runs in voltage control mode which means that the reactive power output will be adjusted to control the voltage. This mode requires the terminal voltage magnitude, operating real power and minimum and maximum reactive power limits to be specified.

A voltage controlled generator is base-loaded with the AVR controlling the field excitation. If either reactive power limit is reached the generator will effectively be operating with fixed active power and reactive power (reactive power control mode).

### 4.1.1 50 ms Symmetrical Fault

The determination of the CCT is implemented using a binary search method. The starting point is fault duration of 50 ms, and this case study investigates the response of the generator to a 50 ms symmetrical bolted fault at the generator terminals.

Specific machine parameters, including machine speed and power angle, at the initiation and clearing times of the fault are tabulated below in table 4.2.

| | Time (ms) | Speed (rpm) | Power Angle (°) | Excitation Voltage (pu) | Bus Frequency (Hz) |
|---|---|---|---|---|---|
| **Fault Initiated** | 500 | 3000.0 | 37.2 | 1.000 | 50.00 |
| **Fault Cleared** | 551 | 3015.7 | 39.6 | 1.451 | 50.22 |

**Table 4.2:** *50 ms Pre-Fault and Post-Fault Machine Parameters*

It can be noted that the interval described in table 4.2 only represents a small time-period of the total system response to the disturbance. The response as a whole is examined in this section.

The rotor power angle is illustrated below in figure 4.1. The power angle initially begins to increase, at a predictable rate, at the moment of fault inception. The power angle continues to increase subsequent to the point of fault clearance. The power angle reaches a peak value, after which the peaks follow a decaying envelope until a steady-state is attained. In this case the post-fault and pre-fault steady-states are equivalent.

The oscillations and the decaying peak envelope are clearly visible as well as the resulting stable condition. The first swing magnitude is typically the major concern in transient stability studies.

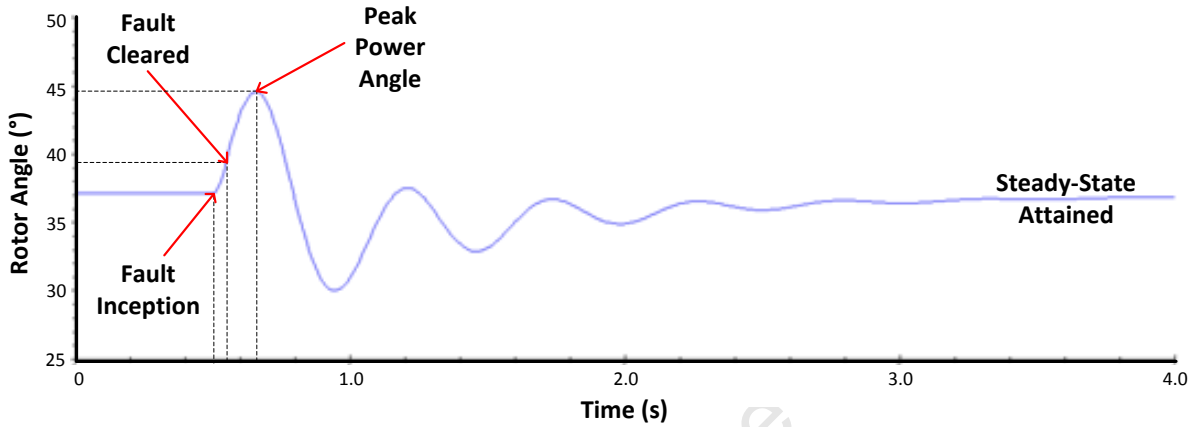


**Figure 4.1:** *Power Angle Response to 50 ms Symmetrical Fault*

The generator exciter response is illustrated below in figure 4.2. The response of the excitation system is to force the excitation voltage to its ceiling during the fault condition. This, in combination with the increased generator speed at the moment of clearing, results in a high post-fault power.

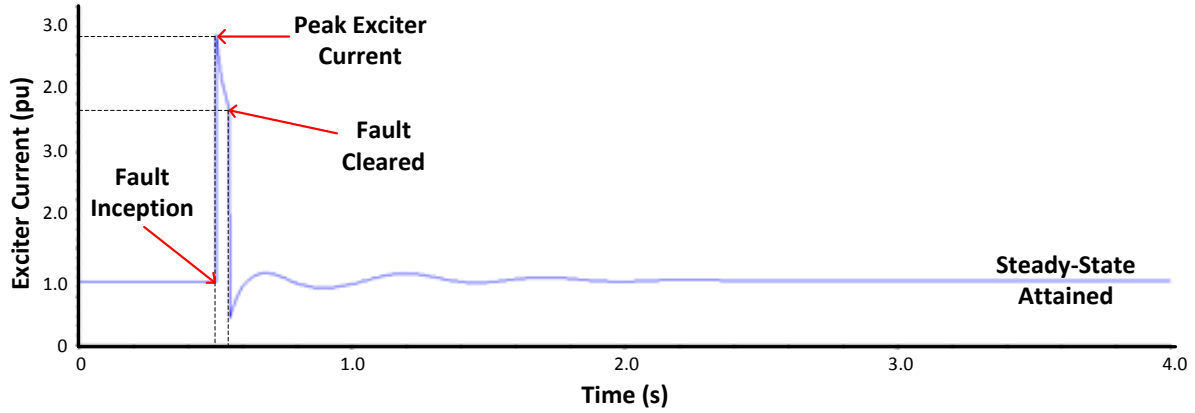


**Figure 4.2:** *Exciter Current Response to 50 ms Symmetrical Fault*

The time delay associated with the excitation system response is visible below in figure 4.3. It is preferable that the ceiling voltage is reached before the fault is cleared to ensure that the post-fault decelerating power is as large as possible. There is a thermal limit which imposes a limit on the maximum time that the excitation voltage can be forced to its ceiling value.

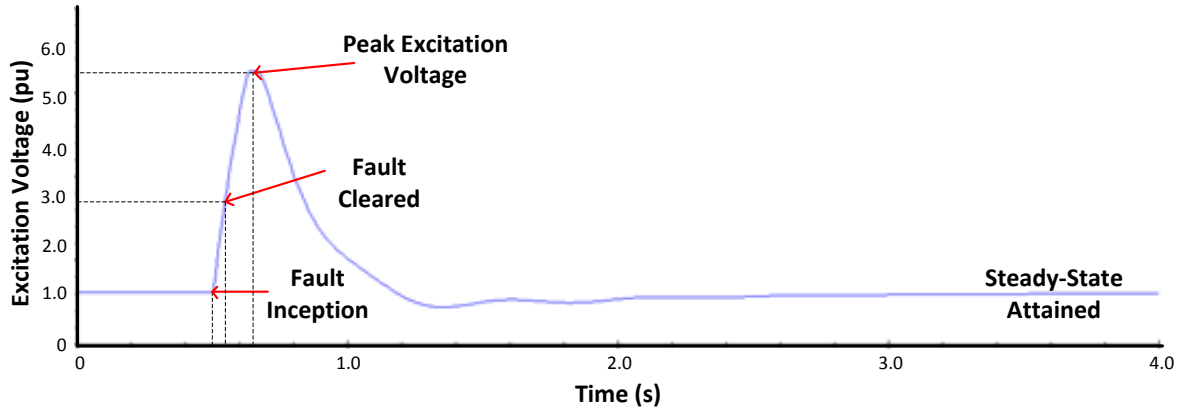


**Figure 4.3:** *Exciter Voltage Response to 50 ms Symmetrical Fault*

The electrical power naturally decreases to zero during the bolted symmetrical fault which results in a net accelerating torque. A symmetrical short-circuit has the effect of pulling the synchronous generator terminal voltage to zero as is shown in figure 4.6.

The zero-voltage effectively blocks power transfer during the fault period, which is expected from the power transfer equation, since the power transfer is proportional to the product of the terminal voltage and system voltage.

When the fault is cleared the generator electrical power will oscillate until steady-state is reached, provided stability is maintained. The generator power response is shown in figure 4.4.

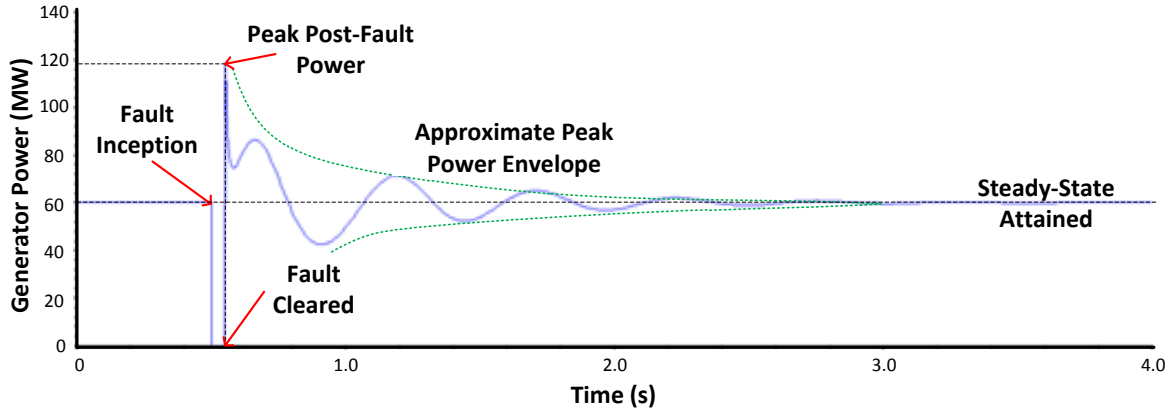


**Figure 4.4:** *Electrical Power Response to 50 ms Symmetrical Fault*

The generating unit speed response is illustrated in figure 4.5. The generator speed will initially increase steadily until the fault is cleared. This is due to the imbalance between mechanical input power and electrical output power during the fault which causes the synchronous generator to accelerate.

Once the fault is cleared the speed waveform displays an oscillatory characteristic of decaying magnitude until a steady-state is reached. It is desirable to return to the steady state as soon as possible, since the machine speed is directly linked to system frequency. System frequency is critical for quality of supply, and significant deviations from nominal frequency may cause tripping of plant [14].

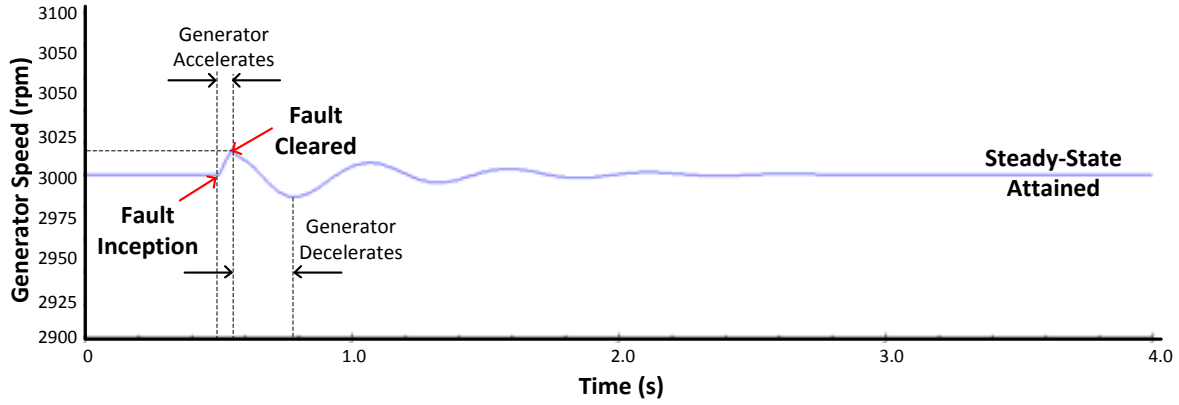


**Figure 4.5:** *Generator Speed Response to 50 ms Symmetrical Fault*

The generator bus voltage is illustrated below in figure 4.6. The bus volts/hertz waveform returns to the nominal value after a relatively short time delay. The generator bus voltage drops to zero as would be expected for a symmetrical bolted fault.

The volts/hertz ratio is indicative of the fluxing of the synchronous machine magnetic circuit. The profile displayed in figure 4.6 corresponds to the typical profile described in figure 3.1.

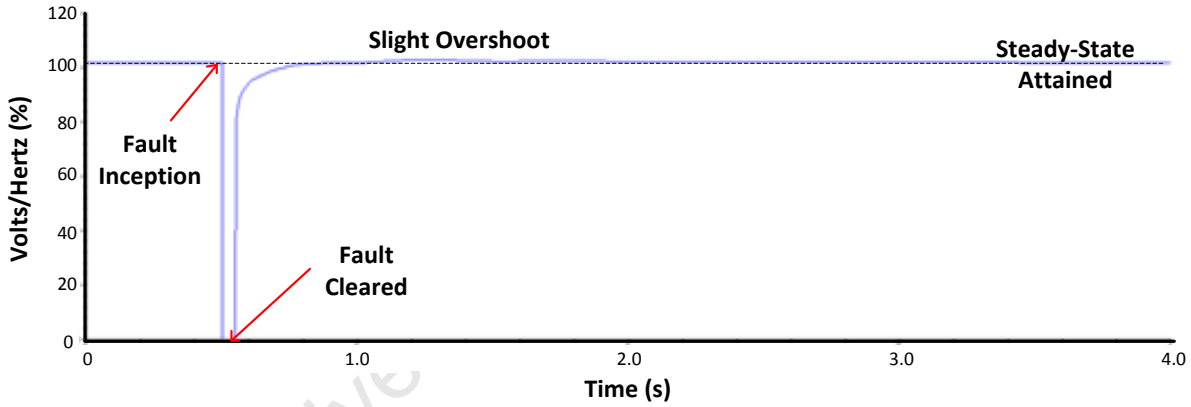


**Figure 4.6:** *Generator Bus Volts/Hertz Response to 50 ms Fault*

The bus volts/hertz waveform is illustrated below in figure 4.7 for the 132 kV voltage level. The voltage impact on the transmission level is clearly visible. The bus voltage drops to below 95% for the fault duration.

This voltage dip is too short for any compensating action to have taken place. In the event that the system voltage dips for a prolonged period the constant kVA loads will draw higher than nominal current. This can have thermal implications and may also affect equipment life.

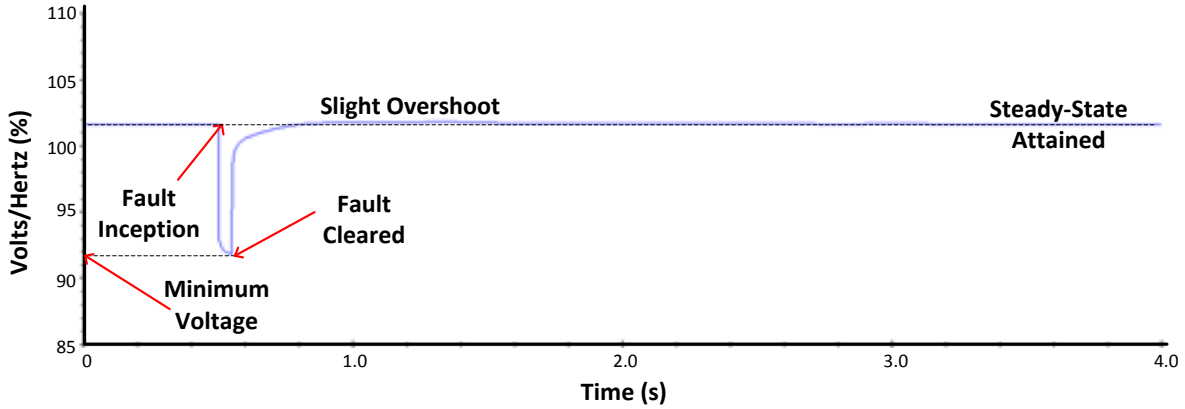


**Figure 4.7:** *Transmission Bus Volts/Hertz Response to 50 ms Fault*

The common characteristic of the waveforms in this section (except for volts/hertz) is that the system displays a large initial response characteristic followed by decaying oscillations. Ultimately a steady-state is reached for all cases which match the pre-fault equilibrium set.

It can be concluded that the generator displays transient stability when subjected to a bolted symmetrical fault at the generator terminals for 50 ms.

It can be concluded, therefore, that the CCT is longer than 50 ms in this case and that the peak power angle of 45° will not result in an unstable condition. A more useful measure is that the critical angle, at which the fault is cleared, is greater than 39.6°.

### 4.1.2 300 ms Symmetrical Fault

Specific machine parameters, for a 300 ms fault, at the initiation and clearing of the fault are tabulated below in table 4.3.

| | Time (ms) | Speed (rpm) | Power Angle (°) | Excitation Voltage (pu) | Bus Frequency (Hz) |
|---|---|---|---|---|---|
| **Fault Initiated** | 500 | 3000 | 37.2 | 1.000 | 50 |
| **Fault Cleared** | 800 | 3100.8 | 128.6 | 2.004 | 51.36 |

**Table 4.3:** *50 ms Pre-Fault and Post-Fault Machine Parameters*

The absolute power angle is visible below in figure 4.8. It is clear that synchronism has been lost and the power angle increases in an unrestrained manner.

The representation of absolute power angle has limited use. The resolution is very low and the area of interest, which is around the moment of loss-of-synchronism, is difficult to examine. This representation also creates the impression that the initial power angle is 0°, and not the actual 37.2° as shown in table 4.3.

It is important to note that in a real power system the protection would never allow a situation such as the one described in this section to persist.

The intention is to pursue the simulation beyond the point of loss-of-synchronism to analyse the longer-term response and potentially damaging conditions.

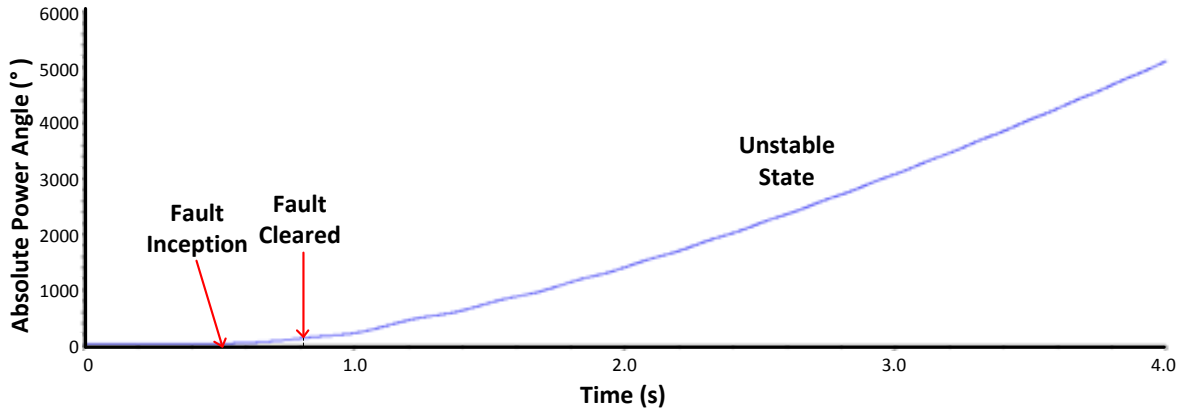


**Figure 4.8:** *Absolute Power Angle Response to 300 ms Fault*

The generator exciter current waveform is visible below in figure 4.9. The characteristic peak is visible followed by oscillations of increasing frequency.

The currents are induced due to the changing flux caused by pole-slipping. The most extreme deviation of excitation current is the negative excitation current shown below.

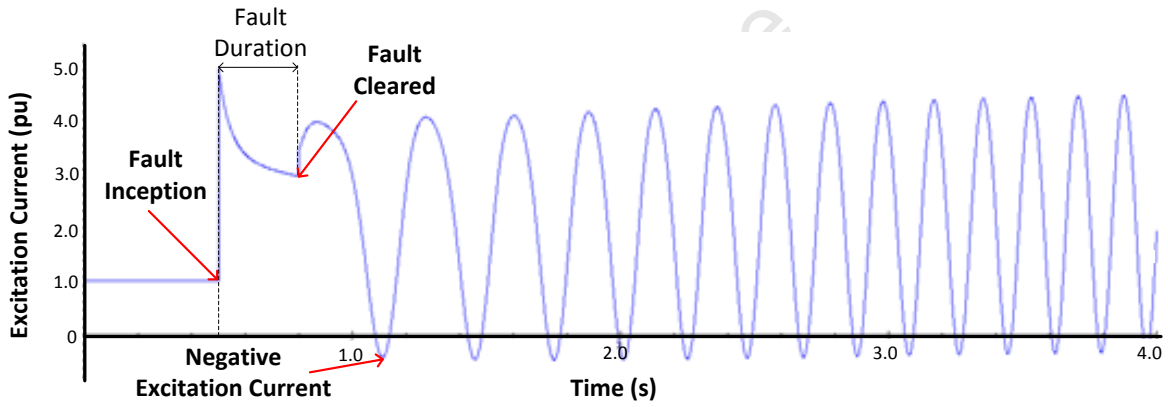


**Figure 4.9:** *Exciter Current Response to 300 ms Fault*

The excitation voltage is visible below in figure 4.10. The voltage is ramped up, with the inherent time delay of the voltage regulator, and then maintained at ceiling voltage.

The ceiling voltage would have an associated time limit programmed into the protection settings which would decrease the excitation voltage after a defined time. This is done to avoid damage to the generator due to thermal overload of the rotor circuit.

The exciter and AVR have an inherent limit on the ramp rate which is represented below as the ratio of the rate of change of excitation voltage to the time taken for the increase.

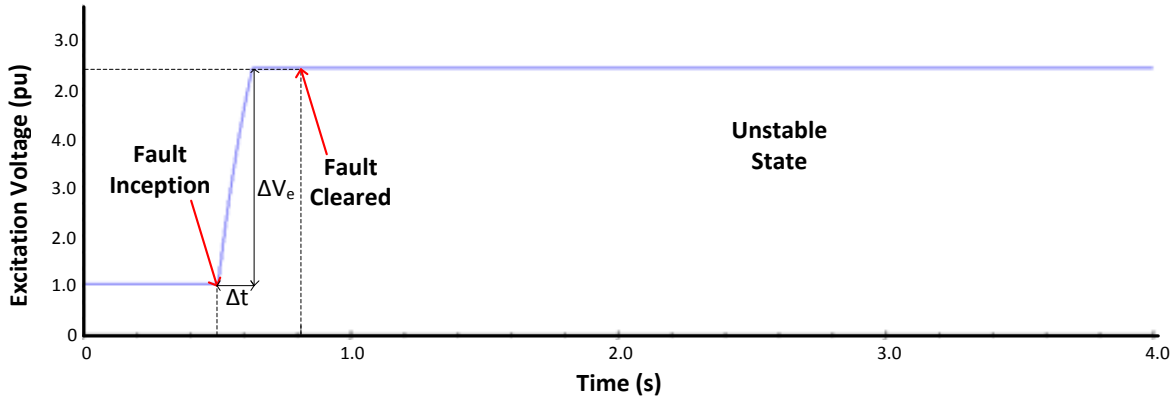


**Figure 4.10:** *Exciter Voltage Response to 300 ms Fault*

The reactive power waveform is illustrated below in figure 4.11. The reactive power is related to the excitation current and the correlations between the waveforms are visible. The average post-fault reactive power is negative compared to the positive pre-fault reactive power. This indicates that the pre-fault generator is a reactive power source which is to be expected; while the post-fault generator is a reactive power sink.

The kink in the reactive power waveform corresponds to the negative excursion of the generator excitation current illustrated in figure 4.9.

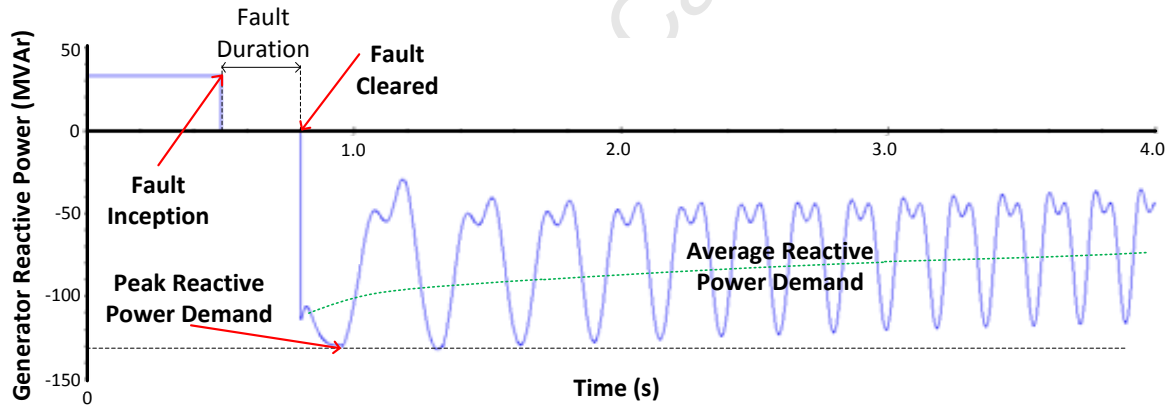


**Figure 4.11:** *Generator Reactive Power Waveform*

The active power waveform is visible below in figure 4.12. The characteristic dip in power during the fault as well as the high post-fault power is evident. The waveform then displays oscillations of increasing frequency and very high magnitude.

These oscillations far exceed the rating of the unit and would result in extreme thermal overload, and possible mechanical damage, of the generator and auxiliary equipment if allowed to persist.

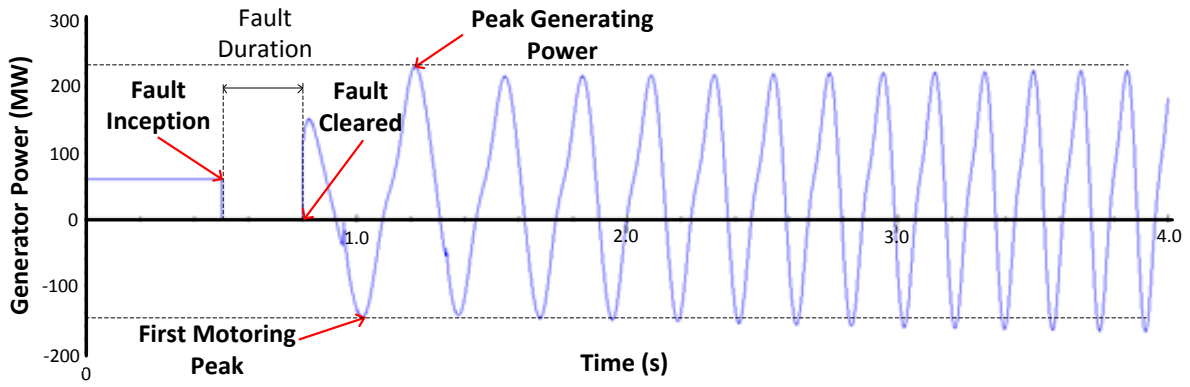


**Figure 4.12:** *Generator Active Power Waveform*

The generator speed, which is related to frequency, is illustrated below in figure 4.13. The waveform displays a steady increase during the fault, followed by an uncontrolled increasing waveform with an oscillatory characteristic.

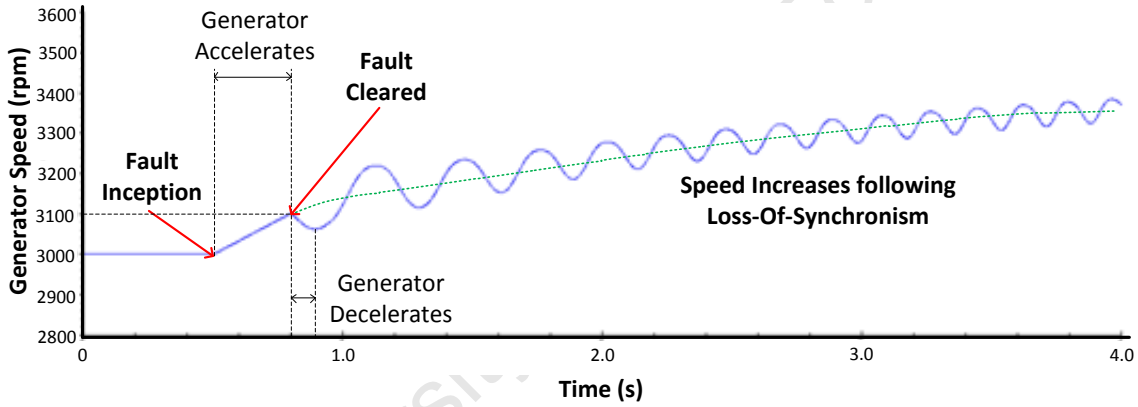


**Figure 4.13:** *Generating Unit Speed Waveform*

The relative power angle waveform is visible in figure 4.14. The sharp discontinuities represent the slipping of a pole. The point of loss of transient stability occurs before the pole is actually slipped. The critical point from which the system cannot recover is known as the CCT and is related to the critical angle.

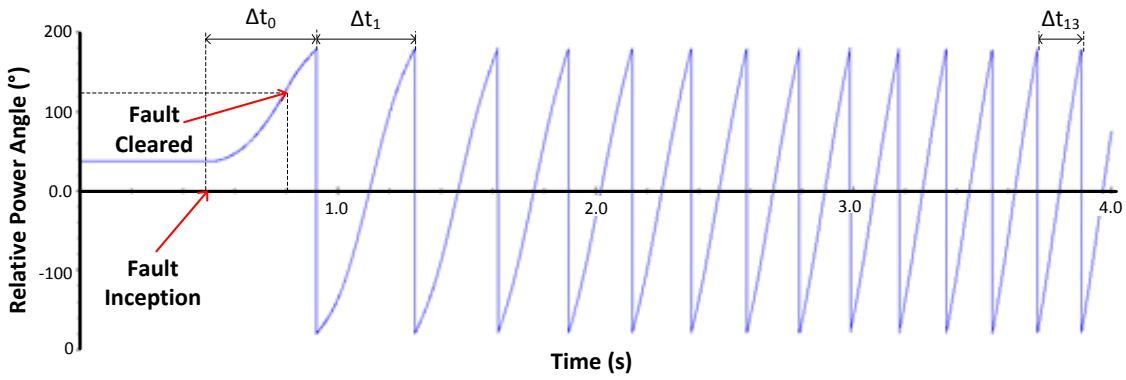


**Figure 4.14:** *Generator Relative Power Angle*

The frequency of the discontinuities shown in figure 4.14 can be regarded as the rate of pole slipping. It is clear from table 4.4 that the average rate of slippage increases with time.

| Interval (Δt) | Time (ms) | Angular Velocity (°/ms) |
|---|---|---|
| $\Delta t_0$ | 424 | 0.336 |
| $\Delta t_1$ | 384 | 0.938 |
| $\Delta t_2$ | 320 | 1.125 |
| $\Delta t_3$ | 277 | 1.300 |
| $\Delta t_4$ | 245 | 1.469 |
| $\Delta t_5$ | 230 | 1.565 |
| $\Delta t_6$ | 211 | 1.706 |
| $\Delta t_7$ | 201 | 1.791 |
| $\Delta t_8$ | 195 | 1.846 |
| $\Delta t_9$ | 188 | 1.915 |
| $\Delta t_{10}$ | 183 | 1.967 |
| $\Delta t_{11}$ | 175 | 2.057 |
| $\Delta t_{12}$ | 170 | 2.118 |
| $\Delta t_{13}$ | 169 | 2.130 |

**Table 4.4:** *Rate of Pole-Slipping for 60 MW Generator*

The average rate of change of power angle is defined as the angular velocity in table 4.4. Each point plotted in table 4.4 represents the average angular velocity during that specific interval. It can be noted that the angular velocity is increasing at a decreasing rate.

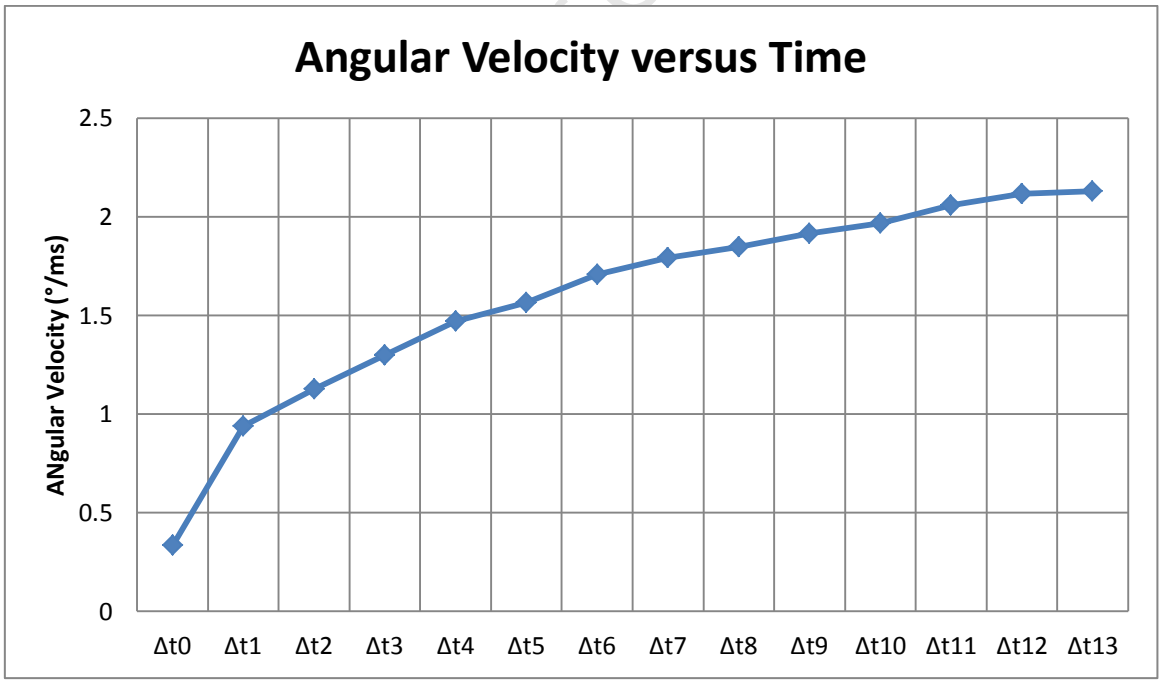


**Figure 4.15:** *Angular Velocity versus Time for Loss-of-Synchronism Event*

The effect of the loss-of-synchronism on the larger system is evident by the effect on the transmission level frequency which is illustrated in figure 4.15. The unregulated waveform shown in figure 4.16 is unacceptable from a quality of supply perspective, but more importantly the knock-on effect of a single generator on the whole system is verified.

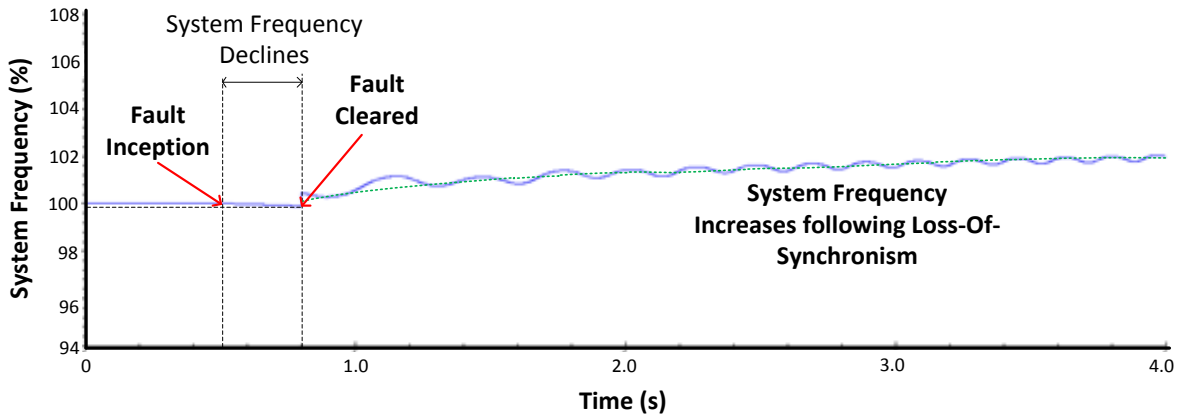


**Figure 4.16:** *System Frequency Response to Slipping Generator*

The waveforms explored in this section are typical of system displaying the characteristics of transient instability. The fundamental problem of transient stability, which is loss-of-synchronism, is evident in the behaviour of the generating unit when subjected to a 300 ms symmetrical fault.

The transient conditions to which the simulated equipment has been exposed are destructive and may have been likely to cause catastrophic failures if permitted to persist.

The section on protective relaying determines the limits of operation before a generating unit is tripped. A power swing exceeding 120° would typically result in tripping of the unit. This value can be selected based on practical limits and the typical operating conditions.

The next point in the search for the CCT would be 200 ms, which departs from the principle of a strict binary search, but is valid based on the relatively low peak angle produced as a result of a 50 ms fault. The CCT is determined to be 281 ms.

The steps in the binary search algorithm are as follows:

1. Estimate lowest and highest CCT limits (50 ms and 300 ms)
2. Test at mid-point of limits (175 ms)
3. Determine if CCT is above or below mid-point
4. Determine mid-point of upper or lower interval depending on result of step 3
5. Repeat process until the CCT is determined

The binary search method is not an elegant method if applied bluntly, but this method can yield a result in surprisingly few steps if reasoning and understanding of the resulting waveforms are applied.

The CCT for this specific case was found to be within 280 ms and 290 ms within six iterations. These limits were then applied to the remaining generators as logical starting limits which reduced computation time considerably.

## 4.2 Two Motor System

The arrangement of the system for this case study is representative of the arrangement at oxygen trains 1 to 7 West and 7 East. This arrangement was selected due to the parallel connection of a 36 MW synchronous motor and a 13.7 MW induction motor on the same bus fed by a single transformer.

The intention is to cause a loss-of-synchronism event in order to determine the influence of the induction motor on system transient stability.

***The aims of this two-motor system study are as follows:***

1. To determine the power angle response and power response for a system with and without a large induction motor in parallel to the synchronous motor to a fault.
2. To determine the effect of the motor model (sub-transient, transient and equivalent) on the power angle response to a fault.
3. To determine the effect of the synchronous motor inertia (including inertia of driven equipment) on the power response, power angle response and machine speed response to a fault.
4. To determine the effect of the fault type on the system response to the fault.

### 4.2.1 System Study

The two large motors are connected via a three-winding transformer to the utility supply. The utility supply is modelled as a swing bus with a fault-level corresponding to the system 132 kV fault-level.

The ratings of the synchronous motor (36 MW), which drives the air compressor, are described below in table 4.5.

| Parameter | Value |
|---|---|
| **Real Power** | 36 MW |
| **Apparent Power** | 40.7 MVA |
| **Power Factor** | 90 % |
| **Efficiency** | 98.19 % |
| **Full Load Current** | 2138 A |
| **Poles** | 2 |
| **Speed** | 3000 rpm |

**Table 4.5:** *Synchronous Motor Parameters*

The fault-level analysis reveals the symmetrical fault-level to be 41.3 kA of which the synchronous motor contributes 11.85 kA and the induction motor contributes 4.71 kA. The remaining 24.75 kA is contributed by the utility.

A 100 ms symmetrical fault is simulated at the motor bus and the results are analysed below. The simulation is done for the induction motor in service and with the induction motor out of service as two separate cases.

The power angles are visible for both cases in figure 4.17. The second case is with the induction machine out of service. The second waveform has a higher frequency which corresponds to a lower overall system inertia. It is important to note that the initial power angle is negative in the case of a synchronous motor.

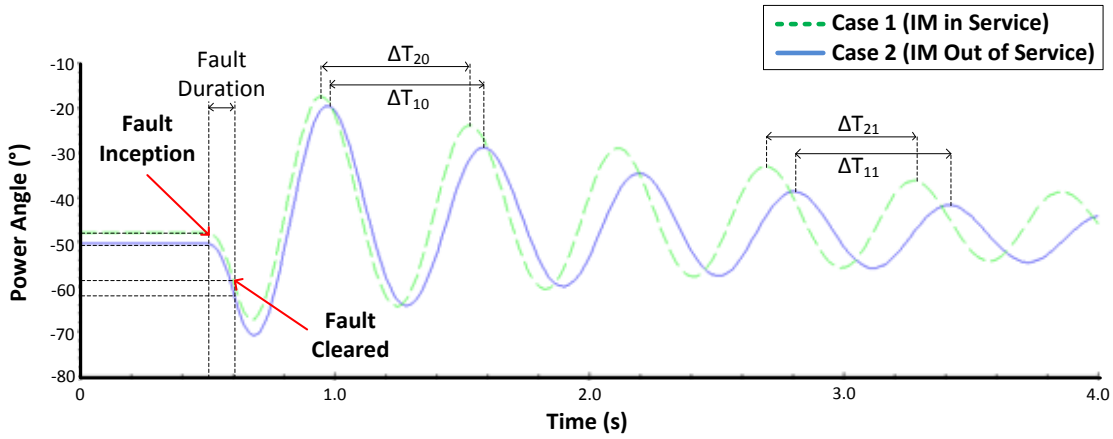


**Figure 4.17:** *Motor Power Angle Responses to 100 ms Symmetrical Fault*

The two power angle waveforms have different frequencies, as shown below in table 4.6, which result in drifting of the peaks relative to each other.

The frequency of both cases is in the region of 1.6 Hz with case 2 having a slightly higher frequency. The slightly higher frequency causes the peaks of the case 2 power angle waveform to occur progressively sooner in time that the peaks of the case 1 power angle waveform.

| Interval | Period (ms) | Frequency (Hz) |
|---|---|---|
| $\Delta T_{10}$ | 605 | 1.65 |
| $\Delta T_{20}$ | 578 | 1.73 |
| $\Delta T_{11}$ | 611 | 1.64 |
| $\Delta T_{21}$ | 590 | 1.69 |

**Table 4.6:** *Interval and Frequency for Power Angle Waveform*

The induction machine appears to have a damping effect on the power angle waveform, and consequently on the stability margin of the synchronous motor. All other waveforms related to this case will display oscillations related to the frequency set by the rotor power angle oscillation.

The electrical power waveforms for both cases are illustrated below in figure 4.18. The oscillations in the second case take longer to decay. The characteristic power dip during the fault is visible.

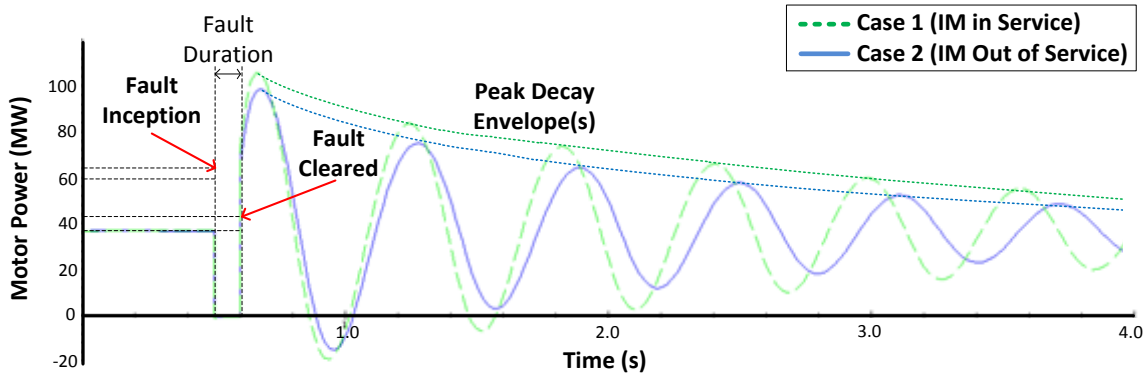


**Figure 4.18:** *Motor Power Responses to 100 ms Symmetrical Fault*

An interesting case arises with a clearing time of 250 ms. 240 ms is stable and 260 ms is first swing unstable. The oscillations increase in magnitude leading to instability despite first swing stability. The loss-of-synchronism event occurs 1500 ms seconds after the fault clearance.

The machine rotor angle is illustrated below in figure 4.19. The power angle undergoes two negative peaks before synchronism is lost.

This case illustrates borderline stability. The system is first-swing transiently stable but is still transiently unstable.

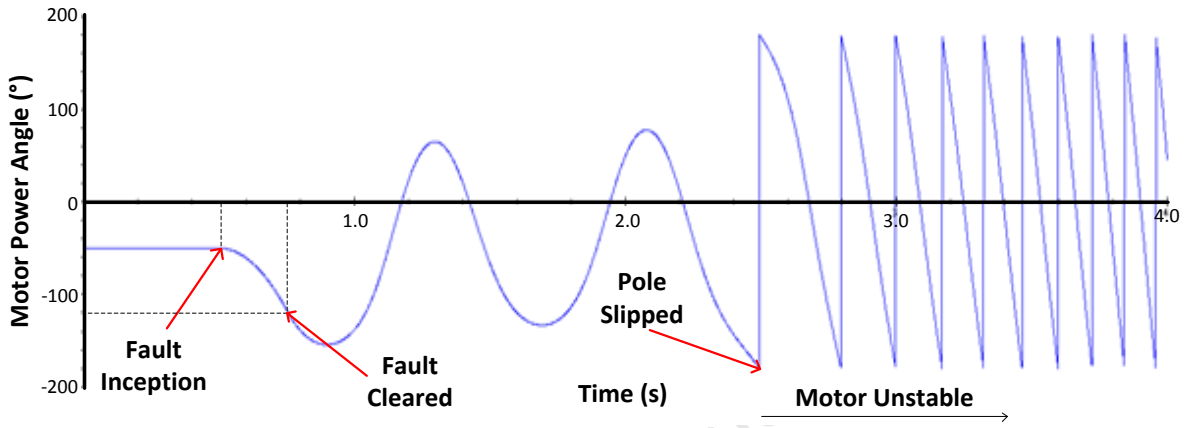


**Figure 4.19:** *Motor Power Angle Responses to 250 ms Symmetrical Fault*

A case such as the one illustrated in figure 4.19 requires OOS protection to detect an impending unstable condition.

### 4.2.2 Motor Model Effect on Response

Simulations were run for the sub-transient, transient and equivalent models. These correspond to case 1, 2 and 3 respectively for a 100 ms symmetrical fault at the motor bus.

The power angle versus time is plotted for all three cases below in figure 4.20. It is clear that these models give different results. The sub-transient model will be used for all simulations since this is the accurate model to use when performing transient stability studies.

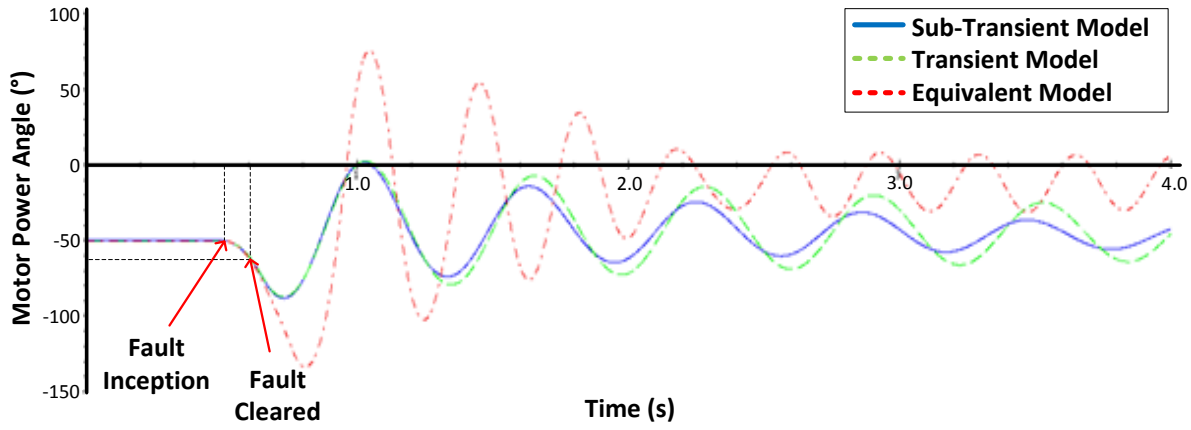


**Figure 4.20:** *Power Angle Response for Different Motor Models*

### 4.2.3 System Inertia Effect on Response

The total inertia (rotor and load) was set at 4.179, 6.179 and 8.179 for cases 1, 2 and 3 respectively. The electrical power is illustrated below in figure 4.21 for all three cases.

The first case with the lowest inertia displayed the highest post-fault accelerating power and the highest oscillation frequency.

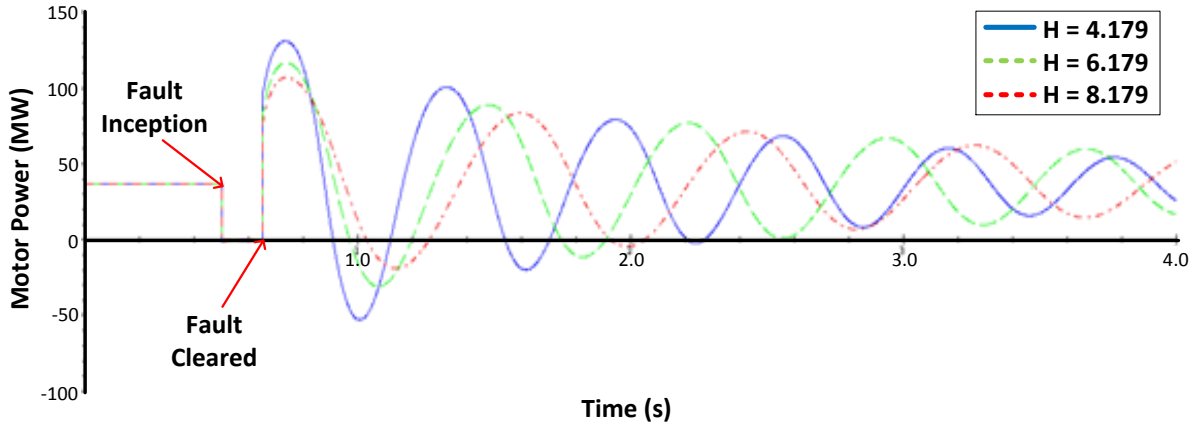


**Figure 4.21:** *Power versus System Inertia for 100 ms Fault*

The motor speed variations are illustrated below in figure 4.22. The first case displays the sharpest speed decline during the fault as well as the quickest recovery and the highest overshoot of all three cases.

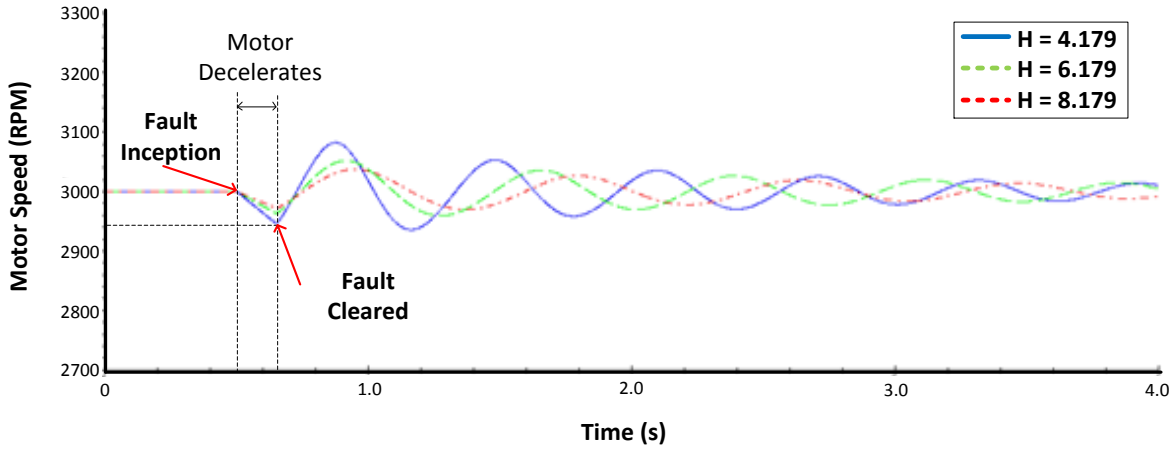


**Figure 4.22:** *Motor Speed versus System Inertia for 100 ms Fault*

The motor power angles are illustrated below in figure 4.23. The first case displays the largest first power angle swing and the largest absolute change in power angle.

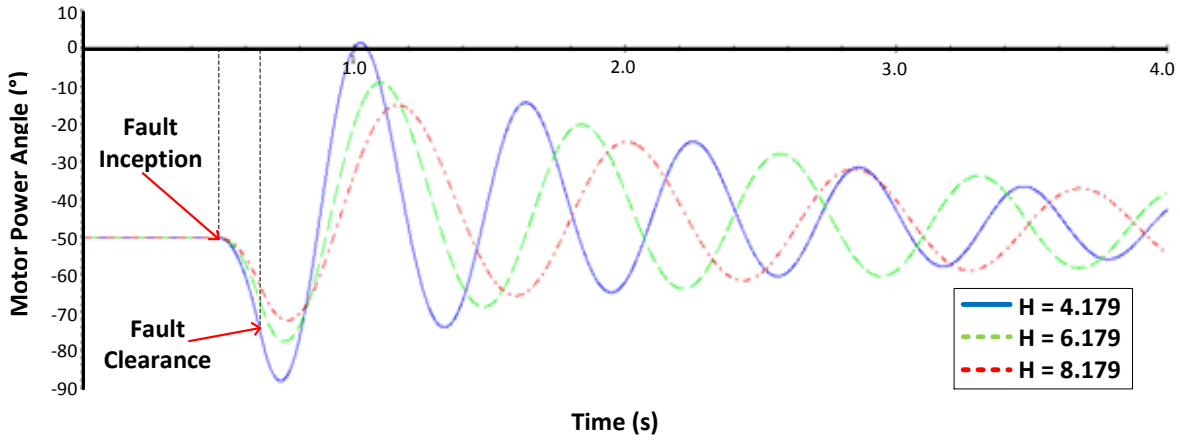


**Figure 4.23:** *Motor Power Angle versus System Inertia for 100 ms Fault*

It can be observed that a higher rotor and driven equipment inertia corresponds to favourable transient stability margin. A very high inertia is, however, not desirable from the perspective of starting the motor.

### 4.2.4 Fault Type Effect on Response

The cases were compared for a 100 ms symmetrical fault versus opening the motor circuit breaker for 100 ms.

The behaviour is similar since no power is transferred to the motor during the transient condition. The voltage is higher in the second case than the first case, which will result in a faster recovery.

The rotor power angles are illustrated below in figure 4.24. The first case is with a symmetrical fault and the second case for an open circuit breaker. The power angle swings are higher in magnitude for the symmetrical fault.

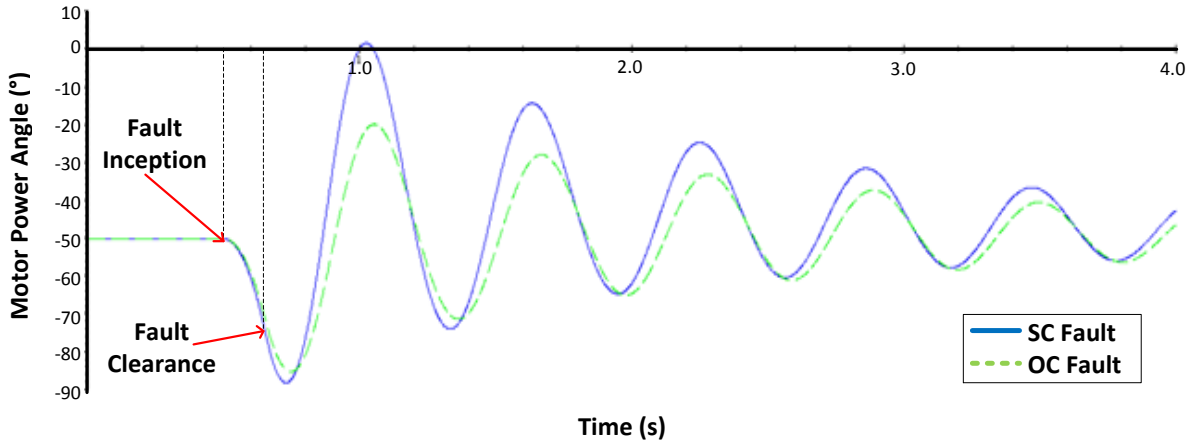


**Figure 4.24:** *Motor Power Angles for SC versus OC Fault*

The electrical power is intuitively zero during the transient condition for both cases and the post-fault power is lower in the second case.

Two cases were compared for a 150 ms symmetrical fault versus 150 ms line-to-ground fault.

A three-phase symmetrical fault is the most severe form of electrical fault and it is expected that the oscillations from a symmetrical fault would be significantly higher in magnitude than for a LG fault of the same duration. The fault was applied for 150 ms for both symmetrical and line-to-ground faults.

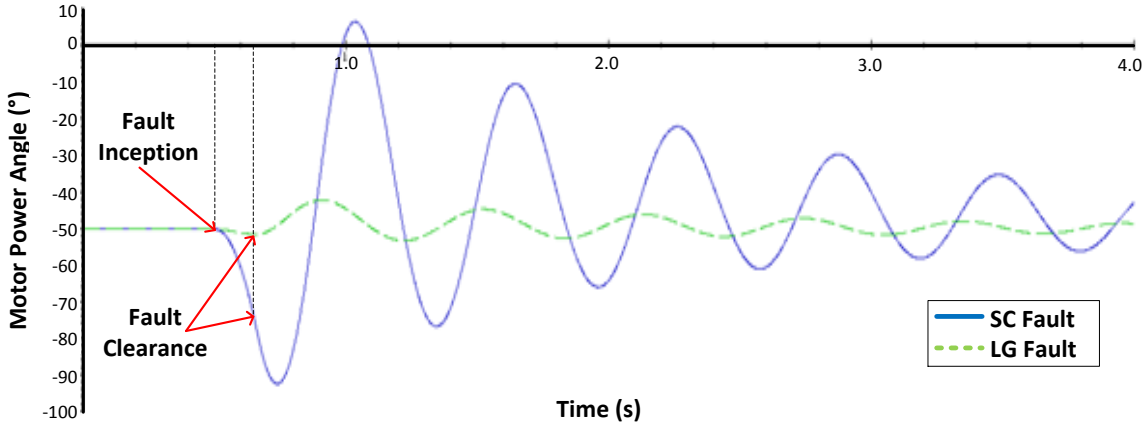


**Figure 4.25:** *Power Angles for Symmetrical versus LG Fault*

The power angles are illustrated above in figure 4.25 and as expected the oscillation following the symmetrical fault is significantly higher in magnitude than the oscillation subsequent to a line-to-ground fault.

# 5 Sasol Synfuels Case Study

This section provides an overview of the Sasol Synfuels Transmission and Distribution Network both for the current system and for projected development.

**Sasol System:**

- Ten 60 MW ST-driven generators
- Two 118 MW GT-driven generators
- Eight 36 MW air compressors (Oxygen T1 to T14)
- Two 55 MW air compressors (MAC)
- Two 22 MW air compressors (BAC)
- Three 17 MW compressors (Turbo Plant)
- Four 20.3 MW methane compressors (Gas Circuit)
- Many induction motors

The Secunda works can be divided into the West plant, the East plant (formerly Sasol 2 and Sasol 3) and the coal mines of which there are five. The original construction had one 132 kV switch-plant per side. In 2010 a third 132 kV switch-plant was commissioned two 118 MW GT-driven generators were connected to this system.

The geographical layout of the Sasol Secunda interconnection to the Eskom grid is illustrated below in figure 5.1.

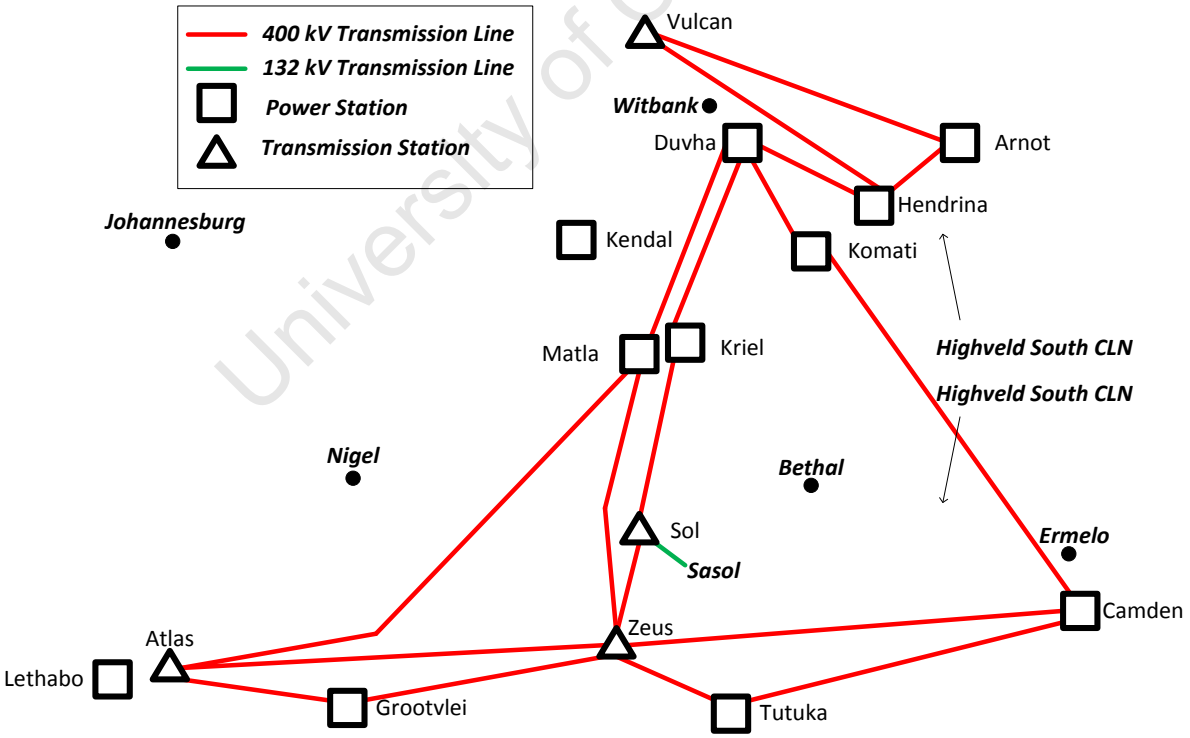


**Figure 5.1:** *Geographical Diagram of Utility HV Lines*

The Sasol system generates a large portion of its power in-house; while the exact generation depends on steam availability, the deficit is imported from Eskom via the SOL Main Transmission Substation (MTS) 500 MVA transformers. The power factor seen by Eskom is controlled by adjusting the excitation of the connected synchronous machines.

A block diagram of the Sasol network is illustrated below in figure 5.2 which shows the three main sub-systems of the distribution system.

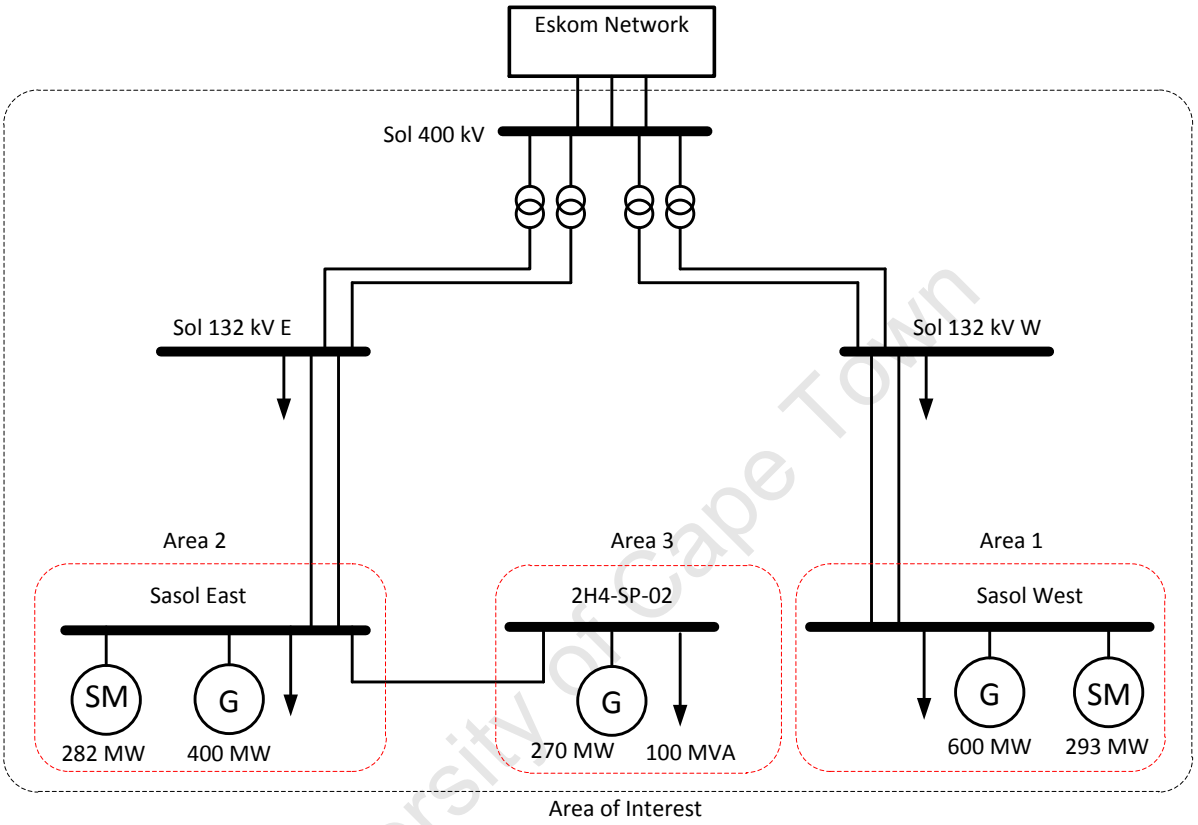


**Figure 5.2:** *Sasol Synfuels Transmission Network Equivalent Diagram (Current Arrangement)*

The SOL MTS no longer has capacity to supply the Secunda area in N-2 conditions. The existing SOL MTS has four 500 MVA transformers with a peak load of 850 MVA. The peak load of the MTS is 1450 MVA without Sasol generation.

Sasol have projected a load increase of 500 MVA in Notified Maximum Demand (NMD) from 1100 MVA to 1600 MVA.

The OCGT plant will be integrated to the 132 kV network and has an initial capacity of 250 MVA, which is projected to increase to 500 MVA in 2016.

These changes necessitate strengthening of the Highveld South Customer Load Network (CLN) by addition of a new 400 kV MTS (SOL B MTS).

## 5.1 Phase 0

The first phase (Phase 0) is the configuration which describes the Sasol Synfuels power system prior to 2010. There are two main 132 kV switch-plants which distribute power throughout the various plants. The SOL MTS is an Eskom transmission substation which was designed with N-2 supply contingency capability.

The East-West tie-line is normally open in this arrangement due to the high fault-level implications of closing the tie.

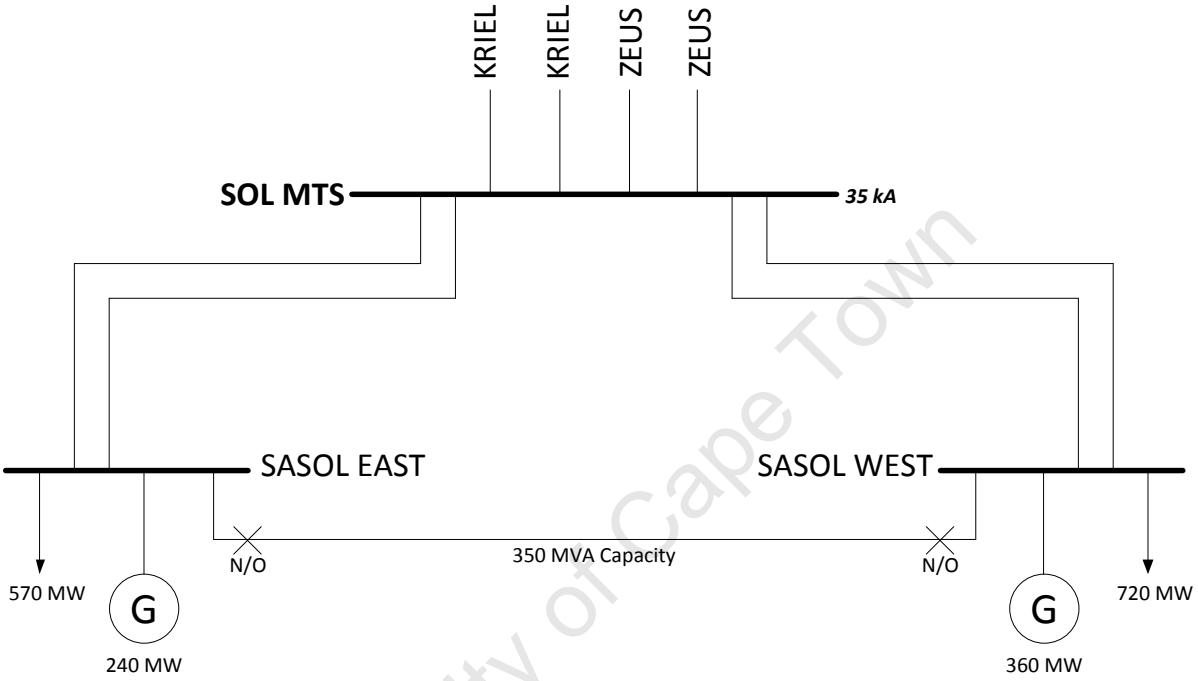


**Figure 5.3:** *Sasol Synfuels and Eskom TDP Phase 0*

Due to natural expansion the electrical load demanded by Sasol Synfuels has increased to the extent that the SOL MTs is no longer able to run in N-2 supply contingency conditions. The situation demanded corrective action to strengthen the supply.

### *5.1.1.1 Initial System Conditions*

The original design has a total of 10 ST-driven generators which generate a possible total of 600 MW. The fault-levels are within the 40 kA switchgear rating at 132 kV.

### *5.1.1.2 Normal Transient Stability Analysis*

The normal transient stability analysis for Phase 0 is effectively included in the normal transient stability analysis of Phase 4, since the old system is unaffected by the infrastructure development.

### *5.1.1.3 N-1 Contingency Transient Stability Analysis*

This system (SOL MTS) is capable of running in N-1 supply contingency conditions. The original design for N-2 supply contingency is no longer possible with the current network loading.

## 5.2 Phase 1

The second phase (Phase 1) involved the construction of a new 132 kV switch-plant (2H4-SP-02) which was connected to the Sasol Synfuels power system. The initial interconnection is via the East-tie cable to 2H4-SP-01. This phase was completed in 2010.

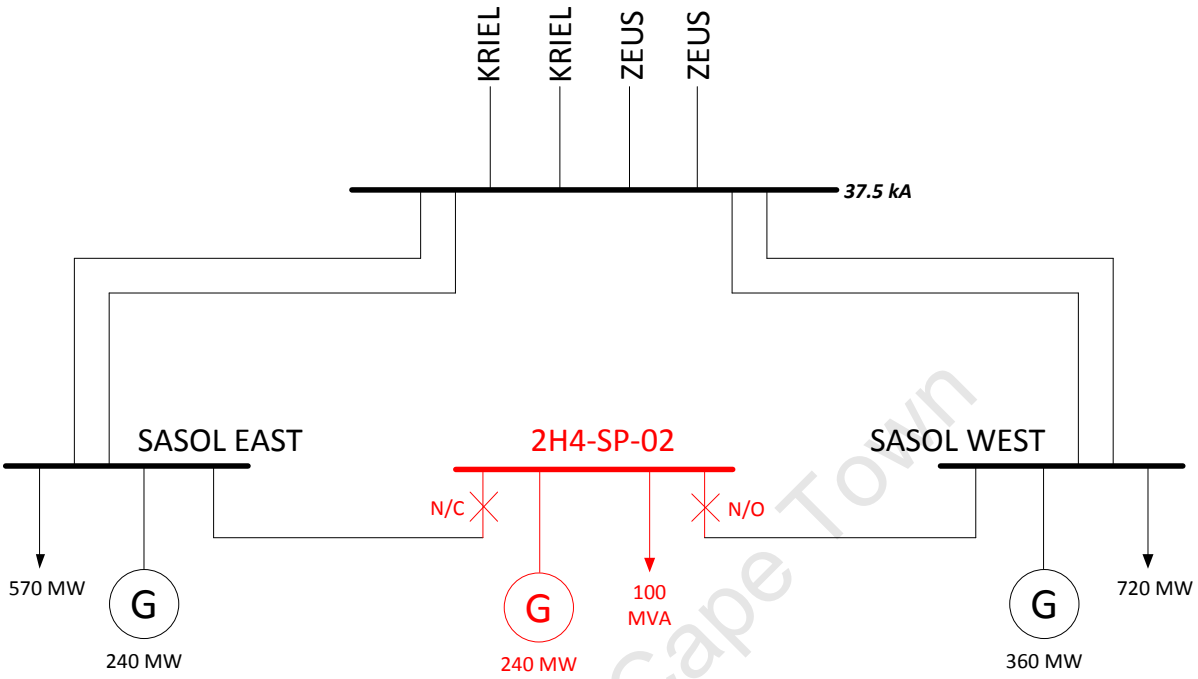


**Figure 5.4:** *Sasol Synfuels and Eskom TDP Phase 1*

Phase 1 included adding 240 MW of generating capacity to the power system, by means of two OCGT generators, and the addition of 100 MVA load.

The network model used for Phase 1 is shown in Appendix 9.1.1.

### *5.2.1.1 Initial System Conditions*

The basic loading and fault-level conditions are as described in table 5.1.

The net incomer apparent power is negative since the sub-system is effectively exporting power in this arrangement.

| Parameter | Value |
|---|---|
| **Incomer Apparent Power** | -152.4 MVA |
| **Incomer Power Factor** | 76.2 % |
| **Bus Voltage** | 100.2 % |
| **Generation** | 235.8 MVA |
| **Load** | 90.3 MVA |
| **Bus Fault-Level** | 45.4 kA |

**Table 5.1:** *Phase 1 System Conditions*

### 5.2.2 Normal Transient Stability Analysis

The synchronous machines in the scope of the transient stability investigation are the two air compressor motors (23 MW and 55MW) and the two GT-driven generators (118 MW).

The deliverables of the transient stability study for Phase 1 are split into four sections. The first section follows:

1. **Bus Fault at 132 kV Level**
    a. Combined power angle plot for synchronous generators
    b. Combined power angle plot for synchronous motors
    c. Volts/hertz response of the 132 kV system
    d. CCTs

***275 ms Symmetrical Fault (Generator Borderline Stability):***

The power angle response of the two GT-driven generators is illustrated in figure 5.5 for a 275 ms symmetrical fault at the 132 kV system bus.

The generators retain transient stability and the system returns to a stable steady-state. The steady-state condition is not shown in figure 5.5.

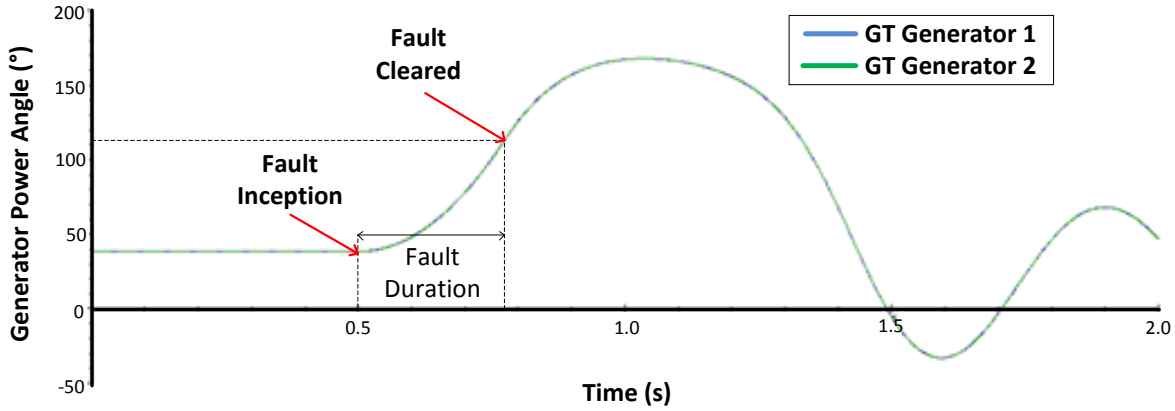


**Figure 5.5:** *GT Generator Power Angle Response to 275 ms Fault*

The generators are marginally stable which can be seen by the large power angle excursion and noticeably non-sinusoidal power angle waveform.

***276 ms Symmetrical Fault (Generator Borderline Instability):***

The power angle response of the two GT-driven generators is illustrated in figure 5.6 for a 276 ms symmetrical fault at the 132 kV system bus.

The generators are both transiently unstable when subjected to this fault type and duration. The point of loss-of-synchronism is, in this case, coincident with the clearing time. This is because the clearing time in this case is the CCT.

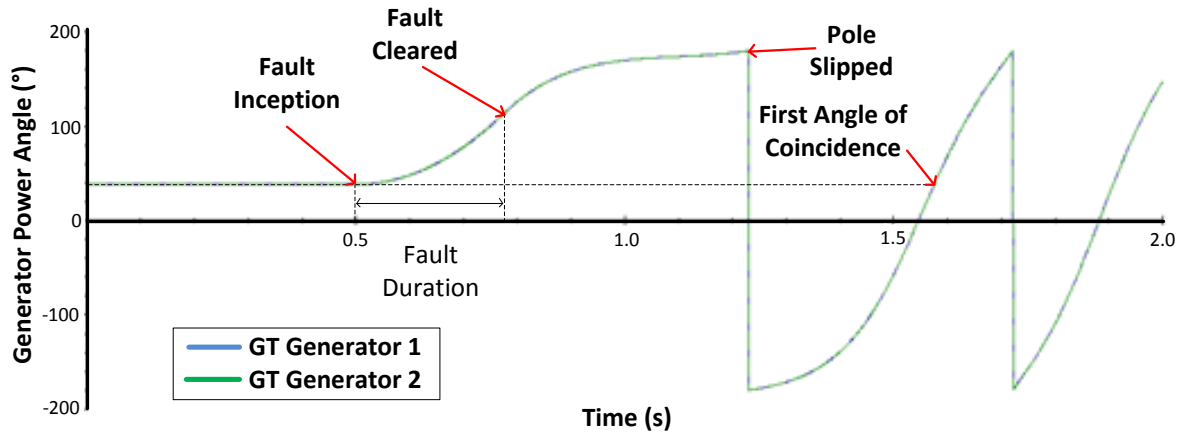


**Figure 5.6:** *GT Generator Power Angle Response to 276 ms Fault*

***213 ms Symmetrical Fault (BAC Motor Borderline Stability):***

The power angle response is shown in figure 5.7 for both the MAC and BAC motors of the 16th Oxygen Train when the 132 kV system bus is subjected to a 213 ms symmetrical fault.

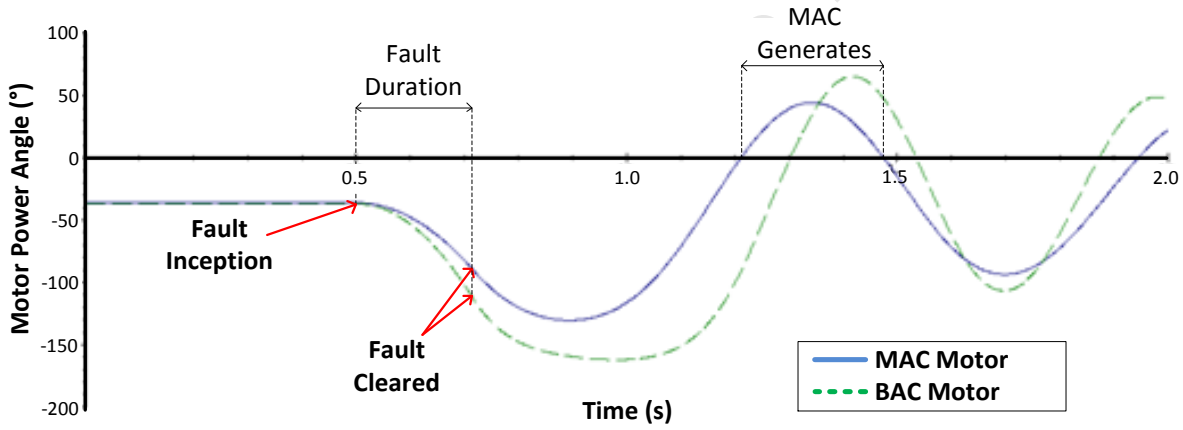


**Figure 5.7:** *MAC and BAC Motor Power Angle Response to 213 ms Fault*

The BAC motor, which is the smaller of the two motors, is on the border of transient stability in this case. This is primarily due to the lower inertia of the rotor and driven equipment.

Both the MAC and the BAC motors display large power angle excursions and even display a positive power angle for a period as indicated in figure 5.7.

***225 ms Symmetrical Fault (MAC Motor Borderline Stability):***

The power angle response is shown in figure 5.8 for both the MAC and BAC motors when the 132 kV system bus is subjected to a 225 ms symmetrical fault.

In this case the BAC motor has lost synchronism and the MAC motor is on the border of stability. This corresponds to the CCT of the MAC motor, which is intuitively longer than the CCT of the BAC motor (higher inertia).

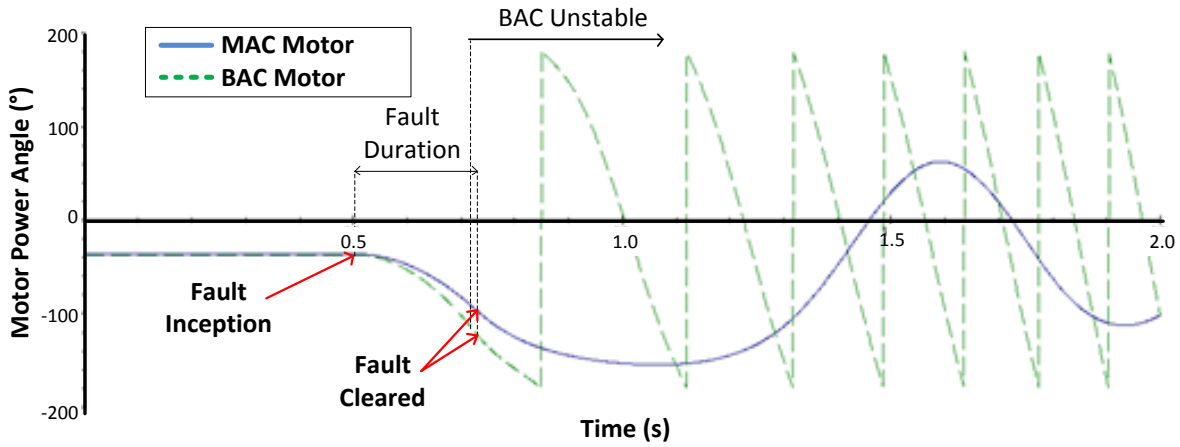


**Figure 5.8:** *MAC and BAC Motor Power Angle Response to 225 ms Fault*

***226 ms Symmetrical Fault (MAC and BAC Motors Unstable):***

The power angle response is shown in figure 5.9 for both the MAC and BAC motors when the 132 kV system bus is subjected to a 226 ms symmetrical fault.

In this case both the MAC and the BAC motors are in an unstable condition which is confirmed by the increasing rate of change of power angle.

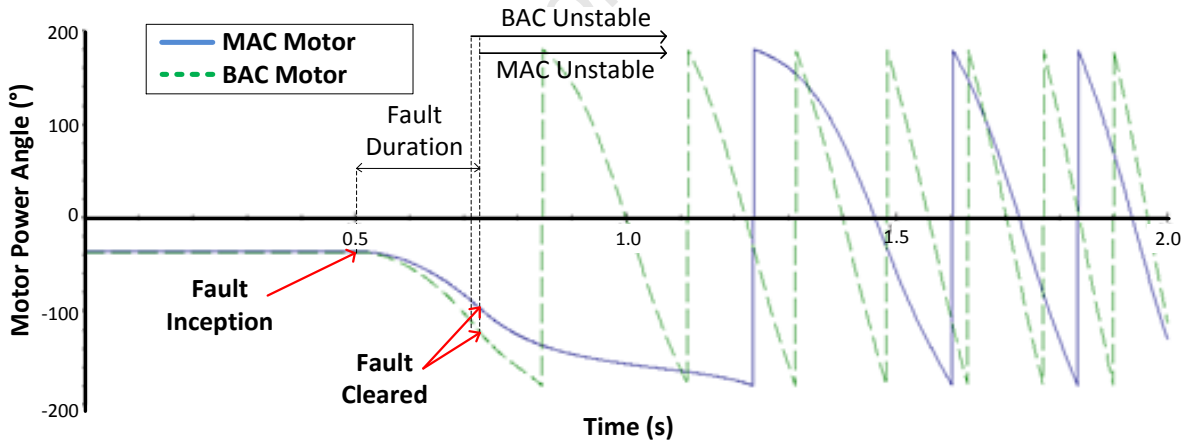


**Figure 5.9:** *MAC and BAC Motor Power Angle Response to 226ms Fault*

It can be concluded that the BAC motor loses synchronism before the MAC motor when both motors are subjected to the same disturbance.

The impact of rotor and equipment inertia was explored in section 4.2.3 for the hypothetical two-motor and has been verified for a practical system in this section.

***200 ms Symmetrical Fault (All Machines Stable):***

The volts/hertz waveform is shown below in figure 5.10 for the case of a 200 ms symmetrical fault at the 132 kV system bus, in which case all synchronous machines in the system remain stable.

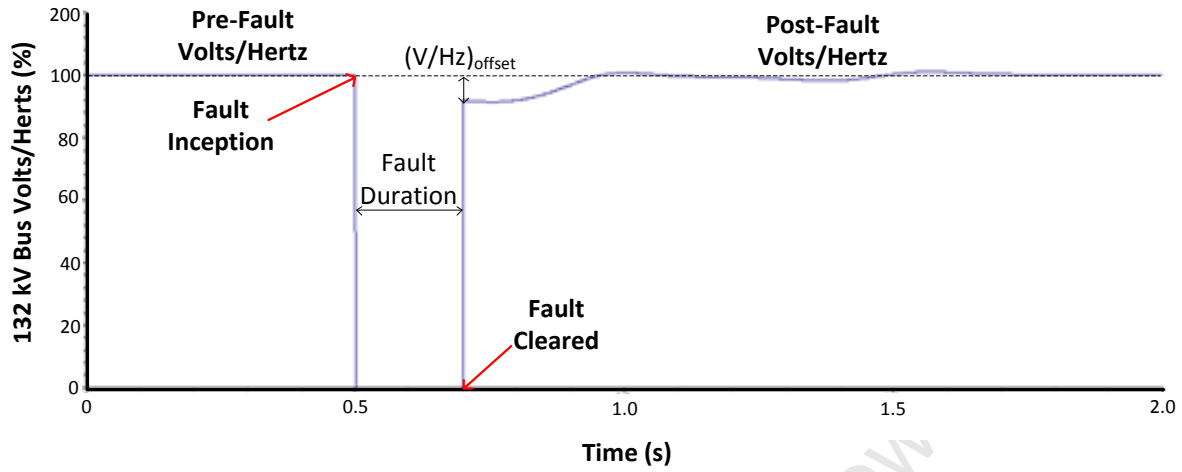


**Figure 5.10:** *132 kV Bus Volts/Hertz Waveform corresponding to 200 ms Fault*

The volts/hertz waveform is pulled to zero during the fault condition, as expected, since the voltage drops to zero during a short-circuit condition. The waveform has an initial offset at the moment of fault clearance, but returns to the pre-fault equilibrium state as illustrated.

***280 ms Symmetrical Fault (All Machines Unstable):***

The volts/hertz waveform is shown below in figure 5.11 for the case of a 280 ms symmetrical fault at the 132 kV system bus, in which case all synchronous machines in the system are unstable.

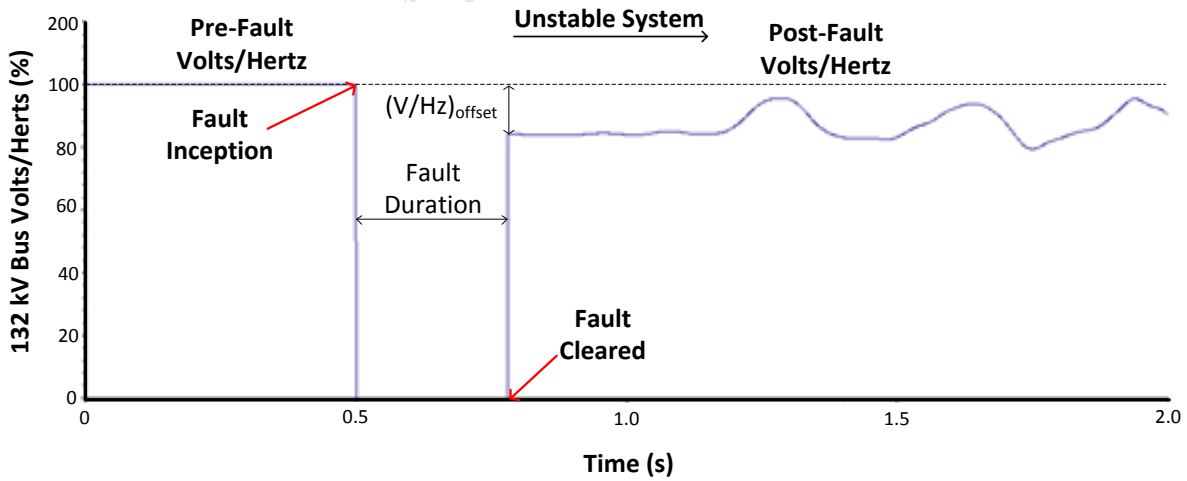


**Figure 5.11:** *132 kV Bus Volts/Hertz Waveform corresponding to 280 ms Fault*

The volts/hertz waveform drops to zero and then returns to a value offset from the pre-fault point. The waveform does not return to the pre-fault equilibrium state. It can be noted that the waveform is a composite of the voltage and frequency responses of several synchronous machines that lose synchronism at different points in time.

The CCTs are tabulated below in table 5.2 for a 132 kV bus fault for the Phase 1 configuration. It can be noted that the generator has the largest transient stability margin, while the BAC motor has the smallest stability margin in these conditions.

| Machine | Fault Type | CCT |
|---|---|---|
| **GT Generator 1** | 132 kV Bus | 275 ms |
| **GT Generator 2** | 132 kV Bus | 275 ms |
| **MAC Motor** | 132 kV Bus | 225 ms |
| **BAC Motor** | 132 kV Bus | 213 ms |

**Table 5.2:** *CCTs for Phase 1 (132 kV Bus Fault)*

The second section of the transient stability study follows:

2. **Bus Fault at Generator 1 Bus (Repeated for GT-Driven Generator 2)**
    a. Combined power angle plot for synchronous generator
    b. Volts/hertz response of the 132 kV system
    c. CCT

***271 ms Symmetrical Fault (GT-Driven Generator 1 Borderline Stability):***

The power angle response to a 271 ms symmetrical fault at the GT-driven generator 1 terminal bus is illustrated in figure 5.12. The generator displays borderline stability in this case.

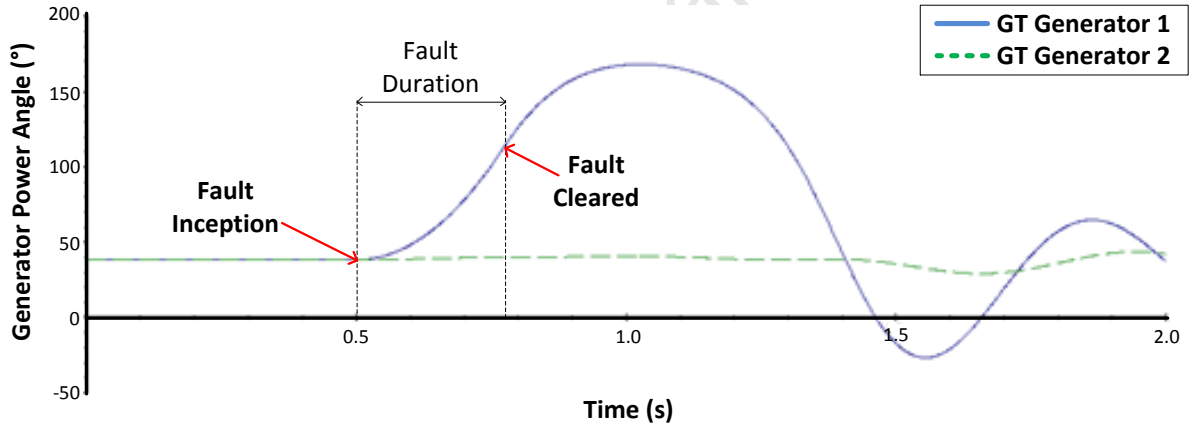


**Figure 5.12:** *GT Generator 1 and 2 Power Angle Response to 271 ms Fault on Generator 1 Bus*

It can be noted that the impact on GT-driven generator 2's power angle is almost negligible when there is a terminal bus fault at GT Gen 1's terminals. The reverse also applies.

The volts/hertz response waveform is visible in figure 5.13 for a 271 ms symmetrical fault at GT-driven generator 1 terminal bus.

The volts/hertz waveform does not drop to zero, as would be expected for a system bus fault, but drops to approximately 94% of the base value.

The waveform returns to the pre-fault equilibrium state, as would be expected, since all synchronous machines are stable in this case.

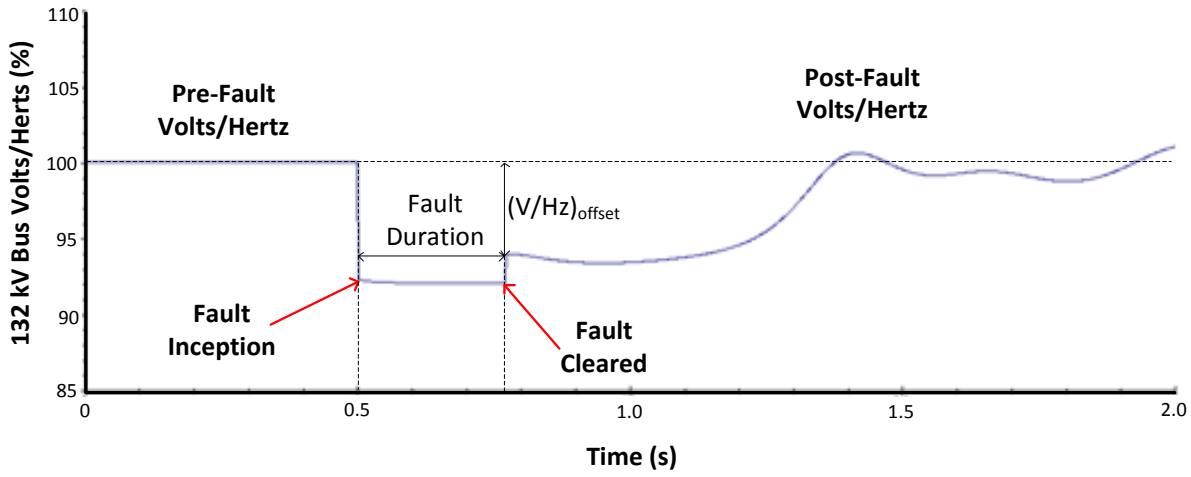


**Figure 5.13:** *132 kV Bus Volts/Hertz Waveform corresponding to 271 ms Fault on Generator 1 Bus*

The volts/hertz waveform returns to the pre-fault setpoint approximately 1 second after fault inception. The time taken to normalise from fault clearance is approximately 730 ms.

***272 ms Symmetrical Fault (GT-Driven Generator 1 Borderline Instability):***

The power angle response to a 272 ms symmetrical fault at the GT-driven generator 1 terminal bus is illustrated in figure 5.14. The generator is unstable in this case.

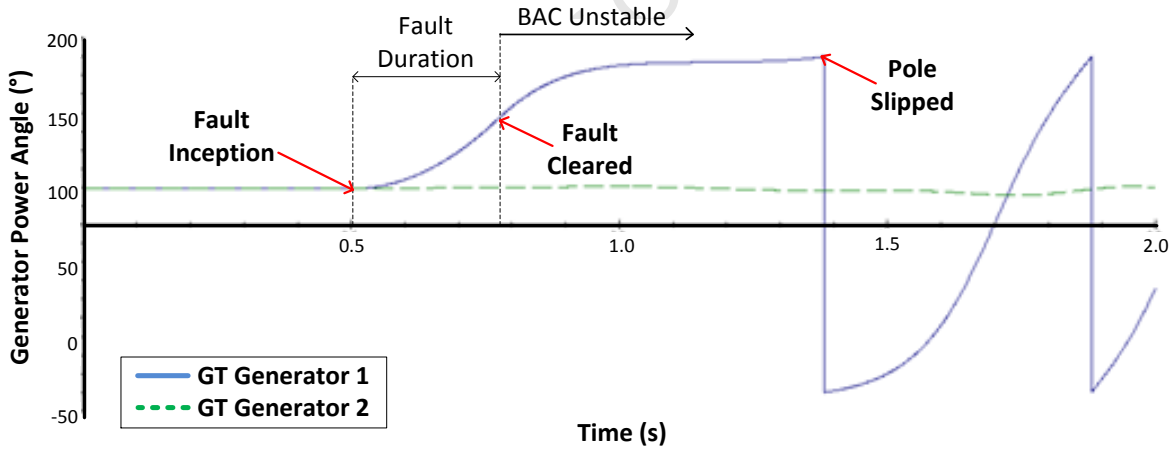


**Figure 5.14:** *GT Generator 1 and 2 Power Angle Response to 272 ms Fault on Generator 1 Bus*

It can be noted that this case displays an unusual case of borderline stability. The generator power angle remains at approximately 180° for approximately 500 ms until the pole is finally slipped. The machine was lost stability, however, long before the pole was slipped.

The volts/hertz response waveform is visible in figure 5.15 for a 272 ms symmetrical fault at GT-driven generator 1 terminal bus.

The volts/hertz waveform illustrates a response characteristic of an unstable system.

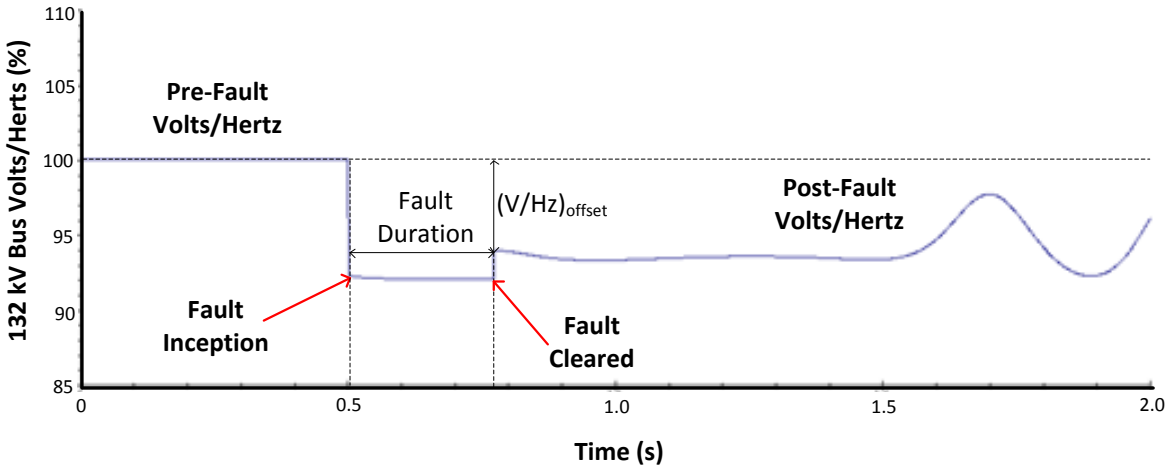


**Figure 5.15:** *132 kV Bus Volts/Hertz Waveform corresponding to 272 ms Fault on Generator 1 Bus*

The power angle and volts/hertz responses have been analysed for system bus and terminal bus symmetrical faults for both synchronous generators and synchronous motors. From this point forward the waveforms will no longer be analysed, although they are used to determine the CCT and are recorded.

The third and fourth sections of the transient stability study follow:

3. **Bus Fault at MAC Motor Bus**
    a. CCT
4. **Bus Fault at BAC Motor Bus**
    a. CCT

The CCTs are tabulated below in table 5.3 for a machine terminal bus fault for Phase 1.

| Machine | Fault Type | CCT |
|---|---|---|
| **GT Generator 1** | Machine Bus | 271 ms |
| **GT Generator 2** | Machine Bus | 271 ms |
| **MAC Motor** | Machine Bus | 230 ms |
| **BAC Motor** | Machine Bus | 223 ms |

**Table 5.3:** *CCTs for Phase 1 (Machine Bus Fault)*

It can be noted that the generator CCTs are lower for a machine bus fault than for a system bus fault which implies a smaller stability margin for the machine bus fault-type.

The motor CCTs are higher for a machine bus fault than for a system bus fault which implies a larger stability margin.

A summary of the results of the transient stability analysis of the synchronous machines for the Phase 1 configuration is presented in a column chart form in figure 5.16.

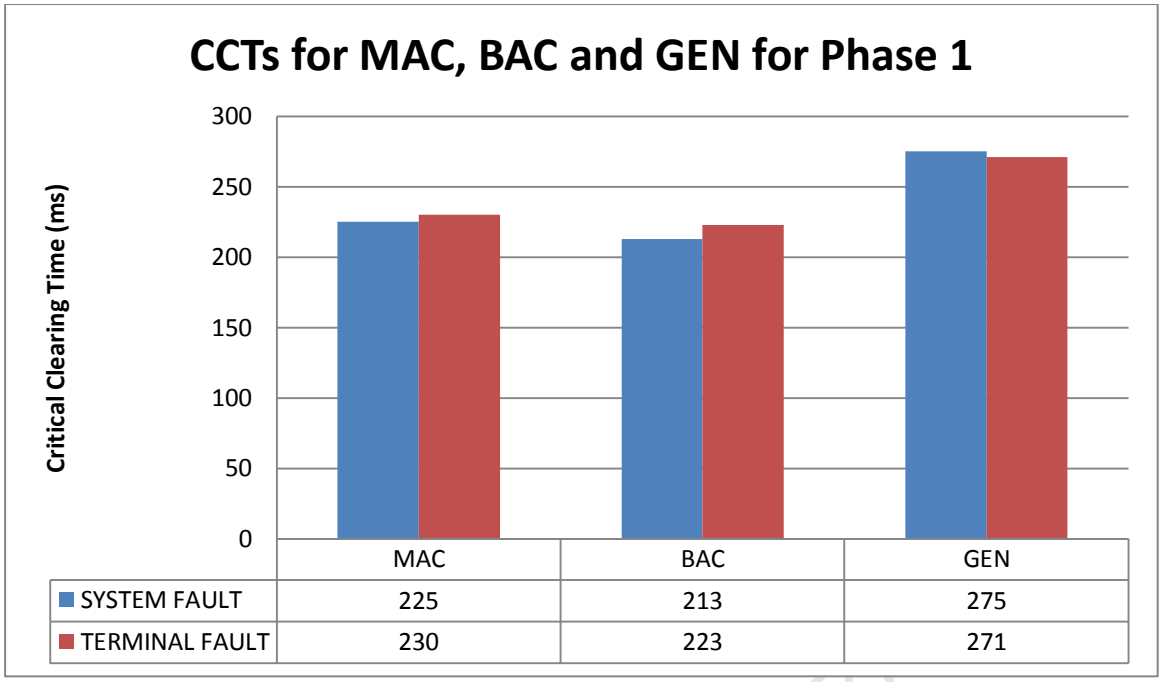


**Figure 5.16:** *Phase 1 Summary Chart for CCTs*

### *5.2.2.1 N-1 Contingency Transient Stability Analysis*

The system (2H4-SP-02) is not designed to accommodate N-1 supply contingency in this configuration since there is only a single incomer. It is possible to consider the GT-driven generators as incomers which implies that the system is capable of N - 2 supply contingency operation; provided the east-tie remains in service.

## 5.3 Phase 2

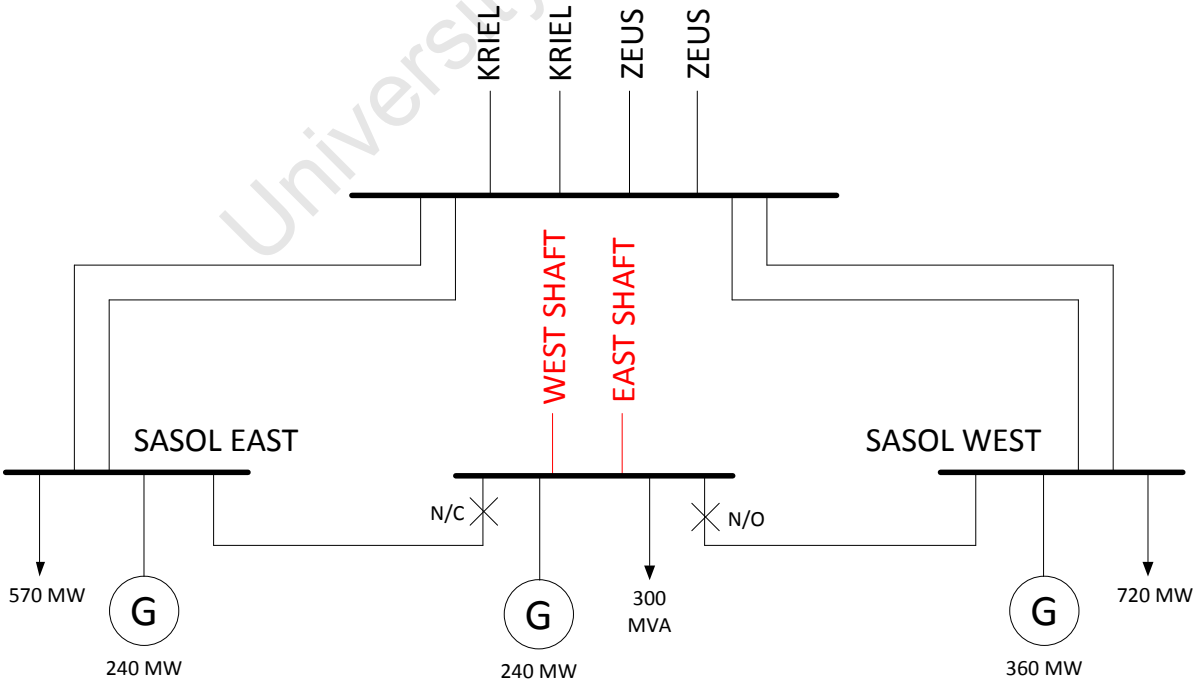


**Figure 5.17** *Sasol Synfuels and Eskom TDP Phase 2*

Phase 2 involves the connection of two incomers, out of a planned three new incomers, to the new switch-plant to accommodate an additional 200 MVA load.

Phase 2 is scheduled to occur between 2010 and 2013. This phase involves an interface between the consumer, Sasol Synfuels, and the utility which is Eskom in this case.

**Summary of changes from Phase 1:**

- 200 MVA additional load
- Two additional incomers

### 5.3.1 Initial System Conditions

The fault-level conditions are described in table 5.4.

| Source | Fault Contribution |
|---|---|
| **East Shaft Incomer** | 14 kA |
| **West Shaft Incomer** | 15 kA |
| **East-Tie Incomer** | 40 kA |

**Table 5.4:** *Phase 2 System Conditions*

### 5.3.2 Normal Transient Stability Analysis

The first configuration is summarised in table 5.5:

| Parameter | State |
|---|---|
| **East Shaft Incomer** | In Service (B Bus) |
| **West Shaft Incomer** | In Service (A Bus) |
| **East-Tie Incomer** | In Service (C Bus) |
| **AC Tie** | Closed |
| **DC Tie** | Closed |

**Table 5.5:** *High Fault-Level Configuration for Phase 2*

The fault-level in this configuration for Bus A/B/C/D is 78.4 kA, which is 157% of the GIS rating and would be unacceptable. The CCTs are determined for this configuration for a 132 kV system bus fault on the A bus. This configuration is shown in appendix 9.1.2.

The power angle response waveforms are not included in the case study for Phase 2 or Phase 3 since they display similar characteristics to the responses recorded for Phase 1.

The CCTs are tabulated in table 5.6 for a symmetrical fault on the 132 kV A Bus. It can be noted that the CCTs are longer for a higher system fault-level when the 132 kV system bus is subjected to a symmetrical fault.

| Machine | Fault Type | CCT |
|---|---|---|
| **GT Generator 1** | 132kV A Bus | 279 ms |
| **GT Generator 2** | 132kV A Bus | 279 ms |
| **MAC Motor** | 132kV A Bus | 232 ms |
| **BAC Motor** | 132kV A Bus | 217 ms |

**Table 5.6:** *CCTs for Phase 2 - High Fault (132 kV Bus Fault)*

The CCTs are tabulated in table 5.7 for a symmetrical fault on the machine terminal buses. It can be noted that the CCTs are longer for a higher system fault-level when the machine bus is subjected to a symmetrical fault.

| Machine | Fault Type | CCT |
|---|---|---|
| **GT Generator 1** | Machine Bus | 273 ms |
| **GT Generator 2** | Machine Bus | 273 ms |
| **MAC Motor** | Machine Bus | 232 ms |
| **BAC Motor** | Machine Bus | 224 ms |

**Table 5.7:** *CCTs for Phase 2 - High Fault (Machine Bus Fault)*

In order to reduce the fault-level for the 132 kV GIS the configuration summarised in table 5.8 is applied.

| Parameter | State |
|---|---|
| **East Shaft Incomer** | In Service (B Bus) |
| **West Shaft Incomer** | In Service (A Bus) |
| **East-Tie Incomer** | In Service (C Bus) |
| **AC Tie** | Open |
| **DC Tie** | Open |

**Table 5.8:** *Normal Fault-Level Configuration for Phase 2*

The important point to note with this configuration, which is illustrated in appendix 9.1.2, is that the normal and critical busses are separated. The east-tie is used for critical supply since the new generators are not configured to supply critical power.

The fault-level for the A/B/D Bus is 37.9 kA, while the fault-level for the C bus is 40.4 kA which are both within the limits of the GIS rating.

The CCTs are tabulated in table 5.9 for a symmetrical fault on the 132 kV A Bus.

| Machine | Fault Type | CCT |
|---|---|---|
| **GT Generator 1** | 132kV A Bus | 271 ms |
| **GT Generator 2** | 132kV A Bus | 271 ms |
| **MAC Motor** | 132kV A Bus | 221 ms |
| **BAC Motor** | 132kV A Bus | 212 ms |

**Table 5.9:** *CCTs for Phase 2 - Normal Fault (132 kV Bus Fault)*

The CCTs are tabulated in table 5.10 for a symmetrical fault on the machine terminal buses.

| Machine | Fault Type | CCT |
|---|---|---|
| **GT Generator 1** | Machine Bus | 270 ms |
| **GT Generator 2** | Machine Bus | 270 ms |
| **MAC Motor** | Machine Bus | 231 ms |
| **BAC Motor** | Machine Bus | 223 ms |

**Table 5.10:** *CCTs for Phase 2 - Normal Fault (Machine Bus Fault)*

In order to reduce the fault-level further in order to accommodate a third incoming line the configuration summarised in table 5.11 is applied.

| Parameter | State |
|---|---|
| **East Shaft Incomer** | In Service (B Bus) |
| **West Shaft Incomer** | In Service (A Bus) |
| **East-Tie Incomer** | In Service (C Bus) |
| **AC Tie** | Open |
| **DC Tie** | Open |
| **E Shaft CLR** | In Service |
| **W Shaft CLR** | In Service |

**Table 5.11:** *Normal Fault-Level Configuration for Phase 2*

A CLR is connected into each of the East Shaft and West Shaft lines to limit the fault contribution from these sources.

The addition of the two CLRs, with 12% impedance on the 2500 A base, reduces the fault-level on the A/B/D bus to 26.5 kA which is a 30% reduction in system fault-level. The 12% impedance for the CLR corresponds to 3.73 Ω with the X/R ratio set to 85.

An additional consideration, which is not addressed here, is the voltage drop across the CLR which may require compensation to maintain the 132 kV system voltage.

The CCTs are tabulated in table 5.12 for a symmetrical fault on the 132 kV A Bus.

| Machine | Fault Type | CCT |
|---|---|---|
| **GT Generator 1** | 132kV A Bus | 264 ms |
| **GT Generator 2** | 132kV A Bus | 264 ms |
| **MAC Motor** | 132kV A Bus | 210 ms |
| **BAC Motor** | 132kV A Bus | 203 ms |

**Table 5.12:** *CCTs for Phase 2 - Reduced Fault (132 kV Bus Fault)*

The CCTs are tabulated in table 5.12 for a symmetrical fault on the machine terminal buses.

| Machine | Fault Type | CCT |
|---|---|---|
| **GT Generator 1** | Machine Bus | 267 ms |
| **GT Generator 2** | Machine Bus | 267 ms |
| **MAC Motor** | Machine Bus | 229 ms |
| **BAC Motor** | Machine Bus | 223 ms |

**Table 5.13:** *CCTs for Phase 2 - Reduced Fault (Machine Bus Fault)*

A summary of the results follows in table 5.13.

| Fault Type | Configuration | MAC | BAC | GEN |
|---|---|---|---|---|
| **132kV Bus** | High Fault | 232 ms | 217 ms | 279 ms |
| | Normal Fault | 221 ms | 212 ms | 271 ms |
| | Reduced Fault | 210 ms | 203 ms | 264 ms |
| **Machine Bus** | High Fault | 232 ms | 224 ms | 273 ms |
| | Normal Fault | 231 ms | 223 ms | 270 ms |
| | Reduced Fault | 229 ms | 223 ms | 267 ms |

**Table 5.14:** *Tabulated Summary of CCTs for Phase 2*

A summary chart of the CCTs for the synchronous machines in the Phase 2 configuration follows in figure 5.18 for a 132 kV system bus fault.

The lowest stability margins correspond to the reduced fault-levels attained using CLRs and a separated bus system.

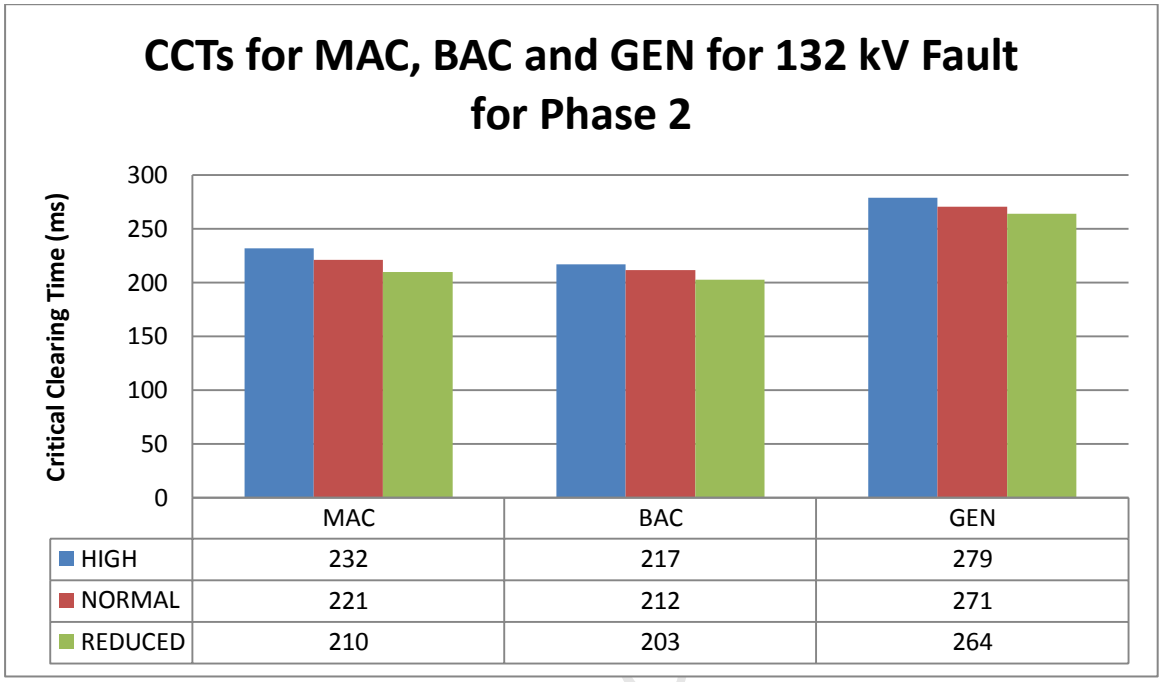


| | MAC | BAC | GEN |
|---|---|---|---|
| HIGH | 232 | 217 | 279 |
| NORMAL | 221 | 212 | 271 |
| REDUCED | 210 | 203 | 264 |

**Figure 5.18:** *Phase 2 Summary Chart of CCTs for 132 kV System Fault*

A summary chart of the CCTs for the synchronous machines in the Phase 2 configuration follows in figure 5.19 for a machine bus fault.

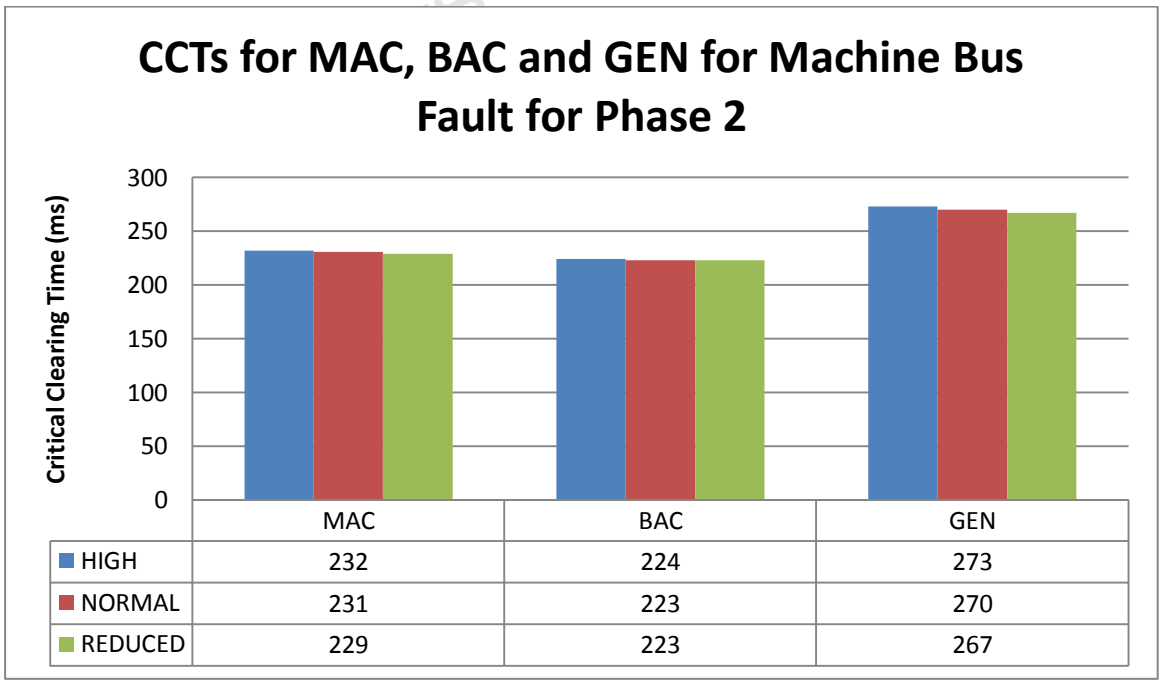


| | MAC | BAC | GEN |
|---|---|---|---|
| HIGH | 232 | 224 | 273 |
| NORMAL | 231 | 223 | 270 |
| REDUCED | 229 | 223 | 267 |

**Figure 5.19:** *Phase 2 Summary Chart of CCTs for Machine Bus Fault*

### 5.3.3 N-1 Contingency Transient Stability Analysis

The system (2H4-SP-02) is capable of N-1 supply contingency operation in this case; provided the east-tie remains in service. The east-tie provides critical power.

The impact of N-1 supply contingency on transient stability is related to the reduction in system fault-level. The fault-level in N-1 supply contingency is either 23.9 kA or 22.9 kA depending on whether the East Shaft Incomer or West Shaft Incomer is out of service. The most marked effect on transient stability will be caused by the West Shaft being out of service. This is the case that will be analysed in this section.

The CCTs are tabulated in table 5.15 for N-1 contingency and a 132 kV Bus A symmetrical fault.

| Machine | Fault Type | CCT |
|---|---|---|
| **GT Generator 1** | 132kV A Bus | 260 ms |
| **GT Generator 2** | 132kV A Bus | 260 ms |
| **MAC Motor** | 132kV A Bus | 205 ms |
| **BAC Motor** | 132kV A Bus | 200 ms |

**Table 5.15:** *CCTs for Phase 2 – N-1 Supply Contingency (132 kV Bus Fault)*

The CCTs are tabulated in table 5.16 for N-1 contingency and a machine bus symmetrical fault.

| Machine | Fault Type | CCT |
|---|---|---|
| **GT Generator 1** | Machine Bus | 265 ms |
| **GT Generator 2** | Machine Bus | 265 ms |
| **MAC Motor** | Machine Bus | 228 ms |
| **BAC Motor** | Machine Bus | 221 ms |

**Table 5.16:** *CCTs for Phase 2 – N-1 Supply Contingency (Machine Bus Fault)*

In the event that CLRs are installed on the incoming West Shaft and East Shaft lines, the system fault-level will be reduced further. The fault-level will be 18.5 kA or 17.5 kA with the East Shaft Incomer or West Shaft Incomer out of service respectively.

The CCTs are tabulated in table 5.17 for N-1 Contingency and a 132 kV Bus A symmetrical fault with CLRs in service.

| Machine | Fault Type | CCT |
|---|---|---|
| **GT Generator 1** | 132kV A Bus | 245 ms |
| **GT Generator 2** | 132kV A Bus | 245 ms |
| **MAC Motor** | 132kV A Bus | 190 ms |
| **BAC Motor** | 132kV A Bus | 188 ms |

**Table 5.17:** *CCTs for Phase 2 – N-1 Supply Contingency (132 kV Bus Fault - CLR)*

The CCTs are tabulated in table 5.18 for N-1 Contingency and a machine bus symmetrical fault with CLRs in service.

| Machine | Fault Type | CCT |
|---|---|---|
| **GT Generator 1** | Machine Bus | 261 ms |
| **GT Generator 2** | Machine Bus | 261 ms |
| **MAC Motor** | Machine Bus | 224 ms |
| **BAC Motor** | Machine Bus | 219 ms |

**Table 5.18:** *CCTs for Phase 2 – N-1 Supply Contingency (Machine Bus Fault - CLR)*

A summary chart of the CCTs for the synchronous machines in the Phase 2 N-1 configuration follows in figure 5.20 for a 132 kV system bus fault.

The lowest stability margins correspond to the reduced fault-levels attained using CLRs and a separated bus system in the N-1 configuration.

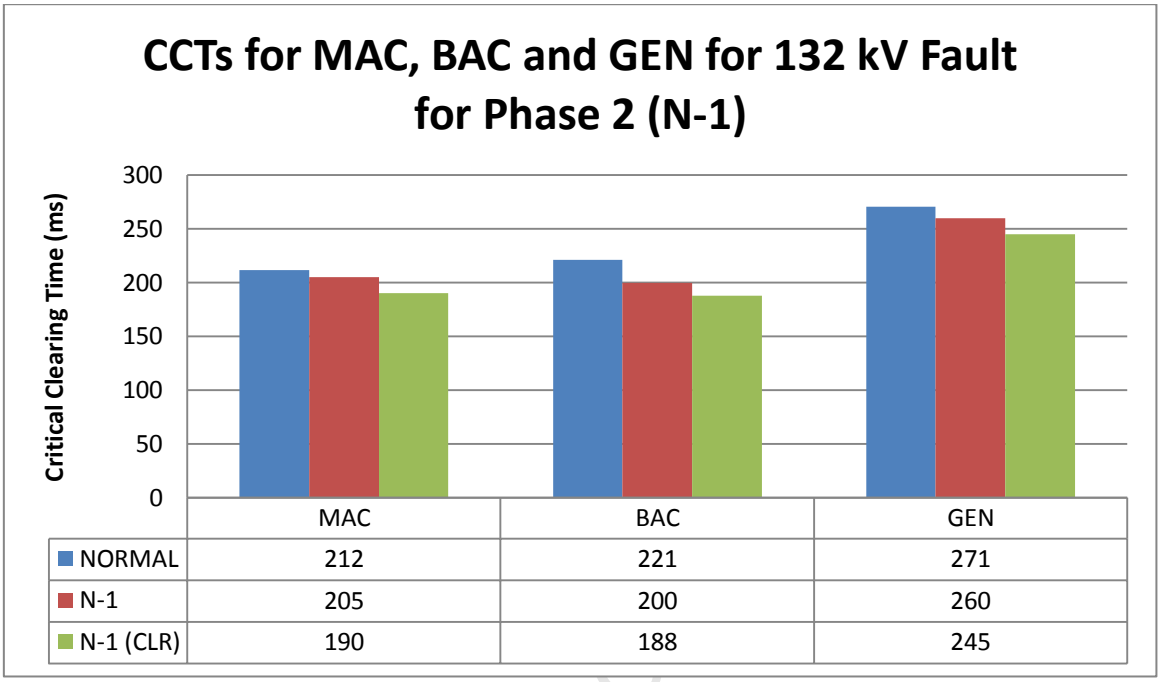


**Figure 5.20:** *Phase 2 Summary Chart of CCTs for 132 kV System Fault (N-1 Contingency)*

A summary chart of the CCTs for the synchronous machines in the Phase 2 N-1 configuration follows in figure 5.21 for a machine bus fault.

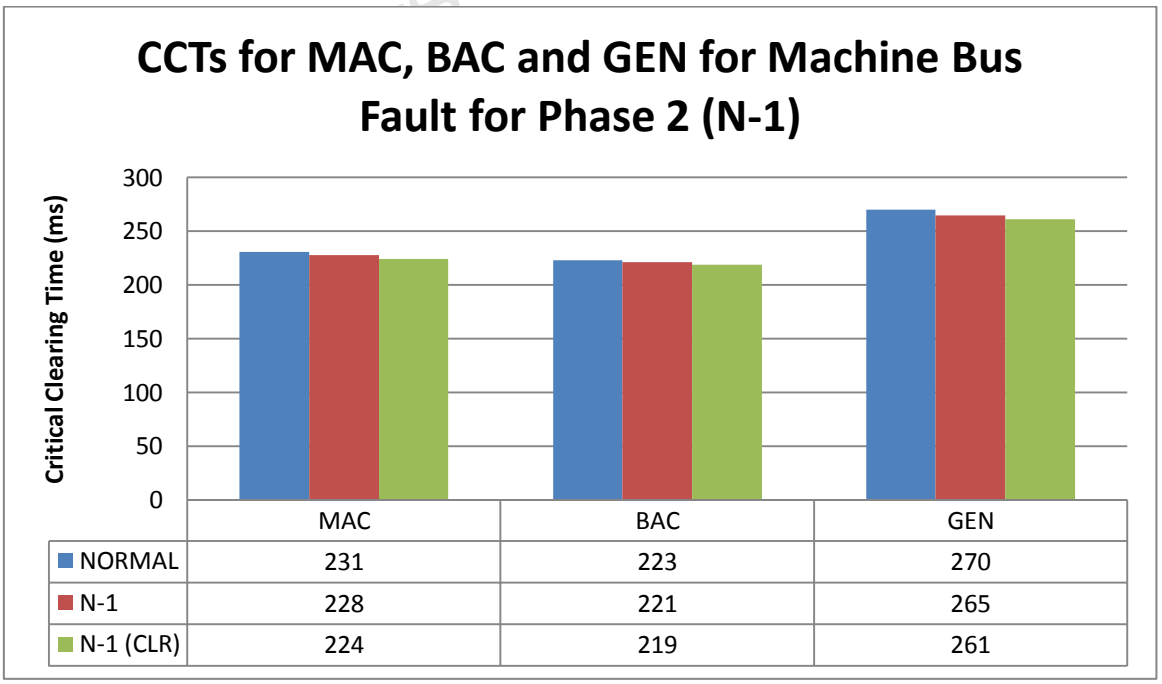


**Figure 5.21:** *Phase 2 Summary Chart of CCTs for Machine Bus Fault (N-1 Contingency)*

## 5.4 Phase 3

The fourth phase (Phase 3) involves significant utility infrastructure upgrades including the construction of a new transmission substation (SOL B MTS).

The new transmission substation will initially be fed by two 400 kV incomers from Kriel and Tutuka power stations.

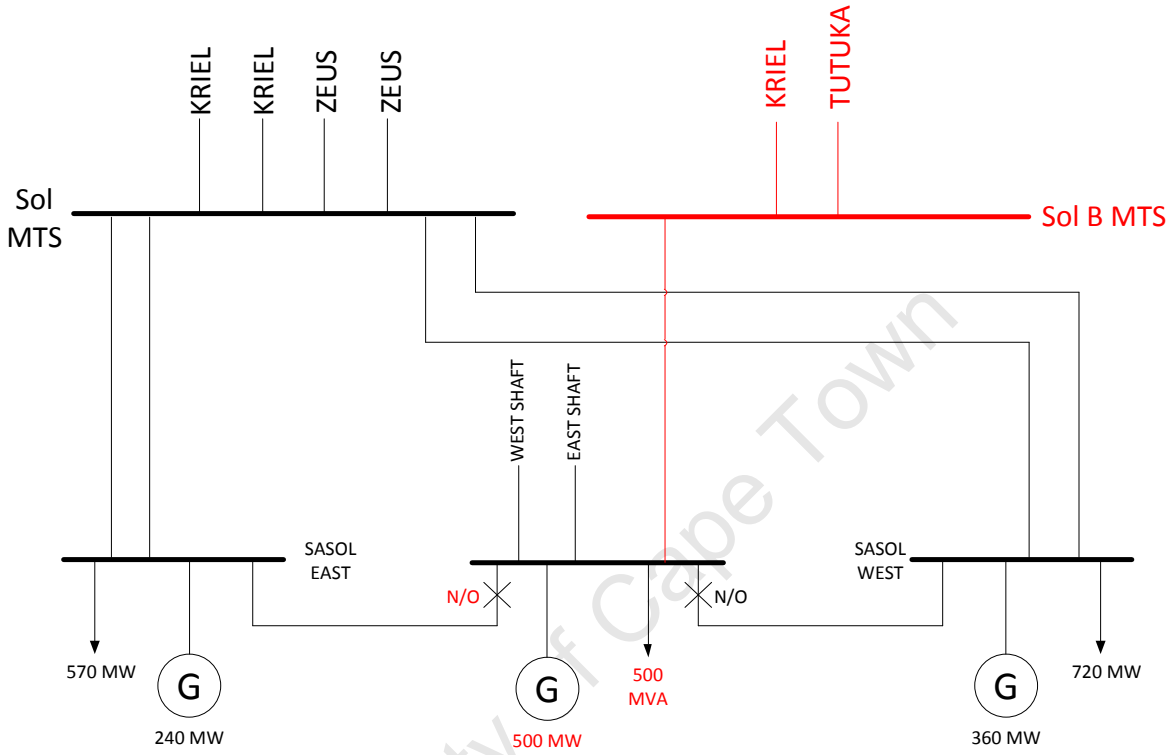


**Figure 5.22:** *Sasol Synfuels and Eskom TDP Phase 2*

The connection of the new transmission substation, SOL B MTS, is coincident with the addition of 200 MVA load and an additional 260 MW of generating capacity.

The switch-plant will also be disconnected from the eastern switch-plant since the power will either be balanced or there will be a net outflow of power due to the increased generating capacity.

At this point the SOL MTS will again have the capability of operation in N-2 supply contingency.

**Summary of changes from Phase 2:**

- 200 MVA additional load
- 260 MW additional generation
- Critical generation capability
- Disconnection from 2H4-SP-01
- Additional incomer to 132 kV D Bus

The additional synchronous generators in Phase 3 are not analysed in this study.

The model used to simulate Phase 3 is illustrated in Appendix 9.1.3.

### 5.4.1 Initial System Conditions

The fault contributions from each of the three incomers are tabulated below in table 5.19.

| Source | Contribution | Contribution (CLR) |
|---|---|---|
| **East Shaft Incomer** | 14 kA | 8.63 kA |
| **West Shaft Incomer** | 15 kA | 9 kA |
| **SOL B Incomer** | 18 kA | 10 kA |

**Table 5.19:** *Phase 3 System Conditions*

Since the methodology has been established only the summary charts will be presented for the normal and N-1 transient stability analyses.

The fault-level for the normal condition with CLRs in service is 45.5 kA, while the fault-level without CLRs is 64.9 kA.

### 5.4.2 Normal Transient Stability Analysis

The four scenarios that will be analysed in this case study are:

- 132 kV Fault for No CLRs
- 132 kV fault for CLRs in service
- Machine Bus Fault for no CLRS
- Machine bus fault for CLRs in service

The CCTs are tabulated below in table 5.20 for both machine bus and system bus symmetrical faults for the normal Phase 3 configuration.

The lowest CCTs, and corresponding stability margins, occur for a 132 kV system bus fault with CLRs in service.

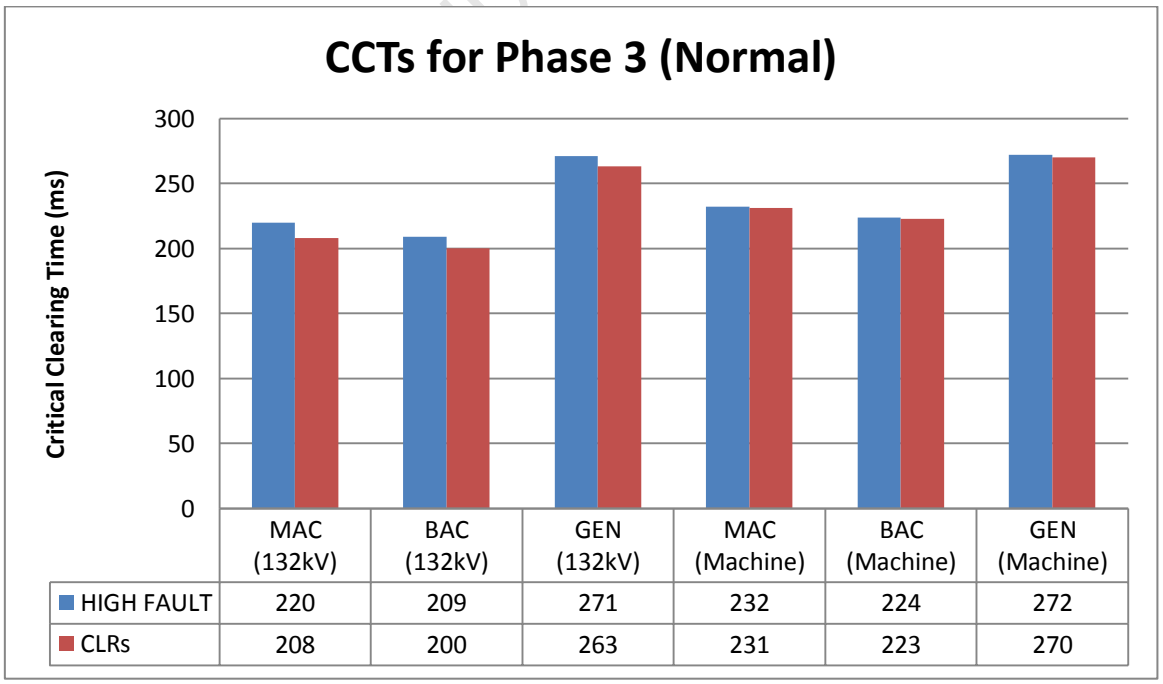


**Table 5.20:** *CCTs for Phase 3 with and without CLRs (Normal Configuration)*

### 5.4.3 N-1 Contingency Transient Stability Analysis

The N-1 supply contingency with the largest impact on the system fault-level is with the new SOL B line out of service. This reduces the fault-level by 18 kA (without CLRs) or 10 kA (with CLRs).

The actual system fault-level is then either 35.5 kA (with CLRs) or 46.9 kA (without CLRs).

The CCTs are tabulated below in table 5.21 for both machine bus and system bus symmetrical faults for the N-1 Phase 3 configuration.

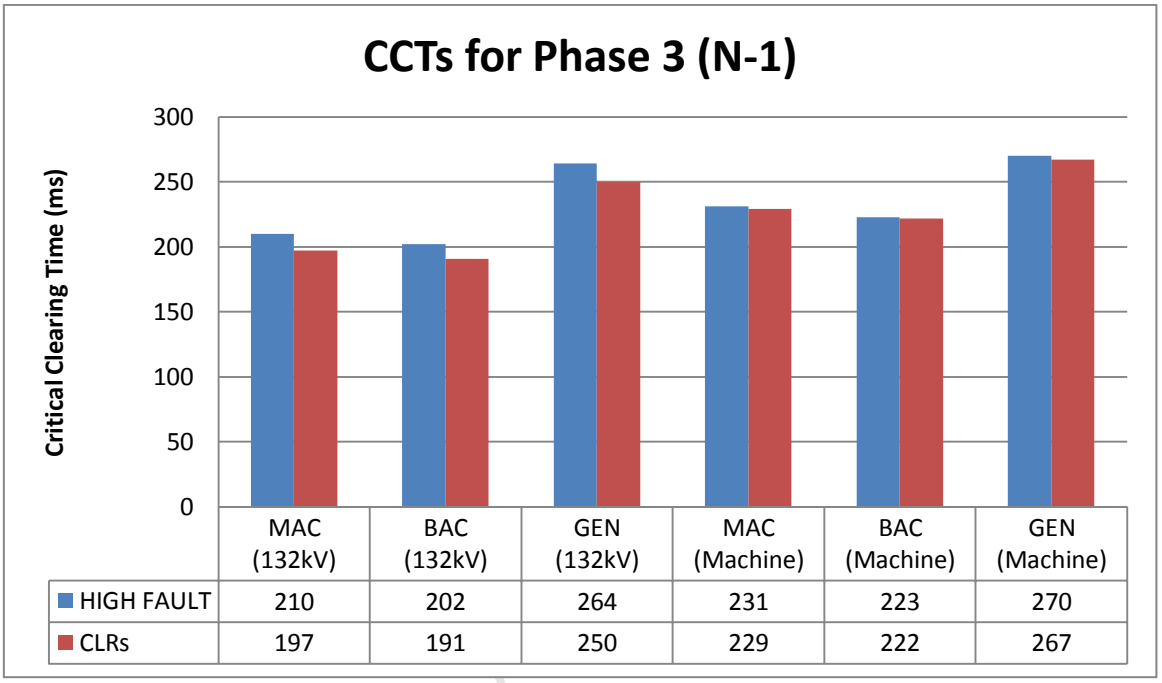


**Table 5.21:** *CCTs for Phase 3 with and without CLRs (N-1 Configuration)*

It can be noted that in general a high fault-level in this system improves the transient stability margin, while a low fault-level reduces the transient stability margin.

There is an apparent trade-off between transient stability margin and fault-level, since it is generally desirable to have a low fault-level and large transient stability margin.

## 5.5 Phase 4

The final phase of the infrastructure upgrade involves a second 400 kV transmission line from Kriel power station being installed and connected.

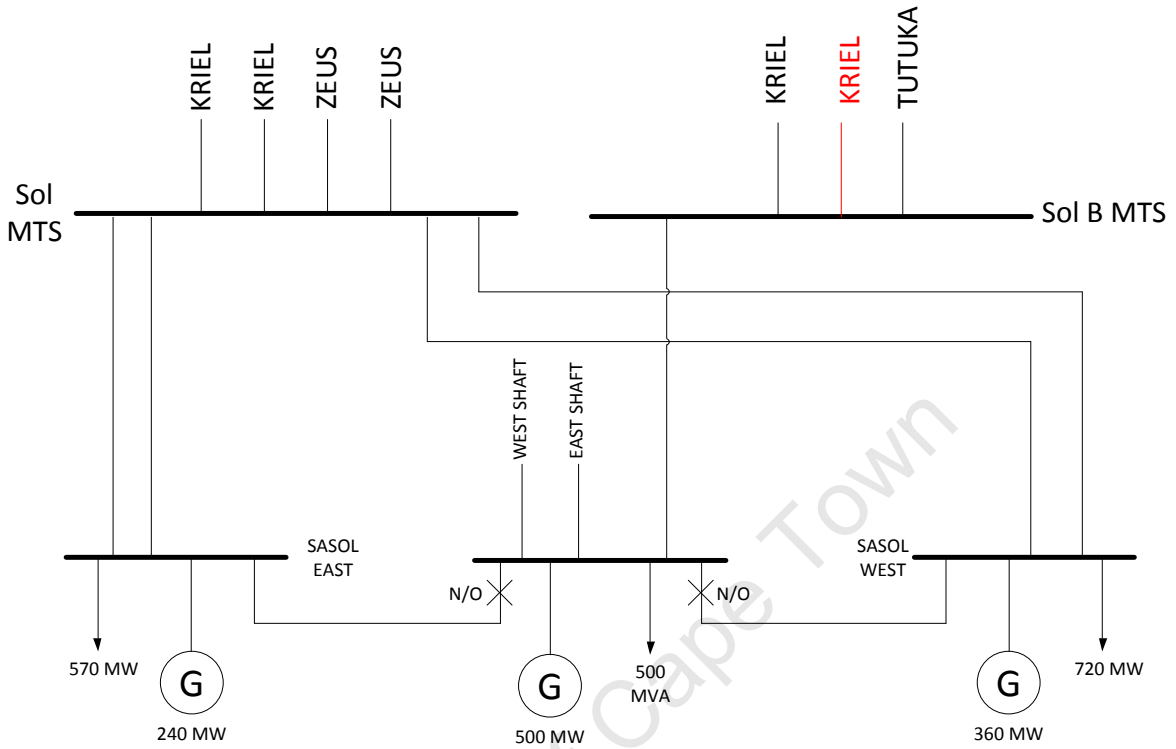


**Summary of changes from Phase 3:**

- Additional incomer to SOL B MTS

### 5.5.1 Initial System Conditions

The fault contributions from each of the three incomers are tabulated below in table 5.22.

| Source | Contribution | Contribution (CLR) |
|---|---|---|
| **East Shaft Incomer** | 14 kA | 8.63 kA |
| **West Shaft Incomer** | 15 kA | 9 kA |
| **SOL B Incomer** | 19.5 kA | 11.5 kA |

**Table 5.22:** *Phase 4 System Conditions*

The fault-level difference at the 132 kV level is not hugely significant compared to the Phase 3 configuration.

The calculation of CCTs for 132 kV bus and machine bus symmetrical faults is presented in the following two sections.

### 5.5.2 Normal Transient Stability Analysis

A summary chart of the CCTs for the synchronous machines in the Phase 3 normal configuration follows below in figure 5.23.

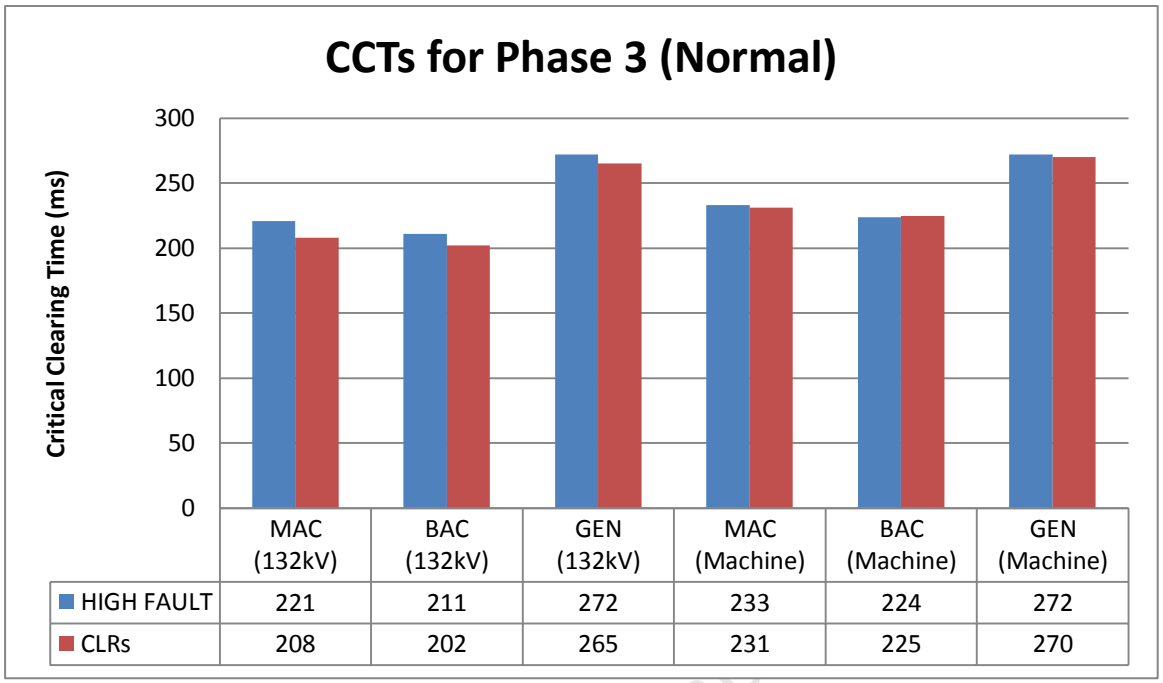


**Figure 5.23:** *CCTs for Phase 3 with and without CLRs (Normal Configuration)*

### 5.5.3 N-1 Contingency Transient Stability Analysis

A summary chart of the CCTs for the synchronous machines in the Phase 3 N-1 configuration follows in figure 5.24.

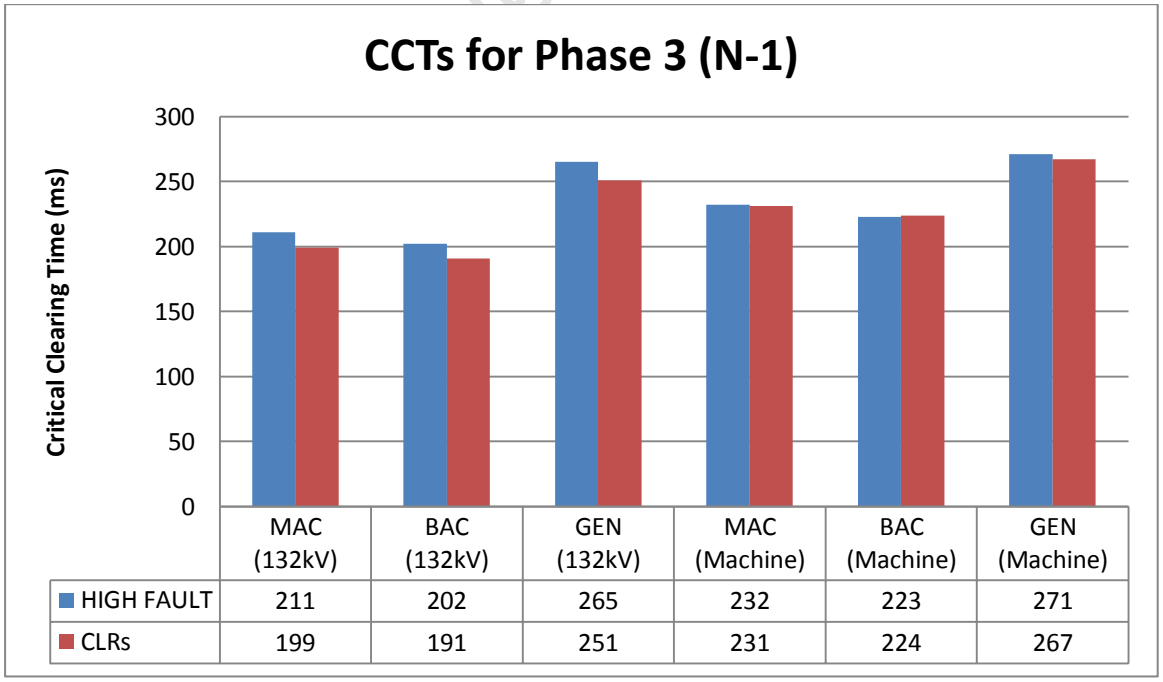


**Figure 5.24:** *CCTs for Phase 3 with and without CLRs (N-1 Configuration)*

## 5.6 Total System CCTs

The first of the case studies involves the determination of the CCTs for every synchronous machine connected to the Sasol Synfuels network in the scope of work. The machines are separated into generators and motors and these divisions are further divided into functional units.

### 5.6.1 Synchronous Generators

Table 5.23 shows the CCTs and angles for generators one to six West for a three-phase fault.

Generator 4 and generator 1 feed two blocks while the remaining four generators each supply one block (boiler-substation), since there are eight boilers on the West plant.

The initial power angle is 39.3 degrees for the generators feeding a single block. The initial power angle is 37.1 degrees for the generators feeding two blocks.

The transient stability margin is defined as the difference between the initial operating power angle and the critical clearing angle.

| Machine | CCT | Critical Angle | Margin |
|---|---|---|---|
| **Gen 1 West** | 292 ms | 122.0° | 84.9° |
| **Gen 2 West** | 290 ms | 124.6° | 84.7° |
| **Gen 3 West** | 290 ms | 124.6° | 84.7° |
| **Gen 4 West** | 292 ms | 122.0° | 84.9° |
| **Gen 5 West** | 290 ms | 124.6° | 84.7° |
| **Gen 6 West** | 290 ms | 124.5° | 84.7° |

**Table 5.23:** *ST-Driven Synchronous Generators West*

Table 5.24 shows the CCTs for generators one to four East for a bolted three-phase fault.

Generator 4 and generator 1 feeds each feed two blocks. There are 9 boilers on Eastern plant and two of the blocks are fed directly from transmission level.

The initial power angle for generator 2 and generator 3 is 45.5 degrees. The initial power angle for generator 1 and generator 4 is 42.5 degrees.

| Machine | CCT | Critical Angle | Margin |
|---|---|---|---|
| **Gen 1 East** | 281 ms | 123.0° | 80.5° |
| **Gen 2 East** | 276 ms | 123.0° | 77.5° |
| **Gen 3 East** | 276 ms | 123.0° | 77.5° |
| **Gen 4 East** | 281 ms | 123.0° | 80.5° |

**Table 5.24:** *ST-Driven Synchronous Generators East*

Table 5.25 shows the CCTs for the two GT-driven generators connected to 2H4-SP-02 for a bolted three-phase fault. The initial power angle for both GT-driven generators is 39.5 degrees.

| Machine | CCT | Critical Angle | Margin |
|---|---|---|---|
| **GT Gen 1** | 267 ms | 111.5° | 72.0° |
| **GT Gen 2** | 267 ms | 111.4° | 71.9° |

**Table 5.25:** *GT-Driven Synchronous Generators*

The GT-driven generators are currently configured in an open-cycle arrangement. The principle of open cycle operation is illustrated below in figure 5.25.

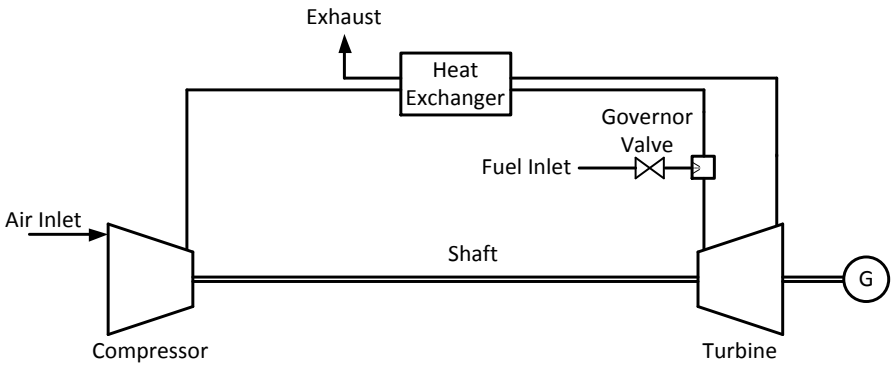


**Figure 5.25:** *Gas Turbine Open Regenerative Cycle Operation*

The intention is to convert these generators to closed-cycle mode in the near future. This will involve the addition of a steam-turbine and generator per unit which will significantly increase the overall efficiency. The principle of close cycle operation is illustrated below in figure 5.26.

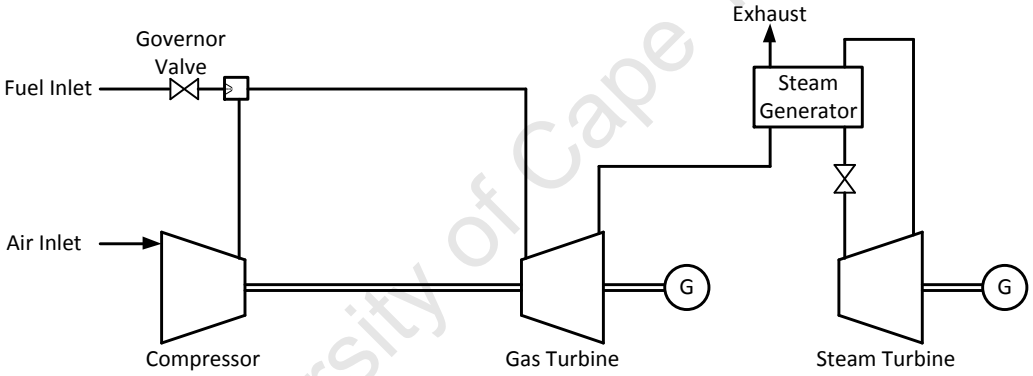


**Figure 5.26:** *Gas Turbine Combined Cycle Operation*

An assessment of the transient stability margin should be done on the new generators as they are connected to the system.

It is possible that the OCGT may be converted to CCGT without implementing ST-driven generators. The steam raised in the heat exchanger may be directed back into the plant steam system.

The transient stability characteristics (including CCT, critical angle and margin) for all synchronous generators in the system are summarised in figure 5.27.

The CCTs of the ST-driven generators are practically the same, and have an average value of 285.8 ms. This is the same as the weighted average since the motors have the same MVA rating and inertia.

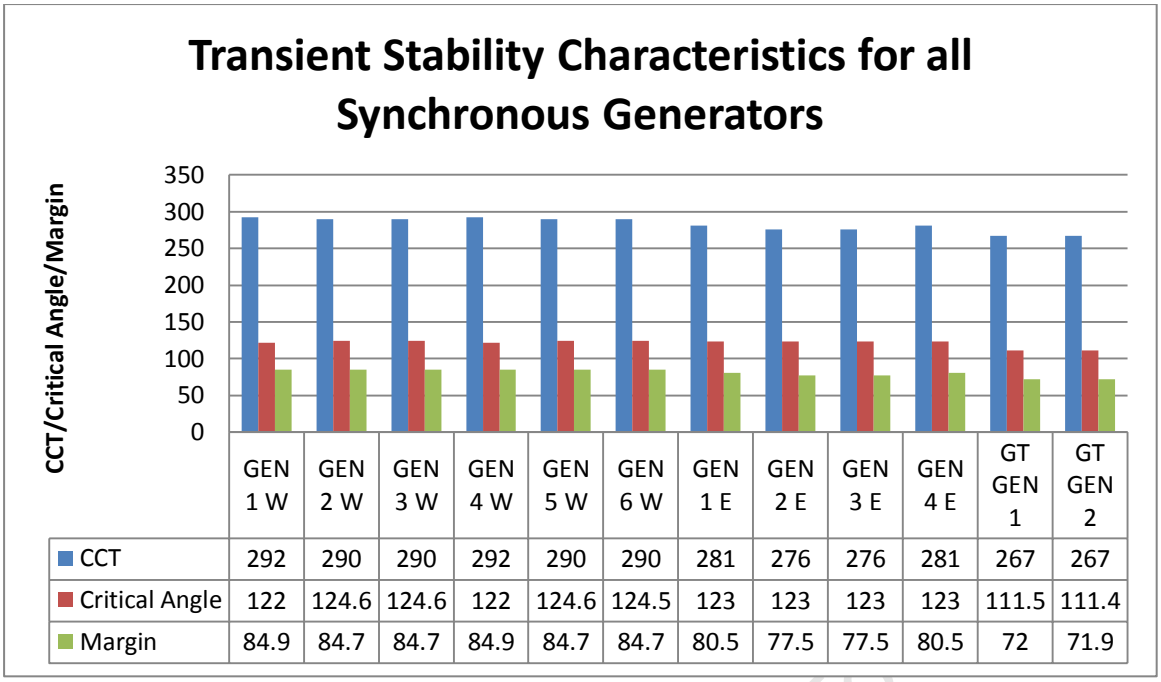


**Figure 5.27:** *Transient Stability Characteristics for all Synchronous Generators*

### 5.6.2 Synchronous Motors

Table 5.26 shows the CCTs for the 36 MW air compressors for oxygen trains one to seven West and train seven east. The initial power angle is -50.3 degrees. This means that the transient stability margin is 71.7 degrees.

| Machine | CCT | Critical Angle | Margin |
|---|---|---|---|
| **36 MW AC Train 1 West** | 258 ms | -122.0° | 71.7° |
| **36 MW AC Train 2 West** | 258 ms | -122.0° | 71.7° |
| **36 MW AC Train 3 West** | 257 ms | -122.0° | 71.7° |
| **36 MW AC Train 4 West** | 257 ms | -122.0° | 71.7° |
| **36 MW AC Train 5 West** | 257 ms | -122.0° | 71.7° |
| **36 MW AC Train 6 West** | 257 ms | -122.0° | 71.7° |
| **36 MW AC Train 7 West** | 257 ms | -122.0° | 71.7° |
| **36 MW AC Train 7 East** | 257 ms | -122.4° | 71.7° |

**Table 5.26:** *36 MW Air Compressors for Oxygen Plant*

Table 5.27 shows the CCTs for the 55 MW MAC motors of oxygen plant train 15 and train 16. The initial power angle is -39.5 degrees for the MAC motors of train 15 and train 16.

| Synchronous Motor | CCT | Critical Angle | Margin |
|---|---|---|---|
| **55 MW MAC Train 15** | 220 ms | -104.6° | 65.1° |
| **55 MW MAC Train 16** | 221 ms | -104.7° | 65.5° |

**Table 5.27:** *Main Air Compressor Motors for Train 15 and 16*

Table 5.28 shows the CCTs for the 23 MW Booster Air Compressor (BAC) motors of oxygen plant train 15 and train 16.

The initial power angle is -35.0 degrees for the BAC motors of Train 15 and Train 16.

| CCT | CCT | Critical Angle | Margin |
|---|---|---|---|
| **23 MW BAC Train 15** | 209 ms | -112.6° | 77.6° |
| **23 MW BAC Train 16** | 210 ms | -114.1° | 79.1° |

**Table 5.28:** *BAC Motors for Train 15 and 16*

The transient stability characteristics (including CCT, critical angle and margin) for all synchronous motors in the system are summarised in figure 5.28.

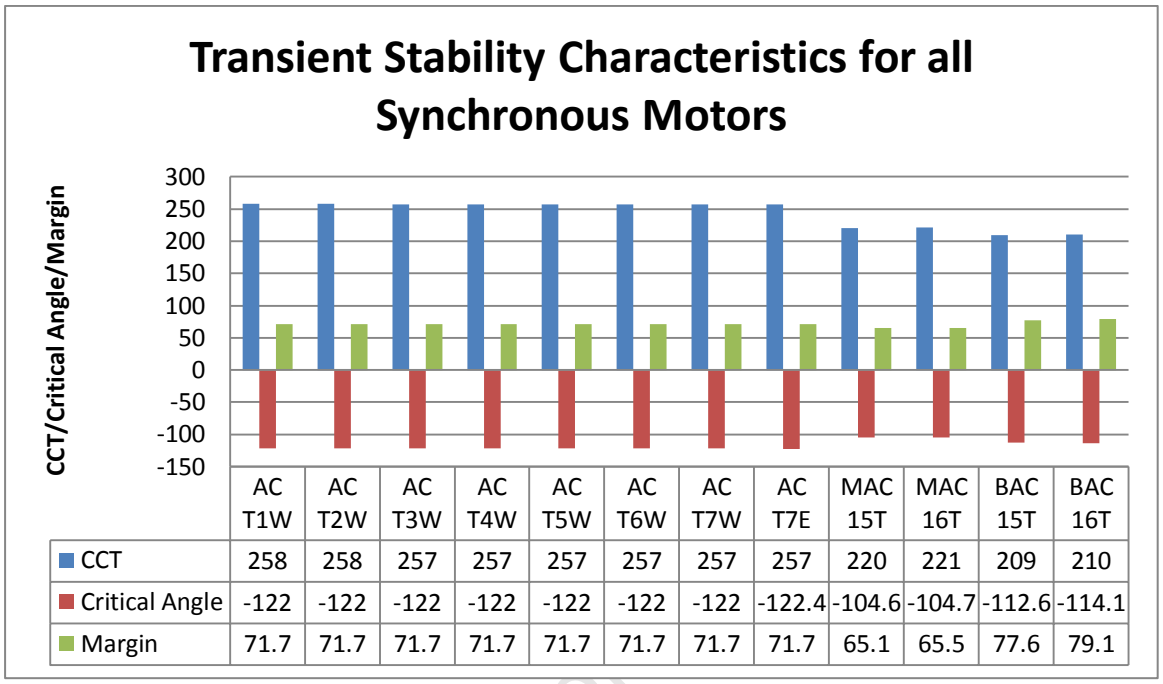


| | AC T1W | AC T2W | AC T3W | AC T4W | AC T5W | AC T6W | AC T7W | AC T7E | MAC 15T | MAC 16T | BAC 15T | BAC 16T |
|---|---|---|---|---|---|---|---|---|---|---|---|---|
| CCT | 258 | 258 | 257 | 257 | 257 | 257 | 257 | 257 | 220 | 221 | 209 | 210 |
| Critical Angle | -122 | -122 | -122 | -122 | -122 | -122 | -122 | -122.4 | -104.6 | -104.7 | -112.6 | -114.1 |
| Margin | 71.7 | 71.7 | 71.7 | 71.7 | 71.7 | 71.7 | 71.7 | 71.7 | 65.1 | 65.5 | 77.6 | 79.1 |

**Figure 5.28:** *Transient Stability Characteristics for all Synchronous Motors*

The lowest motor CCTs correspond to the BAC motors which have the lowest output power and the lowest inertia.

The MAC motors have a CCT which is shorter than the AC motors of the 14 original oxygen trains. The corresponding critical angle for the MAC motors is significantly lower than the critical angle for the existing AC motors.

The average CCT for the 36 MW AC motors is 257.25 ms with little deviation from this value. This is also the weighted average for the 36 MW AC motors.

## 5.7 2H4-SP-02 Load Shedding and Islanding Study

The aim of this case study is to analyse the transient and dynamic response of the 2H4-SP-02 switch-plant to a supply disturbance and N-1 supply contingency conditions.

The switch-plant is designed with three incoming utility lines each of which are connected to a dedicated busbar. The switch-plant makes use of four bus sections, three of which are for normal operation while one is designated as the critical bus. The D bus, which is connected to the third incoming line, is a short-bus section designed purely for accommodating the third line.

The diagram illustrated in figure 5.29 provides a simplified representation of the current and projected arrangement of the switch-plant.

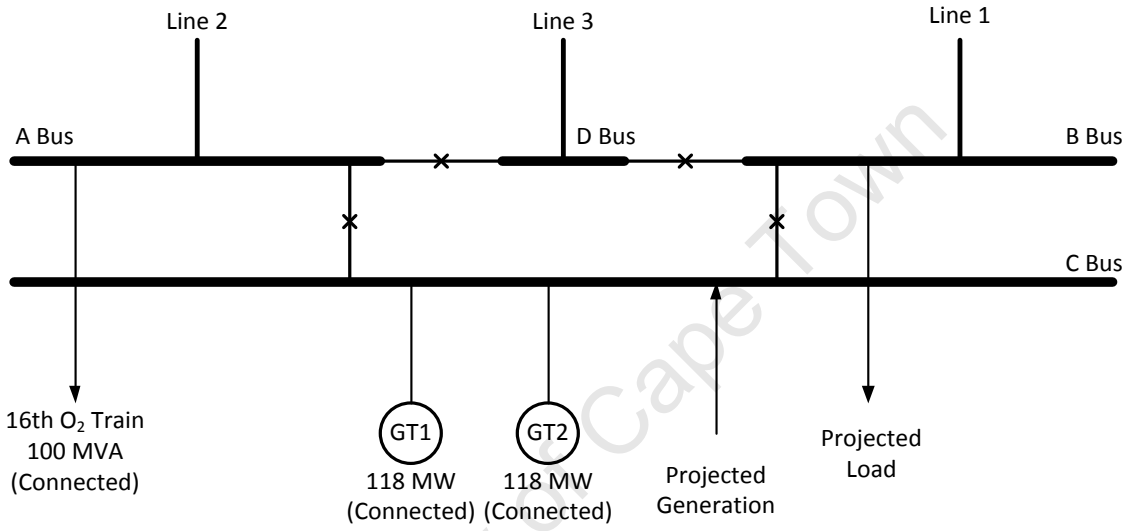


**Figure 5.29:** *2H4-SP-02 Current and Projected Arrangement*

The power system configuration differs from the Phase 4 configuration. It was considered overly optimistic to have 500 MW of additional generation in service by Phase 4.

**Assumptions for Case Study:**

- Two GT generators in service
- Critical power available and connected

### 5.7.1 Load Shedding and Islanding Philosophies

The islanding philosophy is based on a number of factors including the philosophy applied to the existing network, the Eskom requirements for co-generation, the substation capabilities and the plant ability to ride through disturbances.

In the event of a disturbance the three main principles of operation are as follows:

1. Allow time for corrective action
2. Island critical loads
3. Island total substation

Bus C is connected to the critical loads and will be islanded as a first option. The total substation will be islanded, if the disturbance persists, by opening the Eskom lines. The islanding philosophy recognises the fact that Sasol generation cannot support the Eskom frequency in overload conditions. Exposure to abnormal under-frequency conditions will result in damage to plant.

The design of the GT-driven generators does not allow for these generators to be small-islanded (supply only their own auxiliaries). These generators are also not suitable for supplying critical load.

The initial arrangement will not have any Eskom lines connected. The substation will be connected to existing generation via the east-tie. The GT-driven generators will be connected to the A and B bus and the 16$^{th}$ oxygen train will be connected to the A bus. This is designed as a temporary arrangement to ensure beneficial operation of the GT-driven generators while the Eskom lines are built.

The final connection will have all GT-driven generators connected to the A and B buses. All critical loads will be connected to the C bus. The Eskom lines will be connected to buses A, B and C. All ties will be closed in normal running conditions, excluding the eastern and western ties.

### 5.7.2 Normal Power Flow

The normal power flow conditions are described in table 5.29. This simulation assumes the imports are divided equally amongst the three lines.

| Line | Real Power | Reactive Power | Apparent Power | Power Factor |
|---|---|---|---|---|
| **Line 1 (B)** | 186.8 MW | 29.7 MVAr | 189.2 MVA | 98.8 % |
| **Line 2 (A)** | 186.8 MW | 29.7 MVAr | 189.2 MVA | 98.8 % |
| **Line 3 (D)** | 186.8 MW | 29.7 MVAr | 189.2 MVA | 98.8 % |
| **Total** | 560.4 MW | 89.1 MVAr | 567.6 MVA | 98.8 % |

**Table 5.29:** *Line Flows for Normal Conditions*

### 5.7.3 Contingency Power Flows

The contingencies that are allowed for in the design are one generator out of service and one line out of service.

The N-1 supply contingency will result in the power flows described in table 5.30.

| Line Out | Line 1 | Line 2 | Line 3 |
|---|---|---|---|
| **Line 1 (B)** | 0 MVA | 279.9 MVA | 279.9 MVA |
| **Line 2 (A)** | 279.9 MVA | 0 MVA | 279.9 MVA |
| **Line 3 (D)** | 279.9 MVA | 279.9 MVA | 0 MVA |

**Table 5.30:** *Power Flows for N-1 Supply Contingency*

### 5.7.4 Critical Bus Islanding Philosophy

The intention of islanding the critical bus (Bus C) is to protect the critical load against upstream network disturbances.

The scheme should be sensitive enough to protect load while also allowing for natural network recovery before the bus is islanded.

The critical bus will be islanded by opening the A-C and B-C ties. This will require that the critical bus is connected to a critical generator, which is not currently the case.

The two parameters used to detect a disturbance are the incomer voltage and the incomer frequency. The voltage check also incorporates a reverse current check. A voltage discrepancy typically either represents a transient system fault or a fault in the voltage regulation system.

A frequency deviation, as discussed in chapter 2, is indicative of an overloaded system. This situation may be transient if there is an effective UFLs scheme in place or sufficient spinning reserve to eliminate the imbalance. The proposed undervoltage settings are 200 ms and 80% of nominal voltage. These settings allow a compromise between ride-through and fast tripping in the event of a severe disturbance.

The UF settings typically allow longer operation in low-frequency conditions since the power system is less susceptible to UF than UV conditions. The rate of change of frequency will be used as a primary indicator in the critical bus islanding scheme. A high df/dt typically indicates a severe network fault such as loss of significant generation, while a low df/dt typically indicates a power imbalance. If the initial rate of change of frequency is greater than 0.3 $Hz.s^{-1}$ then the critical bus will be islanded. In the case of a low rate of change of frequency the critical bus will be islanded if the frequency decays below 48.5 Hertz for 1.5 seconds.

#### *5.7.4.1 Normal Bus Islanding Philosophy*

The intention of islanding the normal buses is to protect the Sasol generators from a utility network disturbance. The normal bus islanding sequence should always occur after the critical bus islanding sequence. In the event of a high df/dt the priority is to disconnect the utility lines regardless of islanding sequence.

The first islanding option is a long-bus island which involves opening the utility incomers and the east-tie.

The second option is to island each busbar and open line 1 and line 2 as well as the A-D and B-D ties. Line 3 will remain connected to bus D. This is a short-bus island condition.

For a sustained UV condition the island will be initiated if there is a minimum of 5 % reverse power; which indicates an external fault. The UV settings for the normal islanding scheme are proposed to be 500 ms for 80 % nominal voltage. The time delay can be set to 200 ms if a high directional overcurrent is detected.

The UF settings are proposed to be 100 ms delay for 0.3 $Hz.s^{-1}$ and a 0.5 second delay for a sustained UF event below 47.5 Hz. The UF element will be blocked if the voltage is below 70% since the UV element will control islanding in this situation. The islanding settings are summarised below in table 5.31.

| Protection | Limit | Delay |
|---|---|---|
| **UV Critical** | 80 % | 200 ms |
| **UF Critical** | -0.3 $Hz.s^{-1}$ | 0 |
| **UF Critical** | 48.5 Hz | 1500 ms |
| **UV Normal** | 80 % | 500 ms |
| **UF Normal** | -0.3 $Hz.s^{-1}$ | 100 ms |
| **UF Normal** | 47.5 Hz | 500 ms |

**Table 5.31:** *UF and UV Proposed Settings*

### 5.7.5 **Critical Bus Islanding Logics**

The critical bus islanding logics are described in figure 5.30 shown below. The logics are simplified for the purposes of readability. The conditions for remote initiating are not shown in this diagram.

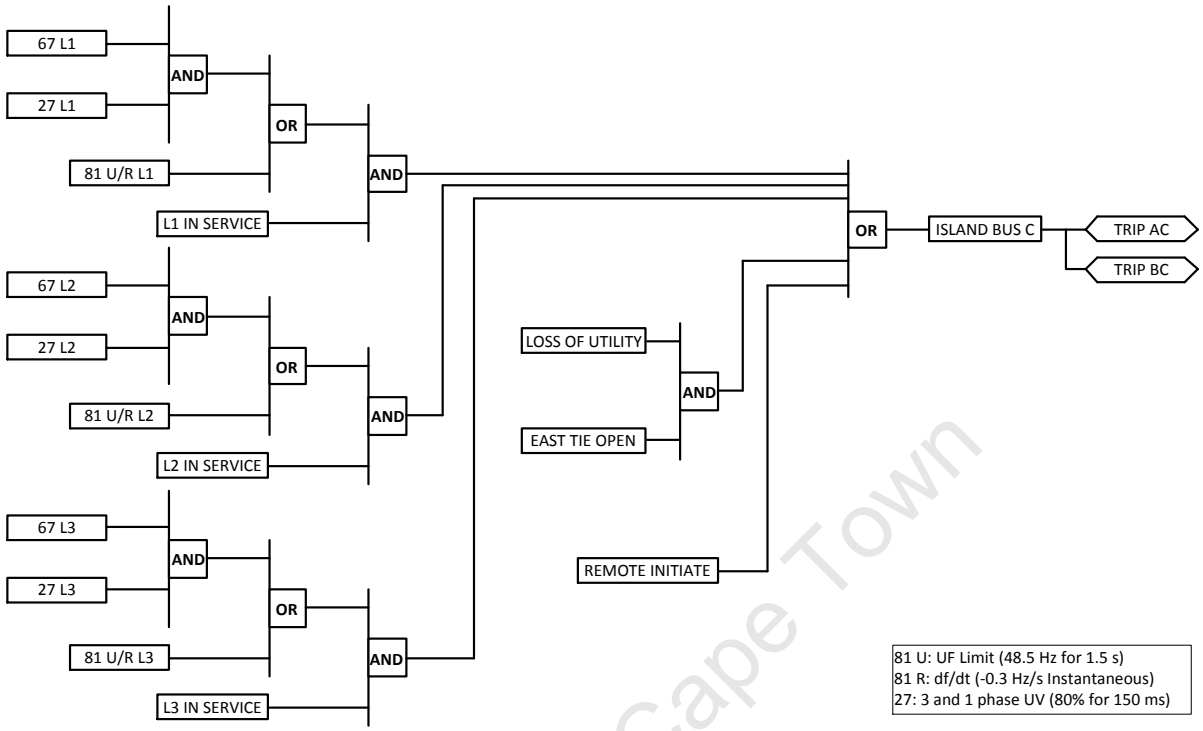


**Figure 5.30:** *Critical Bus Islanding Logics*

The basic requirement for islanding the critical bus, as described in the islanding philosophy, is that a reverse current in combination with an undervoltage condition will initiate critical bus islanding.

Critical bus islanding will also be initiated by an underfrequency event or a loss of the utility supply lines.

The inputs to the islanding logics are the outputs of the measurement elements and the outputs of the islanding logics are two trip signals to the AC and BC ties respectively.

The remote initiate function requirements are that the AC, BC and the east-tie are all closed as well as other conditions from 2H4-SP-01.

The underfrequency (ANSI 81) and undervoltage (ANSI 27) elements which are represented as two elements per line will in reality be four elements per line. This is done since the undervoltage element requires single and three phase measurement, and the underfrequency element requires frequency and rate of change of frequency measurements.

### 5.7.6 **Normal Bus Islanding Logics**

The normal bus islanding logics are described in simplified form in figure 5.31 below. There is no remote initiate function for the normal islanding logics.

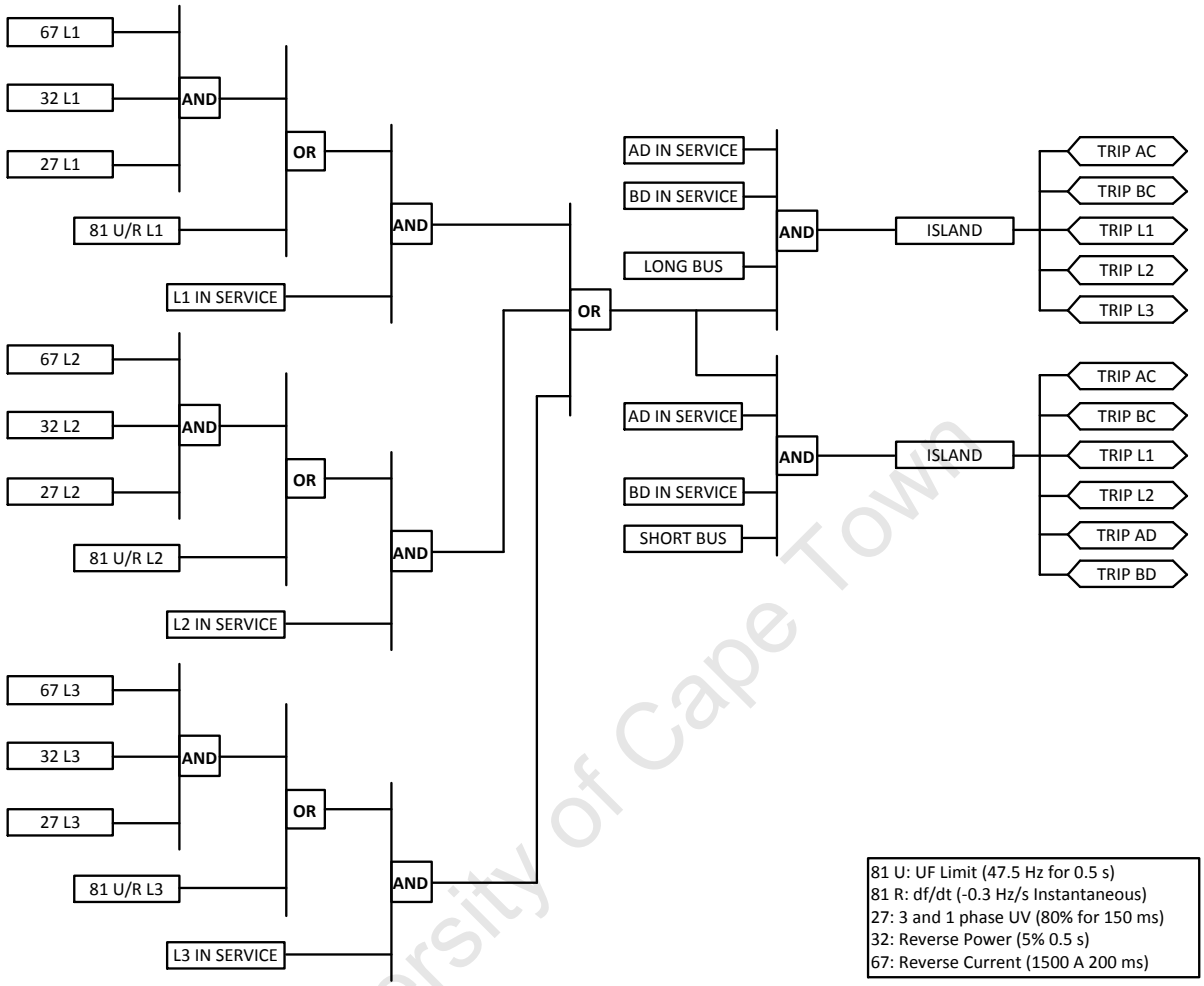


**Figure 5.31:** *Normal Bus Islanding Logics*

The normal bus logics cater for both short-bus and long-bus islanding philosophies. Both of these schemes are described in the normal bus islanding philosophy section.

The critical bus should be islanded by the time that a normal bus island initiate command is issued, but the AC and BC ties are re-tripped for security reasons.

The basic requirement for normal bus islanding is that an undervoltage occurring with a reverse current and reverse power condition exists. This condition will initiate the island.

An underfrequency or high rate of change of frequency will also initiate islanding.

The inputs to the islanding logics are the outputs of the measurement elements and the outputs of the islanding logics are five or six trip signals depending on whether short-bus or long-bus islanding is selected.

### 5.7.8 Islanding Tripping Matrix

The following matrices aim to provide an indication of the breakers to be tripped in any contingency situation. There are a total of eight breakers that are controlled by the islanding scheme.

The first matrix, defined in table 5.32, describes the islanding scheme for both critical and normal bus islanding when a long-bus islanding scheme is implemented. It is assumed that critical generation does not exist at 2H4-SP-02.

| Condition | AC | BC | AD | BD | L1 | L2 | L3 | E- Tie |
|---|---|---|---|---|---|---|---|---|
| L1 3-ϕ UV (20%) (200 ms) | X | X | | | | | | |
| L1 1-ϕ UV (20%) (200 ms) | X | X | | | | | | |
| L1 3-ϕ UV (20%) (500 ms) | | | | | X | X | X | X |
| L1 1-ϕ UV (20%) (500 ms) | | | | | X | X | X | X |
| L1 UF (48.5 Hz) (1500 ms) | X | X | | | | | | |
| L1 UF (47.5 Hz) (500 ms) | | | | | X | X | X | X |
| L1 UF (-0.3Hz.s$^{-1}$) (0 ms) | X | X | | | | | | |
| L1 UF (-0.3Hz.s$^{-1}$) (100 ms) | | | | | X | X | X | X |

**Table 5.32:** *Tripping Matrix (Long Islanding)*

The second matrix, defined in table 5.33, describes the islanding scheme for both critical and normal bus islanding when a short-bus islanding scheme is implemented.

| Condition | AC | BC | AD | BD | L1 | L2 | L3 | E- Tie |
|---|---|---|---|---|---|---|---|---|
| L1 3-ϕ UV (20%) (200 ms) | X | X | | | | | | |
| L1 1-ϕ UV (20%) (200 ms) | X | X | | | | | | |
| L1 3-ϕ UV (20%) (500 ms) | | | X | X | X | X | | X |
| L1 1-ϕ UV (20%) (500 ms) | | | X | X | X | X | | X |
| L1 UF (48.5 Hz) (1500 ms) | X | X | | | | | | |
| L1 UF (47.5 Hz) (500 ms) | | | X | X | X | X | | X |
| L1 UF (-0.3Hz.s$^{-1}$) (0 ms) | X | X | | | | | | |
| L1 UF (-0.3Hz.s$^{-1}$) (100 ms) | | | X | X | X | X | | X |

**Table 5.33:** *Tripping Matrix (Short Islanding)*

It is possible that an island condition may exist without an islanding signal having been given. Table 5.34 describes all possible island conditions for 2H4-SP-02.

| Condition | AC | BC | AD | BD | L1 | L2 | L3 | E- Tie |
|---|---|---|---|---|---|---|---|---|
| Bus C Island | X | X | | | | | | X |
| Long Island (A/B/D) | X | X | | | X | X | X | X |
| Bus A Island | X | | X | | | X | | X |
| Bus B Island | | X | | X | X | | | X |

**Table 5.34:** *Possible Island Conditions*

It is possible to infer from the post-fault status of the breakers that specific group of disturbances may have occurred. The fault-finding can be further aided by load recordings offered by the incomer IEDs.

### 5.7.9 Incomer Line Disturbances

This case study will investigate the effect of voltage dips of varying depth and duration on the system response.

The following are the required deliverables for each case:

- **Power Flows**
  - Power Flow at Initiation
  - Post Island Power Flow
- **Islanding response**

The system response to a disturbance can be divided into the following distinct stages:

- **Stage 1**: Pre-disturbance conditions
- **Stage 2**: Transient response to disturbance
- **Stage 3**: Steady-state conditions during disturbance
- **Stage 4**: Critical bus islanding response
- **Stage 5**: Transient response to critical island initiation
- **Stage 6**: Steady-state critical island conditions
- **Stage 7**: Normal bus islanding response
- **Stage 8**: Transient response to normal island initiation
- **Stage 9**: Steady-state total island conditions

It is not required that the transient response be analysed for every disturbance. The transient response will only be analysed for the worst case condition where power swings and rotor angle sings may be a transient stability concern.

The line disturbances will be assumed to be a utility disturbance and will affect all three lines equally.

The occurrence of a 20 % undervoltage condition for 500 ms will result in critical and normal bus islanding.

A 500 ms voltage dip is regarded as a loss of supply and the utility lines are tripped. It would make no difference to the industrial system if the condition persisted beyond 500 ms.

#### i) Stage 1: Pre-Disturbance Conditions

The pre-disturbance conditions are summarised below in table 5.35 in the form of the line power flows.

| Line | Real Power | Reactive Power | Apparent Power | Power Factor |
|---|---|---|---|---|
| **Line 1 (B)** | 186.8 MW | 29.7 MVAr | 189.2 MVA | 98.8 % |
| **Line 2 (A)** | 186.8 MW | 29.7 MVAr | 189.2 MVA | 98.8 % |
| **Line 3 (D)** | 186.8 MW | 29.7 MVAr | 189.2 MVA | 98.8 % |
| **Total** | 560.4 MW | 89.1 MVAr | 567.6 MVA | 98.8 % |

**Table 5.35:** *Pre-Disturbance Conditions*

### ii) Stage 2: Transient Response to Disturbance

The GT Gen 1 and GT Gen 2 rotor power angles are visible below in figure 5.32 for 200 ms after the fault initiation. The initial angle is 37.2° and the angle 200 m after fault initiation is 41.0°. The settling angle for a sustained 20% undervoltage would be 27.2°. A steady-state voltage dip decreases the power angle in the case of a synchronous generator.

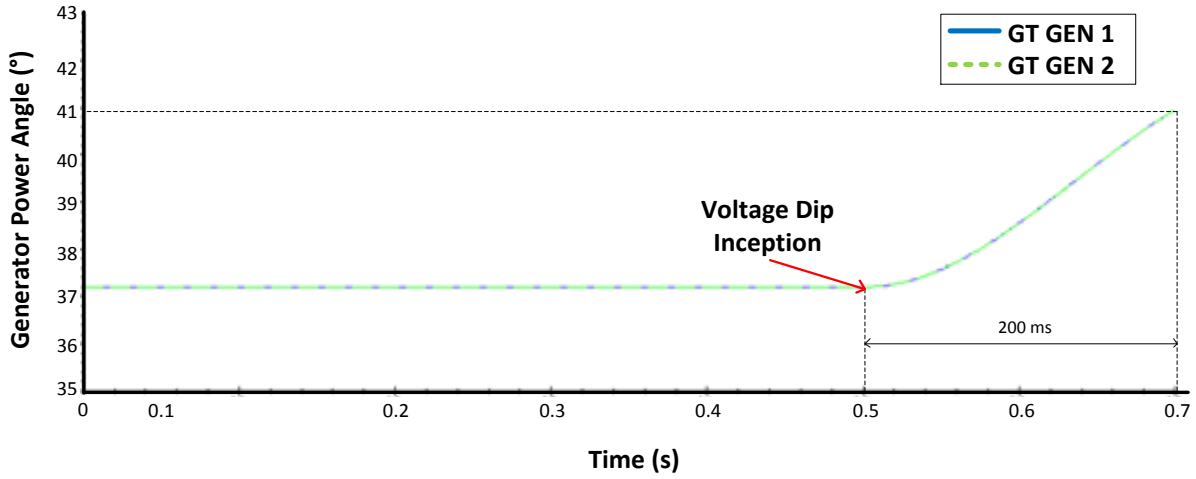


**Figure 5.32:** *Generator 1 & 2 Power Angles (200 ms Fault)*

The electrical power for GT Gen 1 and GT Gen 2 is shown below in figure 5.33. The electrical power suffers an impact decrease and then increases with significant overshoot. The electrical power would return to the pre-disturbance value.

The initial real power is 106.4 MW. At the moment of disturbance the real power drops to 88.2 MW and increases to a maximum of 114.3 MW after 200 ms.

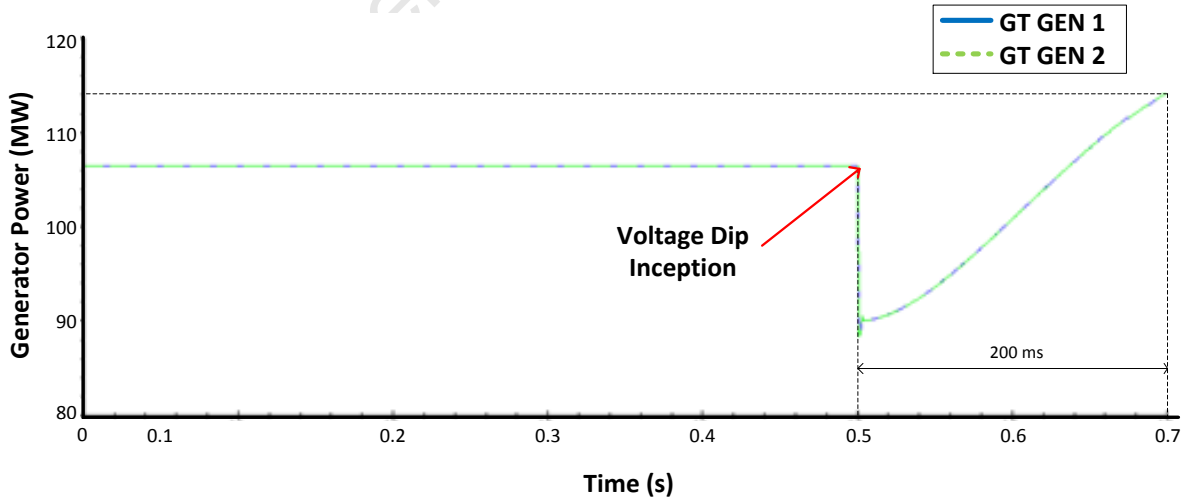


**Figure 5.33:** *Generator 1 & 2 Real Power (200 ms Fault)*

The synchronous motor rotor power angles are visible below in figure 5.34 for 200 ms after the fault initiation.

The initial power angle is for the MAC motor is -40.5° and the angle 200 ms after fault initiation is -43.6°. The settling angle for a sustained 20% undervoltage would be -30.2°.

The initial power angle is for the BAC motor is -37.9° and the angle 200 ms after fault initiation is -41.3°. The settling angle for a sustained 20% undervoltage would be -19.9°.

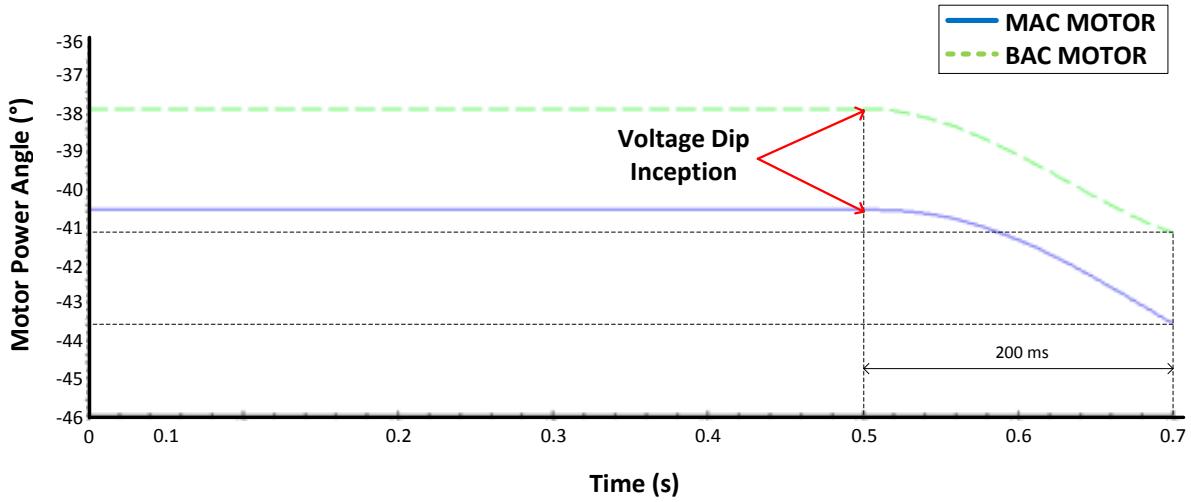


**Figure 5.34:** *Train 16 MAC and BAC Motor Power Angles (200 ms Fault)*

The MAC and BAC motor electrical real powers are shown below in figure 5.35.

The initial power consumed by the MAC motor is 55.7 MW at unity power factor. The power consumed dips to 44.1 MW at the moment of disturbance and reaches a peak of 56.7 MW after 200 ms.

The initial power consumed by the BAC motor is 23.4 MW at unity power factor. The power consumed dips to 18.5 MW at the moment of disturbance and reaches a peak of 25.1 MW after 200 ms.

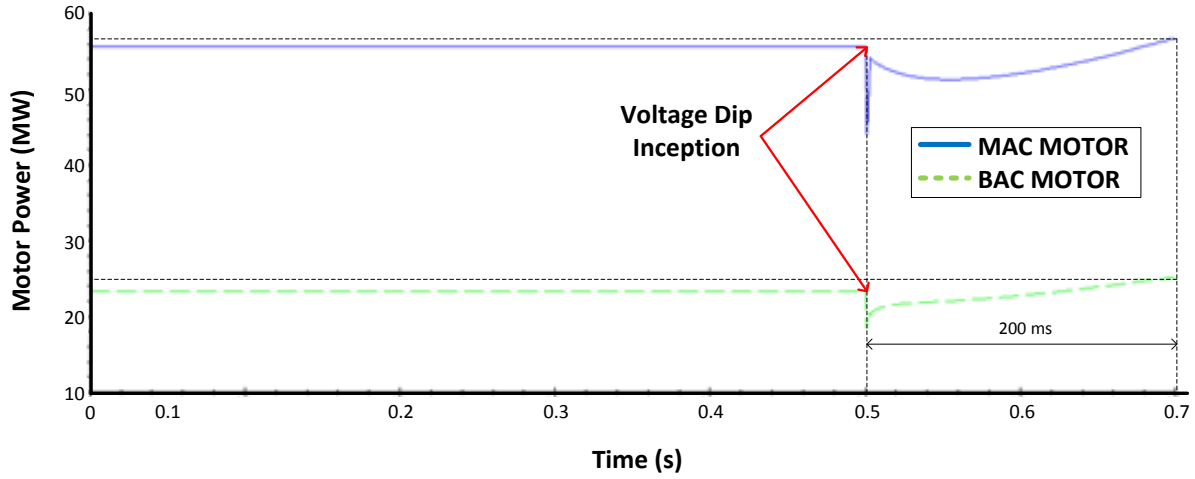


**Figure 5.35:** *Train 16 MAC and BAC Motor Power (200 ms Fault)*

### iii) Stage 3: Steady-State Conditions During Disturbance

The steady-state power flows are shown below in table 5.36 for a 20% voltage dip on the utility supply.

| Line | Real Power | Reactive Power | Apparent Power | Power Factor |
|---|---|---|---|---|
| **Line 1 (B)** | 174.5 MW | 49.6 MVAr | 182.4 MVA | 96.2 % |
| **Line 2 (A)** | 174.5 MW | 49.6 MVAr | 182.4 MVA | 96.2 % |
| **Line 3 (D)** | 174.5 MW | 49.6 MVAr | 182.4 MVA | 96.2 % |
| **Total** | 523.5 MW | 148.8 MVAr | 547.2 MVA | 96.2 % |

**Table 5.36:** *Steady-State Power Flows during 20% UV Disturbance*

The apparent power transfer is 3.6 % lower than the pre-disturbance flow. The reactive power is 67% higher than the pre-disturbance flow. The active power is 6.6 % lower than the pre-disturbance flow. The power factor as seen by the utility is 96.2 %.

### iv) Stage 4: Critical Islanding Response

The response of the critical islanding scheme is determined by the tripping matrix and the critical bus islanding logics. The result of the 200 ms undervoltage condition will be to initiate a Bus C Island.

The following ties will be opened:

- AC Tie
- BC Tie

It is essential that critical generation is connected to the critical bus. The critical supply will be the east-tie until generators suitable for critical operation are connected.

### v) Stage 5: Transient Response to Critical Island Condition

The islanding of the critical bus means that any critical load will be disconnected from the normal bus A/B and will appear to the normal generators and utility as a partial load rejection.

Accurate modelling of this stage requires that the exact loading of the critical plant is known. The critical generation is represented using a utility source in the ETAP model which is connected at the moment of islanding.

The initiation of a critical bus island means the there is a limit of 300 ms for the utility supply disturbance to be removed or a normal bus island will be initiated.

A normal bus island means that plant connected to 2H4-SP-02 will be shut down. The plant is not intended to run on critical power, but rather to shut down safely.

The generator 1 and generator 2 rotor power angles are visible below in figure 5.36 for 500 ms after the fault initiation. The angle 500 ms after fault initiation is 38.6°.

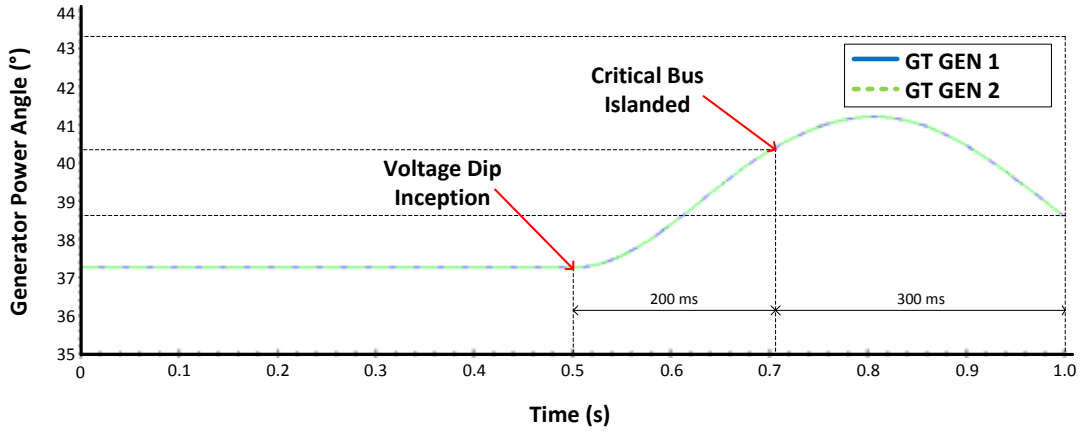


**Figure 5.36:** *Generator 1 & 2 Power Angles (500 ms Fault)*

The electrical power for generator 1 and generator 2 is shown below in figure 5.37. The electrical power experiences a sudden dip 200 ms after the disturbance is initiated. This is due to the sudden disconnection of the critical load from the normal network.

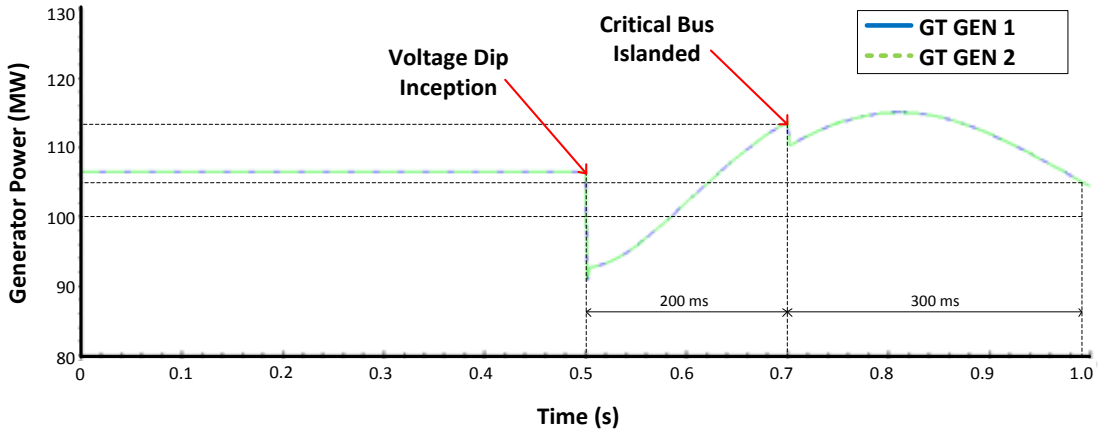


**Figure 5.37:** *Generator 1 & 2 Power (500 ms Fault)*

The power angles are visible for the MAC and BAC motors below in figure 5.38. The angle 500 ms after the disturbance is -41.7° for the MAC motor, and -32.0° for the BAC motor.

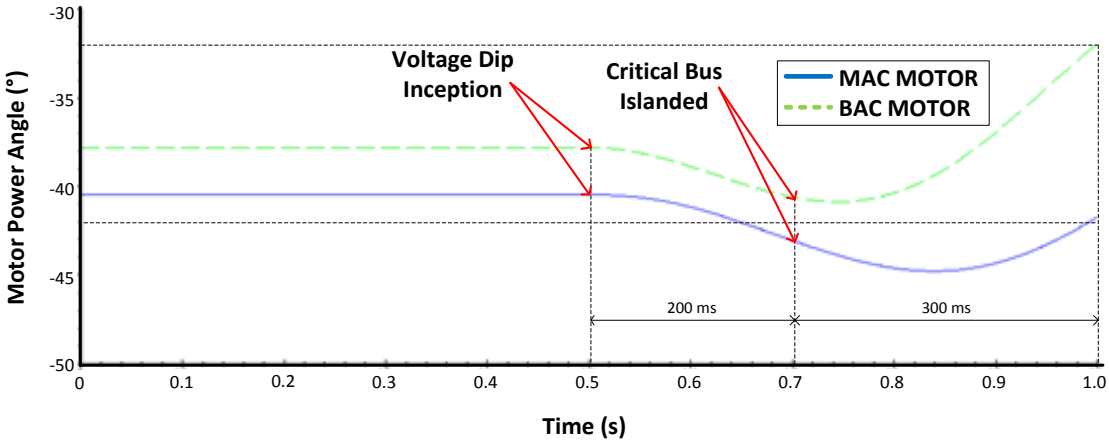


**Figure 5.38:** *Train 16 MAC and BAC Motor Power Angles (500 ms Fault)*

The electrical power is visible below in figure 5.39. There is a slight notch visible at the moment of islanding as the critical load is disconnected. The power response of these motors is largely unaffected by the critical islanding procedure.

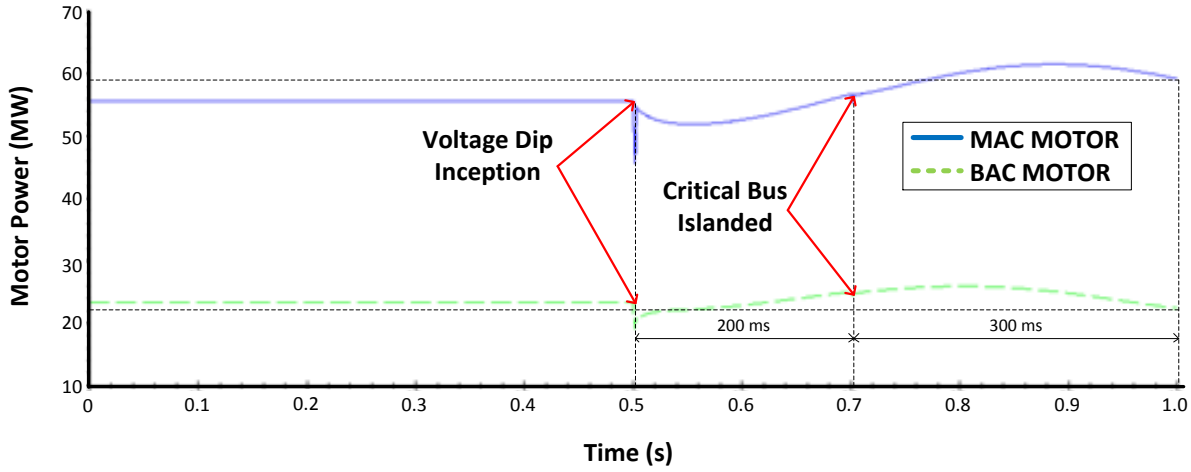


**Figure 5.39:** *Train 16 MAC and BAC Motor Power (500 ms Fault)*

The bus voltages for Bus A, B, C and D are visible below in figure 5.40. All four buses are connected to the utility supply until the moment of islanding. They all, therefore, have the same voltage waveform. At the moment of islanding the critical bus is disconnected from the utility supply and will return to nominal voltage.

The normal bus voltage will see a slight dip at the moment of islanding since the critical supply would have been forcing the voltage to slightly above the 80 % voltage dip.

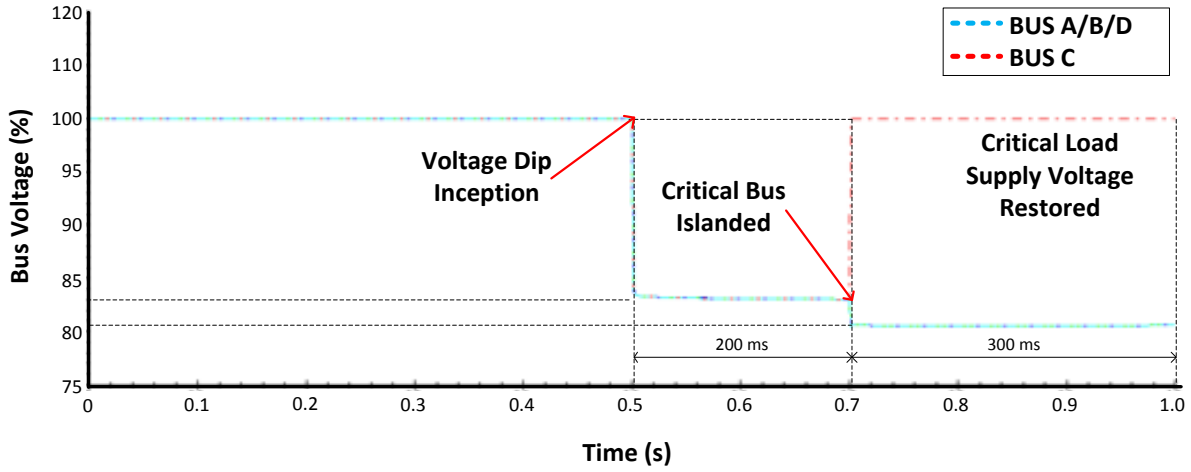


**Figure 5.40:** *Bus Voltage Response to Critical Islanding Scheme*

### vi) Stage 6: Steady-State Critical Island Conditions

The critical power requirements are tabulated below in table 5.37.

The critical power required by any plant is power to equipment that is classified as key to a safe shut down of the process.

| Line | Real Power | Reactive Power | Apparent Power | Power Factor |
|---|---|---|---|---|
| **Critical Power** | 52.6 MW | 32.6 MVAr | 61.9 MVA | 85.0 % |

**Table 5.37:** *Critical Power Requirements*

The line power flows are tabulated below in table 5.38. The line power flows have decreased in proportion to the load disconnected by the critical islanding operation.

| Line | Real Power | Reactive Power | Apparent Power | Power Factor |
|---|---|---|---|---|
| **Line 1 (B)** | 159.4 MW | 38.9 MVAr | 164.1 MVA | 97.1 % |
| **Line 2 (A)** | 159.4 MW | 38.9 MVAr | 164.1 MVA | 97.1 % |
| **Line 3 (D)** | 159.4 MW | 38.9 MVAr | 164.1 MVA | 97.1 % |
| **Total** | 478.2 MW | 116.7 MVAr | 492.3 MVA | 97.1 % |

**Table 5.38:** *Critical Island Power Flow*

#### vii) Stage 7: Normal Islanding Response

The response of the normal islanding scheme is determined by the tripping matrix and the normal bus islanding logics. The result of the 500 ms undervoltage condition will be to initiate a long-bus island.

The following ties will be opened:

- AC
- BC
- L1
- L2
- L3
- East-tie (Unless east-tie is supplying critical network)

The signals to open ties AC and BC are re-sent for security purposes. It is essential that the critical bus be islanded before the normal bus.

At this stage the network is totally isolated from the utility supply. The plant has begun a shutdown sequence and cannot be restored to operation by the removal of the disturbance.

#### viii) Stage 8: Transient Response to Normal Island Condition

The large motors and generators will have been tripped prior to the initiation of a long island condition.

The local generators and motors are not able to maintain the voltage and frequency at nominal value.

The bus voltage is shown below in figure 5.41 for the case that no rotating machinery is connected to the network as the island is initiated. This is a simplified representation useful for illustration of the sequence of events.

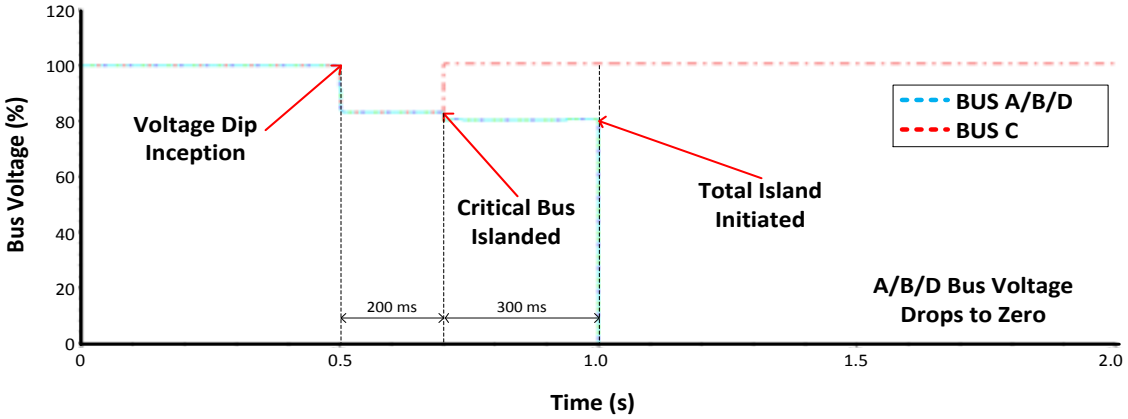


**Figure 5.41:** *Bus Voltage Profile for Islanding Sequence (No Generation)*

The bus voltage is shown below in figure 5.42 for the case that the large synchronous motors are tripped while the generators remain connected to the network after the island is initiated. The voltage profile of the critical bus remains at nominal from the moment the critical island is initiated.

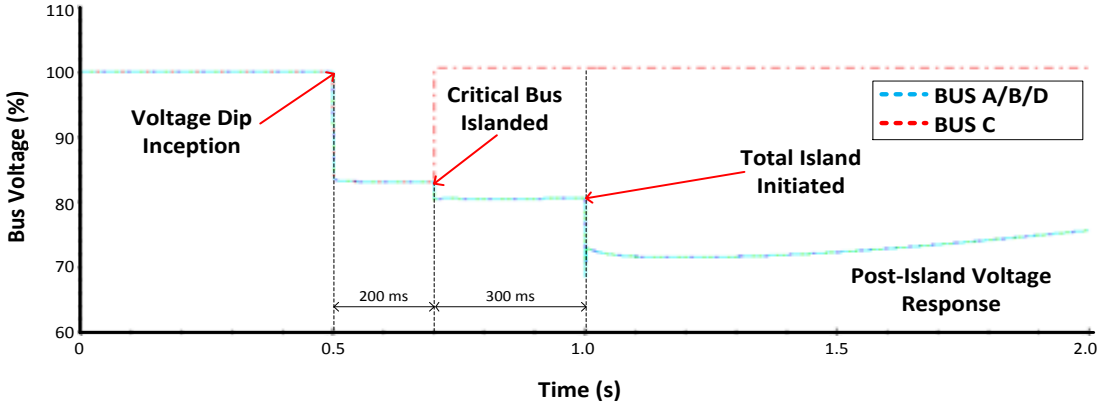


**Figure 5.42:** *Bus Voltage Profile for Islanding Sequence (Generation Connected)*

The generators are running in voltage control mode which explains the apparent increase in voltage after the initial dip. The maintained voltage is accompanied by a frequency decline illustrated below in figure 5.43.

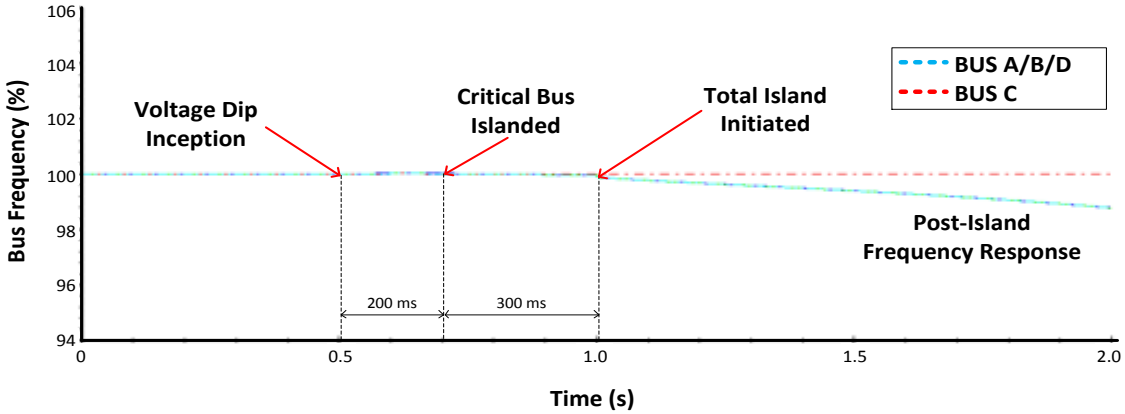


**Figure 5.43:** *Frequency Decline Following Islanding Sequence*

## 5.8 Synchronous Motor Protection Case Study

### 5.8.1 Introduction

The intention of this section is to explore the functioning of the OOS protection applied to the 16th Oxygen Train MAC Synchronous Motor.

The OOS protection is explored with reference to the specific method applied by the Siemens Siprotec 7UM622 Multifunction Relay, which is responsible for protecting the MAC motor, as well as with reference to the available literature on synchronous motor protection.

### 5.8.2 OOS Protection

OOS protection (ANSI code 78) is intended to protect the power system and the synchronous motor from potentially unstable power swings.

When a synchronous motor loses synchronism with the supply frequency it is referred to as an OOS condition. This condition may also be referred to as synchronous motor pull-out (IEEE C37.96-2000).

The following conditions may cause loss-of-synchronism:

- Excessive shaft load
- Reduced supply voltage
- Reduced excitation

Active power swings can lead to synchronous motor pole slipping and motor overloading, both of which are undesirable and potentially damaging conditions.

Torque oscillations applied to the motor shaft may also cause loss-of-synchronism. A frequent cause of loss-of-synchronism is faults on the supply system.

The fault clearing time, fault location, fault type and system configuration are all factors influencing the motor stability (IEEE C37.96-2000).

OOS detection devices for synchronous motors may monitor the power factor angle or the apparent impedance at the motor terminals.

It is also possible to use a CT on the rotor field circuit which would detect the presence of AC in the rotor circuit. The presence of a minimum AC current in the rotor field circuit may indicate an OOS condition (IEEE C37.96-2000).

This section aims to analyse the details of the OOS protection scheme as applied to a specific synchronous motor (16T MAC motor) in the Sasol Synfuels network.

### 5.8.3 OOS using Siemens 7UM622

The OOS protection principle, as applied by the 7UM622 IED, is based on the measurement and assessment of the complex impedance vector locus. The impedance vector is calculated based on the positive sequence fundamental components of the three-phase currents [32].

For the purposes of OOS protection it is suitable to model the synchronous motor as a synchronous generator.

The diagram below forms the basis for the OOS protection principle, where $\mathbf{V_M}$ is the motor voltage vector and $\mathbf{V_S}$ is the system voltage vector.

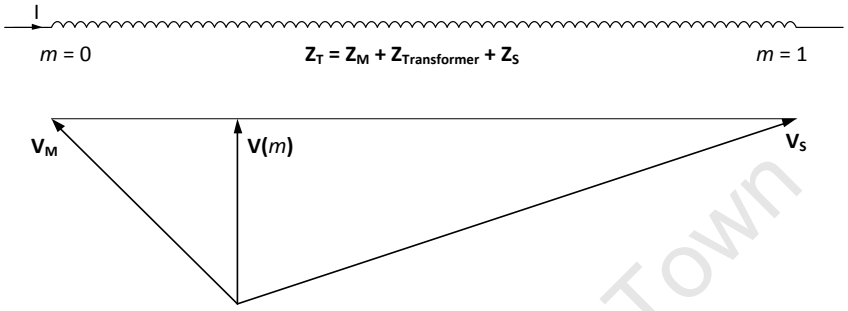


**Figure 5.44:** *Equivalent Model for OOS Protection*

The motor, transformer and network impedances fall between the voltages $\mathbf{V_M}$ and $\mathbf{V_S}$, and are designated by $\mathbf{Z_T}$ which is the total equivalent impedance. It is important to note that these voltage and impedances are complex vectors.

The measurement location, defined by the VT position, divides $\mathbf{Z_T}$ into $m{\cdot}\mathbf{Z_T}$ and $(m\text{-}1){\cdot}\mathbf{Z_T}$. The impedance at the measurement point is given by equation 5.1.

$$\boldsymbol{Z}(m) = \frac{\boldsymbol{V}(m)}{\boldsymbol{I}(m)} \quad \ldots \quad (5.1)$$

The current through the branch is independent of the measurement point and is given by equation 5.2.

$$\boldsymbol{I}(m) = \boldsymbol{I} = \frac{\boldsymbol{V_M} - \boldsymbol{V_S}}{\boldsymbol{Z_T}} \quad \ldots \quad (5.2)$$

The voltage at the measurement position is given by equation 5.3.

$$\boldsymbol{V}(m) = \boldsymbol{V_M} - m \times \boldsymbol{Z_T} \times \boldsymbol{I} \quad \ldots \quad (5.3)$$

It is possible to combine the previous three equations, while converting vector to phasor notation, to derive equation 5.4.

$$\boldsymbol{Z}(m) = \left[\frac{1}{1 - \frac{V_S}{V_M} \cdot e^{-j\delta}} - m\right] \cdot \boldsymbol{Z_T} \quad \ldots \quad (5.4)$$

The primary variable that changes during a power swing is the power angle, δ, which may rapidly vary from 0° to 360°. Equation 5.4 can be used to derive the set of characteristics shown in figure 5.45.

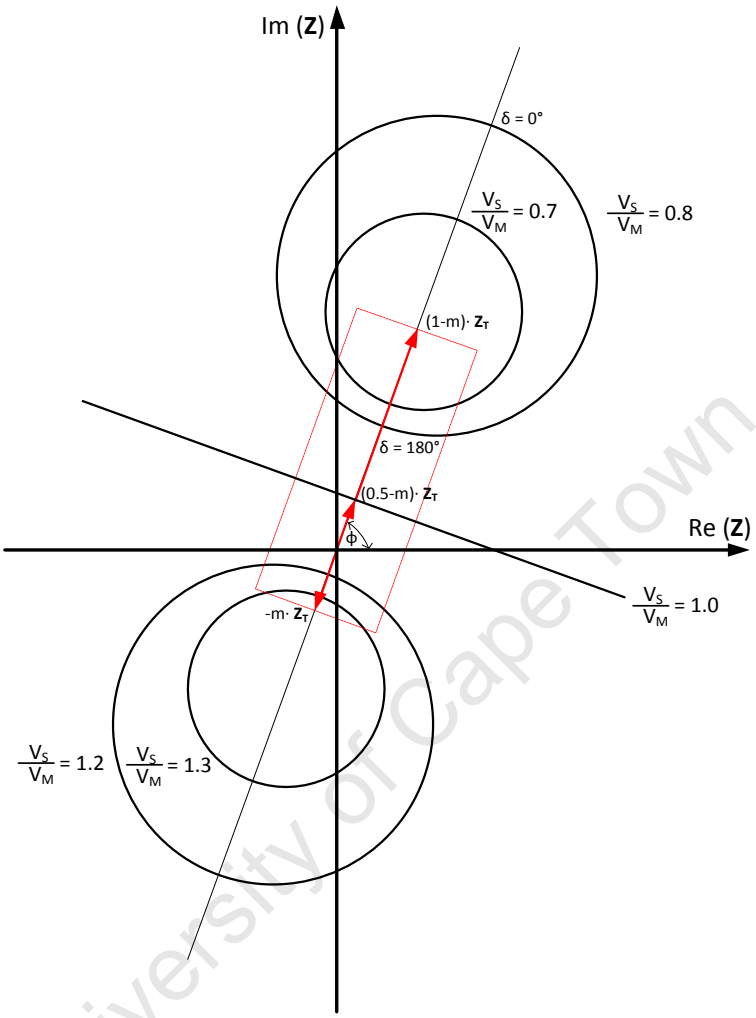


**Figure 5.45:** *Impedance Trajectories for OOS Protection [31]*



If the voltage ratio is kept constant while the power angle is varied a set of circular trajectories occur.

The centres of the trajectories all occur on the total impedance axis. The minimum and maximum impedances occur at 180° and 0° respectively.

The measurement characteristic, as defined by the 7UM622, is a polygon that can be adjusted in all four directions and in its angle of inclination (ϕ) [31].

This polygon is described in greater detail in figure 5.46 shown below.

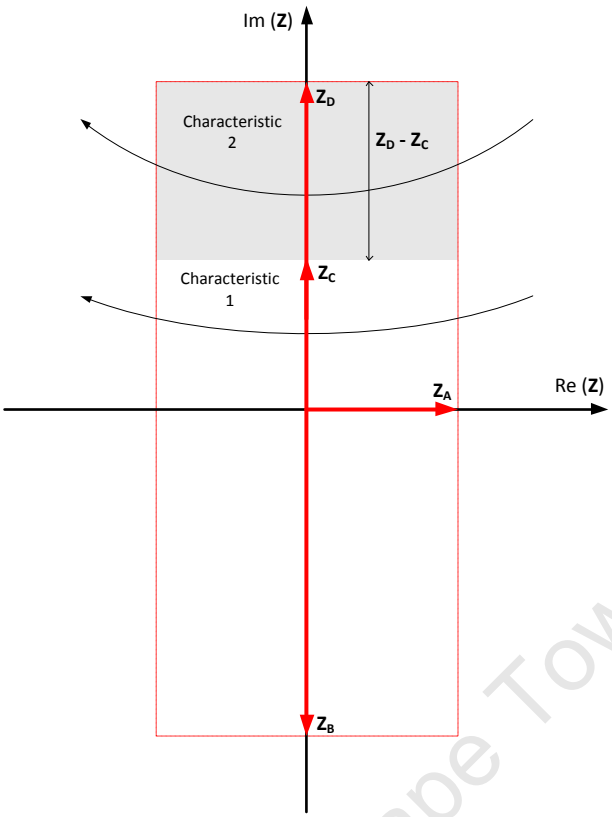


**Figure 5.46:** *OOS Characteristic Polygon*

**Key Characteristics of the OOS Polygon:**

- Setting the ZA, ZB, ZC and (ZD-ZC) parameters determines the polygon size.
- The polygon is symmetrical about the imaginary axis.
- ZB measures into the motor
- ZC measures into the power transformer
- ZD measures into the power network
- The polygon is divided into two characteristics

**Prerequisites for Detecting a Power Swing:**

- Positive sequence current must be above a threshold.
- Negative sequence current must be below a threshold.
- The impedance vector must enter the polygon from one side, cross the imaginary axis, and exit the polygon on the opposite side (real component of complex impedance changes sign).

An annunciation is issued when the impedance vector crosses a power swing characteristic. A counter (n1 or n2) is also incremented. OOS pick-up is initiated when a counter reaches 1. After a specified holding time the counter is reset. The holding time resets after each increment increase of the counter [31].

The operation of the OOS protection is well-defined by the protection logic diagram shown in figure 5.47.

This diagram has been simplified to only show the core protection function, and for this reason does not show annunciations and supplementary information.

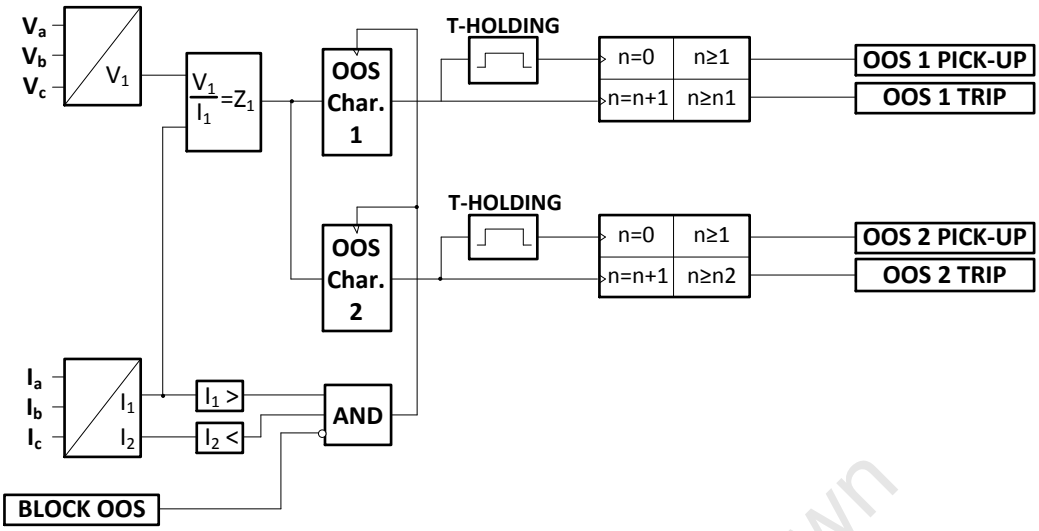


**Figure 5.47:** *OOS Protection Logic Diagram*[5] *[31]*

**Setting Notes:**

- **BLOCK** is a binary input which enables or disables OOS protection.
- **RELEASE1**: positive sequence current must exceed a threshold to release measurement.
- **RELEASE2:** negative sequence current must be below a threshold to release measurement.
- $Z_B$ is approximately equal to the motor secondary transient reactance and can be calculated by equation 5.5.
- $Z_C$ is typically set between 70% and 90% of the short-circuit impedance of the step-up transformer.
- ($Z_D$-$Z_C$) is typically set to cover the remainder of the transformer and extend into the network.

$$Z_B \approx X'_d = \frac{V_{M,Rated}}{\sqrt{3} \cdot I_{M,Rated}} \cdot x'_{d,pu} \cdot \frac{CT_{Ratio}}{VT_{Ratio}} \quad \dots \quad (5.5)$$

$Z_A$ determines the width of the polygon. The value for $Z_A$ depends on the maximum allowable power angle during a swing and is described in figure 5.48 and equation 5.6. Equation 5.6 is derived from the trigonometric laws applied to right-angled triangles for the simplified diagram shown on the right half of the diagram.

$$Z_A = \tan\left(\frac{\delta}{2}\right) \cdot \frac{Z_T}{2} \quad \dots \quad (5.6)$$

The typical value for the maximum power angle is 120°, which means that $Z_A$ should be set to 0.289 times the total impedance. This is the default value of $Z_A$ in the relay settings and is the value applied for the MAC motor OOS protection scheme.

[5] The logics, protection polygon characteristic, equations (5.5 and 5.6) and default settings are adapted from the Siemens Siprotec 7UM622 Technical Manual.

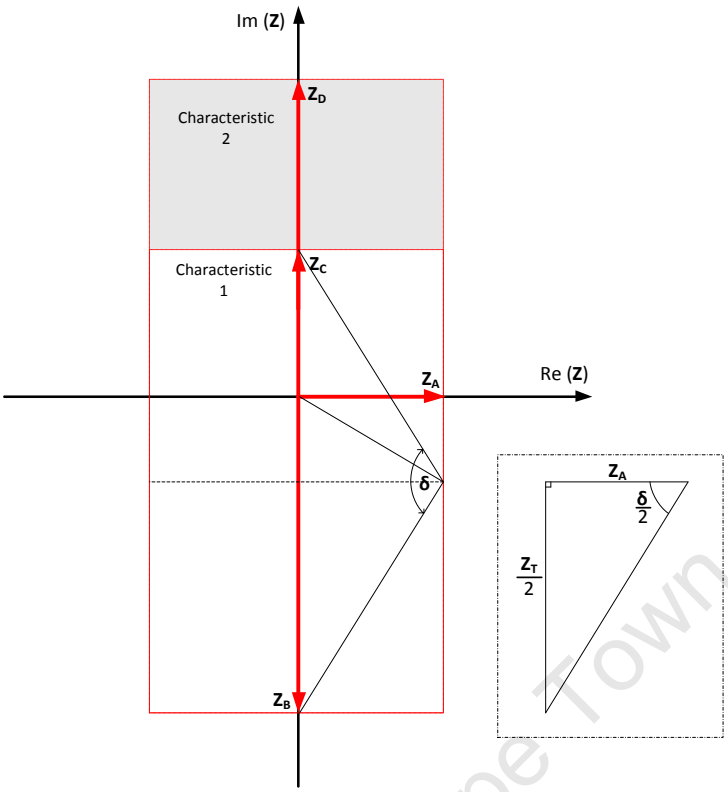


**Figure 5.48:** *OOS Polygon and Impedance Vectors [31]*

The number of power swings allowed may differ between characteristic 1 and characteristic 2. The **REP. CHAR. 1** and **REP. CHAR. 2** addresses set the maximum number of power swings for characteristic 1 and characteristic 2 respectively. **REP. CHAR. 1** is typically set lower than **REP. CHAR. 2** due to the higher likelihood of damaging machine stresses in the characteristic 1 zone. The setting sheet is given below in table 5.39 for the OOS function giving the setting ranges, the default settings and the actual settings on the 7UM622 OOS protection relay for the MAC motor [31].

| Parameter | Range | Default | MAC Setting | Description |
|---|---|---|---|---|
| **OUT-OF-STEP** | OFF/ON/BLOCK | OFF | ON | Enabling Parameter |
| **RELEASE1** | 20 % to 400 % | 120 % | 120 % | Positive Sequence Release |
| **RELEASE2** | 5 % to 100 % | 20 % | 20 % | Negative Sequence Release |
| **$Z_A$** | 0.2 Ω to 130 Ω | 4.5 Ω | 6.77 Ω | Polygon Width |
| **$Z_B$** | 0.1 Ω to 130 Ω | 12 Ω | 15.15 Ω (-100%) | Reverse Polygon Reactance |
| **$Z_C$** | 0.2 Ω to 130 Ω | 3.6 Ω | 8.3 Ω (+85%) | Forward Polygon Reactance 1 |
| **$Z_D$ - $Z_C$** | 0 Ω to 130 Ω | 6.4 Ω | 2.39 Ω (+30%) | Forward Polygon Reactance 2 |
| **PHI POLYGON** | 60° to 90° | 90° | 90° | Polygon Inclination |
| **REP. CHAR. 1** | 1 to 10 | 1 | 2 | Power Swings in Char. 1 |
| **REP. CHAR. 2** | 1 to 20 | 4 | 4 | Power Swings in Char. 2 |
| **T-HOLDING** | 0.2 s to 60 s | 20 s | 20 s | Holding Time for Detection |
| **T-SIGNAL** | 0.02 s to 0.15 s | 0.05 s | 0.05 s | Annunciation Time |

**Table 5.39:** *MAC Motor OOS Protection Settings*

### 5.8.4 System Response to Protection Operation

The intention of this section is to analyse the response of the system to the protection operation in the event of a machine bus fault on the 16th Train MAC Motor Bus (R8L-EE-332A).

The motor response to a 228 ms symmetrical short circuit on the motor bus is illustrated in figure 5.49.

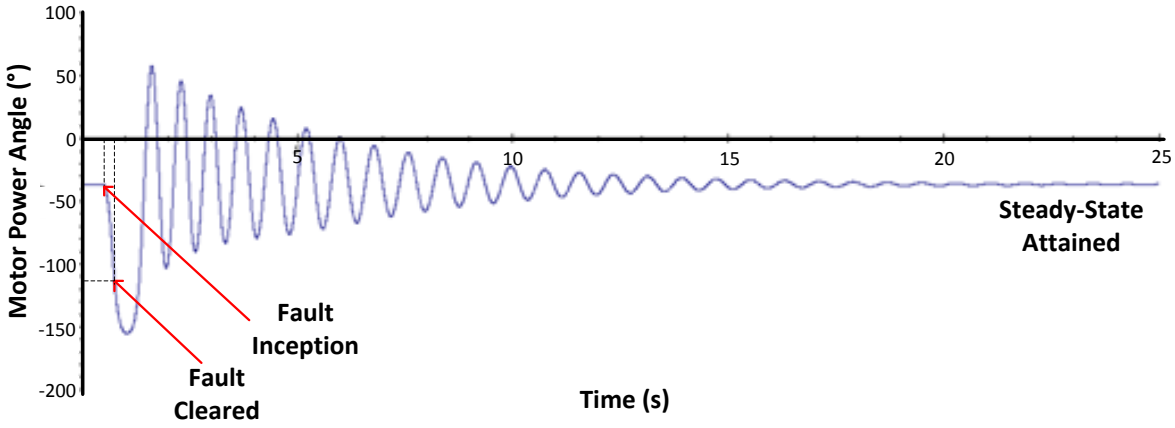


**Figure 5.49:** *MAC Motor Response to 228 ms Motor Bus Fault*

The motor parameters are tabulated in table 5.40 for four significant points during the analysis of a 228 ms motor bus fault. The important point to note is that the power angle reaches 120° at 779 ms and initiates the first unstable swing count.

| Time | Parameter | Value |
|---|---|---|
| **Conditions at 500 ms (Fault Inception)** | Angle | -36.6° |
| | Speed | 1500 RPM |
| | Active Power | 50.141 MW |
| | Reactive Power | 0 MVAr |
| **Conditions at 600 ms (During Fault)** | Angle | -48.5° |
| | Speed | 1480.2 RPM |
| | Active Power | -163 kW |
| | Reactive Power | -320 kVAr |
| **Conditions at 728 ms (Fault Clearance)** | Angle | -97.4° |
| | Speed | 1455.9 RPM |
| | Active Power | 95.965 MW |
| | Reactive Power | 38.755 MVAr |
| **Conditions at 779 ms (OOS Count 1)** | Angle | 120° |
| | Speed | 1468.6 RPM |
| | Active Power | 122.475 MW |
| | Reactive Power | 44.847 MVAr |

**Table 5.40:** *MAC Motor Response to 228 ms Motor Bus Fault*

The next power angle peak occurs at 1960 ms (1460 ms after fault) and is 103.4°, which is below 120°. The OOS protection, therefore, does not issue a trip command in this case.

The critical points of the motor response to a 230 ms symmetrical short circuit on the motor bus are tabulated in table 5.41.

| Time | Parameter | Value |
|---|---|---|
| **Conditions at 777 ms (OOS Count 1)** | Angle | 120° |
| | Speed | 1467.1 RPM |
| | Active Power | 122.582 MW |
| | Reactive Power | 44.573MVAr |
| **Conditions at 1441 ms (OOS Count 2)** | Angle | 120° |
| | Speed | 1402 RPM |
| | Active Power | 172.133 MW |
| | Reactive Power | 6.737MVAr |

**Table 5.41:** *MAC Motor Response to 230ms Motor Bus Fault*

The settings, as detailed in table 5.39, specify that the OOS protection should issue a trip command in this case. The trip command will initiate tripping of the motor running circuit breaker.

The motor electrical power response waveform is illustrated below in figure 5.50. The waveform displays the characteristic zero-power during fault conditions and then the unstable oscillatory characteristic subsequent to the fault. The RCB is tripped at 1441 ms which effectively disconnects the motor from the power system.

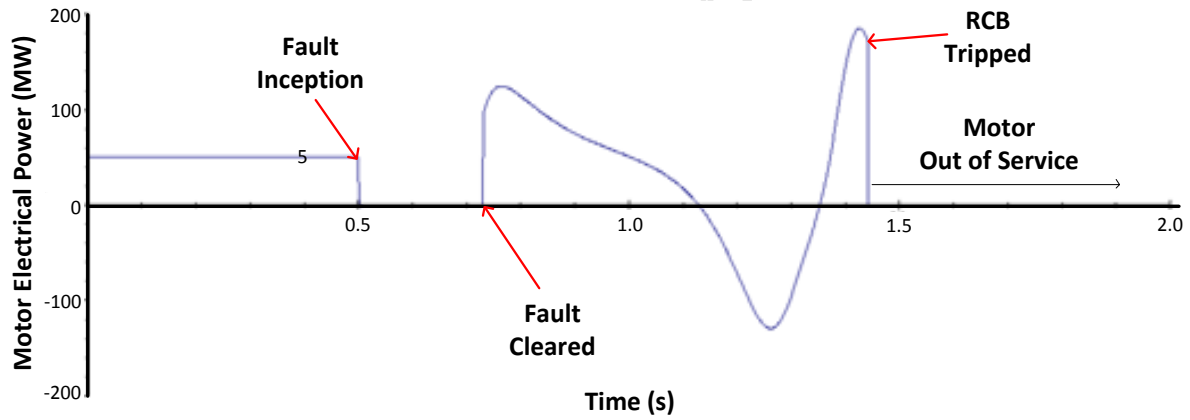


**Figure 5.50:** *Mac Motor Electrical Power Response to 230 ms Fault and OOS Protection*

The GT-driven generators respond to the unstable conditions before the motor is tripped with their own characteristic oscillations. The power angles of the GT-driven generators increase to a maximum of 43.1° and decrease to a minimum of 31.9° before ultimately returning to a stable steady-state.

The 132 kV bus voltage drops to 92.3 % during the fault conditions, but return to the pre-fault setpoint within 5 seconds.

The frequency deviation of the system as a whole, due to the motor bus fault, is less than 0.2 % at its peak. This corresponds to a maximum frequency deviation of 0.1 Hz.

# 6 Improvement of Power System Stability

For any system any one method of improving stability may not be adequate. A combination of methods may be required to achieve the desired result [2].

According to Kimbark, *et al*, (1950) the most effective methods of improving transient stability are the fast clearing of faults and rapid reclosing. High speed clearing can be achieved with faster circuit breakers and protection relays [9]. Reclosing schemes are not applied in the Synfuels network and may only be applicable to the 400 kV utility lines.

**Desired Effects of Methods of Improving Stability:**

- Reduction in disturbance influence by reducing fault severity and duration
- Increase in synchronising forces
- Reduction of accelerating torque by reduction in mechanical power
- Reduction in accelerating torque by applying artificial load

The improvement of steady-state stability has an impact on the transient stability of the power system in a number of ways. The improvement of steady-state stability may entail increasing the maximum power transfer, reducing the system reactance and the installation of additional transmission or distribution lines [1].

By increasing the maximum power transfer it is possible to reduce the impact of a fault since a higher portion of power will be permitted to flow through the unfaulted portion of the network during disturbed conditions. The addition of parallel transmission lines increases the maximum power transfer across the link as well as effectively increasing the availability of the single link [1].

The use of FACTS devices can significantly improve the steady-state stability of the power system. The reduction of the transmission system reactance is discussed in section 6.2. This method effectively increases the maximum power transfer but has the effect of increasing the system fault-levels [1].

The aim of this section, however, is not to focus on the improvement of steady-state stability but rather on the improvement of power system transient stability.

Transient stability improvement methods include:

- High speed fault clearing
- Reduction of transmission system reactance
- Regulated shunt compensation
- Dynamic braking
- Reactor switching
- Steam turbine fast valving
- Generator tripping
- Islanding and load-shedding
- Power System Stabilisers (PSSs)
- Static VAr Compensators (SVCs)

## 6.1 High Speed Fault Clearing

The kinetic energy gained by the generators during a fault is directly proportional to the duration of the fault.

Early circuit breakers, prior to 1930, had interrupting times between 15 and 30 cycles with relays having pick-up times greater than 6 cycles [9].

It must be noted that the clearing time is also dependent on the protection grading and not purely on relay and breaker interrupting time.

Two-cycle breakers in combination with high speed communication and relays are commonly used in locations where high speed fault clearing is required [2].

The effect of fast fault clearing is illustrated below in figure 6.1. Case 1, indicated by the solid line, is for a 50 ms symmetrical fault, while the dashed line corresponds to a 150 ms symmetrical fault. The magnitude of the power swings is clearly higher in the case of a longer clearing time.

The fault duration is also clearly visible as the period where the power transfer is zero.

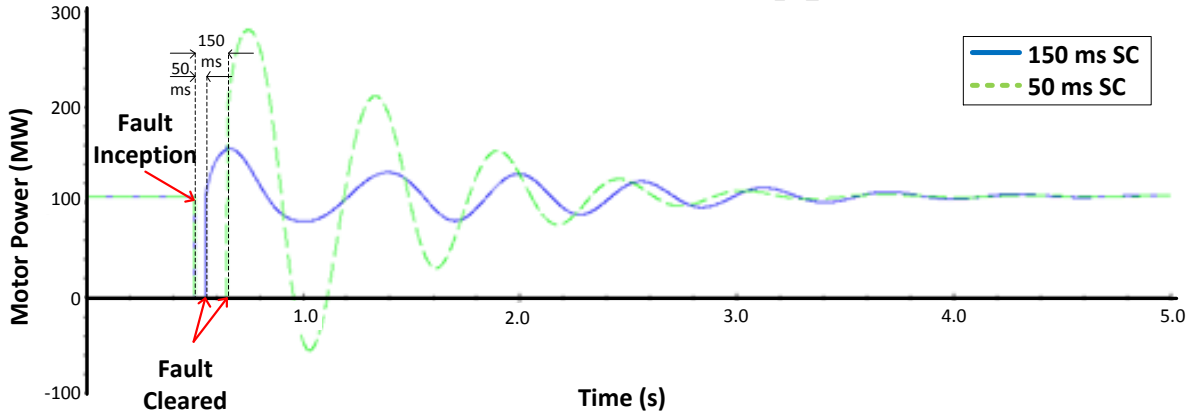


**Figure 6.1:** *Power Swings for 50 ms and 150 ms Symmetrical Fault*

The rotor angle swings for a 50 ms fault versus a 150 ms fault display a similar trend and the severity of the swing is proportional to the fault duration.

The implications of the fault clearing time are best understood with reference to the equal-area criterion which was described in section 2.93. A longer fault clearing time results in a larger power angle difference, and a smaller stability margin.

Provided all other conditions are unchanged, the shorter the clearing time the smaller the power swings and the higher the chances of transient stability being maintained.

The major manufacturers of circuit breakers and related protection systems have the reduction of fault clearing time as a primary target. Their intention is typically to limit equipment damage but the positive spin-off is the improvement of transient stability as a result of these reduced clearing times.

## 6.2 Reduction of Transmission System Reactance

The series inductive reactances of transmission networks are primary determinants of power system stability. A lower transmission network reactance directly equates to a higher post-fault synchronising torque.

Methods of achieving this objective include:

1. Reduction of line reactances
2. Reduction of transformer leakage reactances (typically 0.1 to 0.15 pu)
3. Series capacitor compensation of transmission lines

The main disadvantage of the reduction of transmission system reactance is the corresponding increase in fault-levels. High fault-levels are already an area of concern at the 132 kV level for the Synfuels power system.

The oversizing of transformers is, however, typically not an economically feasible option since an oversized transformer is generally not a justified expense.

In typical industrial distribution systems the design is for N – 1 contingency. This means that on a dual-incomer section the transformers operate below 45 % of design capacity.

The use of series capacitors to increase maximum power transfer capacity of the transmission system is an economically feasible option which may be followed by the Transmission Operator. This has the impact of improving transient stability by effectively increasing the post-disturbance synchronising torque [17].

The increase in transmission system reactance, due to CLRs installed in the 132 kV incomers, has been explored in chapter 5.

## 6.3 Regulated Shunt Compensation

Shunt compensation capable of maintaining voltages at selected buses may improve the synchronising power flow between groups of generators.

Synchronous condensers or SVCs may be used for this purpose. Regulated shunt compensation also increases the maximum power transfer along a line and improves steady-state stability as a result. The use of the SVC as a means of improving power system stability will be addressed in section 7.14.

FACTS devices offer the ability to increase utilisation of existing plant which will result in an increased maximum power transfer. This may have the effect of improving the transient stability of the power system. A UPFC controller is a FACTS device that may be used for this purpose. The device is able to supply or absorb reactive power and is able to maintain the voltage at a specific point in the network [18].

The series voltage can be decomposed into an in-phase and a quadrature component. The in-phase component has the effect of adjusting the voltage while the quadrature component has the effect of adjusting the phase angle. This method is applied by the UPFC [18].

## 6.4 Dynamic Braking

The concept of dynamic braking involves introducing an artificial load following a fault to reduce the possible accelerating torque. A form of dynamic braking involves switching in a shunt resistor for approximately 0.5 seconds following a disturbance. The sudden switching of the resistor causes large stresses on the machine which is undesirable [2].

The use of braking resistors requires a power system that is able to momentarily handle a portion of generation being disconnected from the load. This arrangement would not be suitable in a single machine system or where all the generators function as a group [1].

The use of a braking resistor is implemented exclusively for transient stability improvement. It will absorb excess generation in the event of a fault electrically near to the generator. Modern braking resistor schemes may be in the form of a Thyristor-Switched Braking Resistor (TSBR). A possible TSBR scheme is illustrated in figure 6.2 [3].

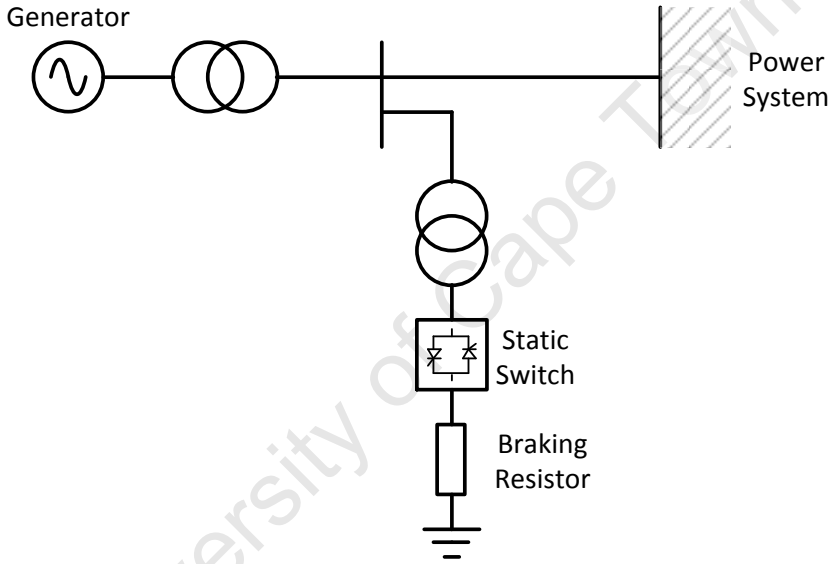


**Figure 6.2:** *Thyristor-Switched Braking Resistor*

A series braking resistor may be switched-in and the power dissipated will depend on generator current. A neutral resistor may be used to add load only in the case of asymmetrical ground faults [2].

The braking resistor should ideally be connected at the instant of fault clearance and disconnected as soon as the rotor speed deviation becomes negative [3].

The insertion of the braking resistor can be conceptualised as a fast load addition at the moment of fault clearance in order to absorb the excess energy. The maximum energy that can be transferred to the resistive load is typically limited by the thermal constraints of the resistor which determine the maximum temperature rise [19].

It is possible to improve the thermal capacity of the resistor by arranging the resistors in parallel banks and by using forced cooling on the resistor banks. Ideally the forced cooling would be triggered by an early warning system.

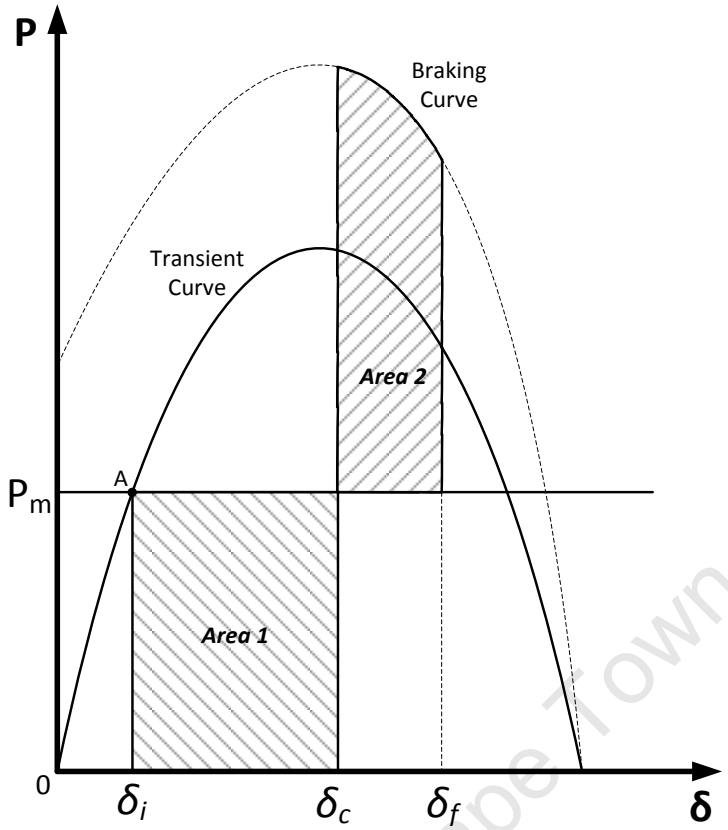


**Figure 6.3:** *Effect of Dynamic Braking on Power Curve*

The effect of the braking resistor is visible in figure 6.3 shown above. The fault is initiated at $\delta_i$ which is the initial power angle. The fault is cleared at $\delta_c$ which is the fault clearing angle. At the same time that the fault is cleared the braking resistor is switched-in which increases the power transfer and effectively shifts the peak of the power curve upwards.

The time that the braking resistor is maintained in operation is based on the time taken for *Area 2* to become equal to *Area 1*, as stipulated by the equal-area-criterion. The fault duration is determined by the fault clearing time and the protection settings and can be predicted. Once the power angle has reached the peak value the braking resistor is removed from the circuit and the normal transient power curve is followed. The timing of the switching sequence is critical for optimisation of the scheme.

Alternative braking arrangements include using a switched resistor-capacitor arrangement and a switched resistor reactor arrangement [19].

A strategy that has been proposed involves using a resistor-reactor combination with the resistor and reactor switched alternately based on rotor velocity deviations. The resistor is responsible for absorbing the excess energy while the generator accelerates and the reactor reduces the generator output while decelerating by reducing the terminal voltage [19].

Another option is to use an alternately switched resistor and capacitor scheme. The capacitor will suppress the voltage surge following the resistor switching and assist in restoring the system to normal conditions [19].

## 6.5 Reactor Switching

A shunt reactor may be permanently connected near to the generator bus. The inductive reactance will increase the generator internal voltage. The reactor may be switched out following a fault to improve stability [2].

A reactor that is permanently connected to the generator bus is typically used to compensate for the capacitive reactance of long transmission lines. The reduced line reactance results in increased power transfer as defined by equation 6.1 below.

$$P_{line} = \frac{V_1 \cdot V_2}{X_{eq}} \quad \ldots \quad (6.1)$$

The power transfer is proportional to the product of the sending-end and receiving-end voltages and inversely proportional to the magnitude of the line reactance. The reactor should be sized so that the peak required power transfer coincides with the lowest line reactance.

The reactor, due to the fact that it is continuously energised, is a source of energy losses and degrades the system efficiency.

This technique follows similar principles to the concept of dynamic braking. The generator will suffer a depressed terminal voltage due to the permanently connected shunt reactor. The voltage regulation system should be designed to compensate for the effect of the shunt reactor.

## 6.6 Independent-Pole Breaker Operation

Independent-pole operation refers to the use of separate operating mechanisms for each phase of the circuit breaker. The failure of one mechanism will not affect the opening of the other two poles. Although the poles operate independently they are normally tripped simultaneously. This arrangement reduces the severity of a three-phase fault with a stuck breaker [2].

Although similar in principle to the concept of single-pole switching the intention is different. While the intention of single-pole switching is to sustain power transfer during a single-phase fault, the intention of independent-pole breaker operation is to minimise the power flow during a symmetrical fault.

The operation of an Independent Pole Operating (IPO) breaker requires that the three poles be mechanically separate and have separate tripping mechanisms. The mechanical failure of one pole will not affect the tripping operation of the other two poles [24].

Each tripping coil has an associated primary and secondary relay, both of which would have to fail for the pole not to open. The complete failure of the breaker, which would entail all three poles not opening, would require the failure of six relays.

The primary relay operates before the secondary, which means that in the event of a failed operation a three phase fault will become a single phase fault and will then be cleared [24].

The system should be designed to incorporate a high level of redundancy while remaining economically feasible to install.

## 6.7 Single-Pole Switching

Single-pole switching uses separate operating mechanisms for each phase. In the case of a single line-to-ground fault only the faulted phase is tripped followed by rapid reclosing. For any other faults all three phases are tripped [2].

**Problems associated with Single-Pole Switching:**

- Secondary-arc extinction.
- Fatigue duty on turbine-generator shafts and turbine blades.
- Thermal duty on nearby generators due to negative sequence currents.

Single-pole switching is one of a number of discrete controls implemented for the improvement of power system transient stability. The use of single-pole switching can reduce the frequency of operation of other discrete controls such as generator tripping or fast-valving. This effectively extends the system life [22].

The considerations that need to be addressed when implementing a single-pole switching scheme include:

- Secondary Arc Extinction

  The reactive nature of long lines tends to result in sustained arcs after the faulted phase is opened. The scheme needs to accommodate secondary arc extinguishing to be effective. Methods for secondary arc extinguishing include slow reclosing, neutral reactors and high speed earthing switches [22].

- Protective Relaying

  The protective relay and associated equipment needs to be able to detect which phase is faulted and to issue a command to only the faulted phase-pole to trip. Protection relays are currently available which accommodate single-pole switching [22].

- Generating Unit Considerations

  The generating unit (generator-turbine combination) is subjected to a 100 Hz frequency due to the presence of a negative sequence current. The generating-unit must be capable of handling this stimulus without any damaging resonant frequencies being excited [22].

The generating-unit is subjected to an instantaneous torque at the moment of single-pole tripping and at the instant of reclosing. The generating-unit is also subjected to abnormal heating during the dead time to the presence of the negative-sequence current [23].

The dead-time should be minimised due to the stresses placed on the generating-unit during this period, and as a consequence slow reclosing should typically not be used as a method of secondary arc extinction.

## 6.8 Steam-Turbine Fast Valving

Fast-valving is a technique applied to thermal units to improve transient stability. Fast-valving relies on rapid closing and opening of valves in a prescribed manner to reduce post-fault accelerating power. These techniques effectively reduce the mechanical input to the generator following a disturbance [2].

Fast-valving is not commonly used to because of the adverse effects it may have on the generating unit. Fast-valving is not as effective as generator tripping; however, the unit remains in service. A typical fast-valving sequence is shown below in figure 6.4.

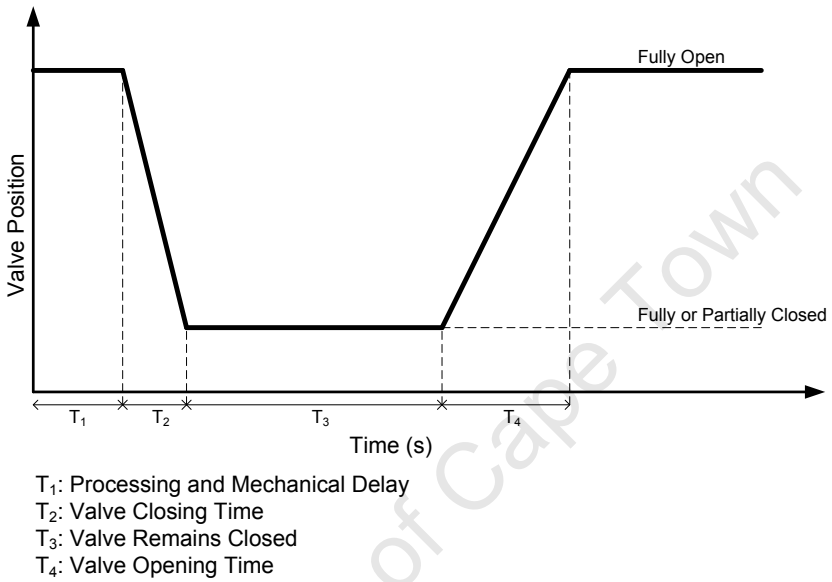


**Figure 6.4:** ***Typical Fast-Valving Sequence***

The terms fast-valving and Early Valve Actuation (EVA) are used interchangeably.

The concerns that need to be addressed when assessing a fast-valving scheme include [20]:

- Whether momentary or sustained fast-valving is to be used.
- The method of initiating fast-valving.
- Whether generator tripping is a preferable scheme.

The general consensus is that fast-valving, momentary or sustained, can be an effective method of stability improvement. It would be preferable to use a reliable and safe method of fast-valving over a unit-tripping scheme. The fast-valving scheme should not compromise steam supply or the availability of the turbine [20].

It is possible to reduce the need to implement the fast valving scheme by installing complementary infrastructure such as single-pole switching and tripping capable breakers as well as the installation of generator neutral resistors. These complementary devices typically remove the need for fast-valving in the event of line-to-ground faults [20].

## 6.9 Generator-Tripping

Selective tripping of generators in the event of severe system disturbances may improve the system stability. Generators can be tripped rapidly and reduce the power that can be transferred to the fault. Unless special facilities are provided the generating-unit follows a normal shut-down and start-up procedure [2].

**The concerns of Generator-Tripping Include:**

1. Turbine over-speed subsequent to generator tripping
2. Thermal stresses caused by rapid load changes
3. High shaft torques as the result of successive disturbances

Generator tripping can be regarded as a discrete supplementary control system for the improvement of transient stability.

The requirement of several transient stability improvement schemes to predict the onset of instability have effectively reformulated the transient stability problem as a pattern recognition problem [21].

A method proposed by Karady, G., for stabilising a power system following a disturbance based on generator tripping has been established. Conventional techniques based on generator tripping have various shortcomings including slow training time, large communication infrastructure requirements and large processing requirements [21].

The proposed method is based on a look-up table which is generated prior to the need for tripping. This eliminates the large processing requirements since the look-up table need only be updated in the rare case when the infrastructure is changed [21].

The basic principle is to track the generator rotor-angle and refer the rotor-angle to the look-up table which tabulates all generator and all feasible contingencies. The generator is classified as either stable or unstable based on the rotor-angle and is tripped accordingly.

The criteria that are analysed are the following:

- First swing
- Second swing with increasing rotor-angle
- Increasing oscillatory rotor-angle
- First swing with decreasing rotor angle
- Second swing with decreasing rotor-angle
- Oscillatory decreasing rotor-angle

The tracking and screening algorithm will allow the scheme to differentiate between stable and unstable cases as well as impending unstable cases. The next step of the algorithm is to select the optimal generator to be tripped to maintain stability while minimising the detrimental impact on the power system [21].

## 6.10 Islanding and Load Shedding

Islanding typically follows an unsuccessful attempt to restore system frequency by shedding load. It is also possible to initiate islanding manually or through other protection functions.

### 6.10.1 Islanding

Islanding, or controlled system separation, may be used to prevent a severe disturbance in one part of an inter-connected system from propagating and causing a widespread system break-up. Once an impending instability condition is detected system separation is initiated in a controlled manner by opening specific tie-lines [2].

Considerations when assessing the possibility of implementing an islanding scheme include planning studies, stability studies and fault-level studies. Planning studies ensure that there is no power imbalance within the proposed island and that steady-state stability is possible. Stability studies ensure that the island will maintain transient and voltage stability. Fault-level studies ensure that the new fault-levels in the islanded system are within acceptable limits [26].

### 6.10.2 Load Shedding

It may be necessary to shed pre-selected loads in specific areas after islanding has occurred in order to balance the load and generation.

It may be sufficient in certain instances to shed load without initiating controlled separation [2].

Three typical load shedding schemes follow:

- Reactive

  Reactive load shedding requires no operator intervention to initiate the load shedding sequence. This method relies on the absolute frequency value and refers to a look-up table to determine the load to be shed [25].

- Proactive

  A proactive load shedding scheme also requires no operator intervention but this scheme has a higher level of built-in intelligence than the reactive scheme. This scheme considers the rate of change of frequency and possibly even the acceleration of the frequency in order to initiate load shedding [25].

- Manual

  Manual load shedding is the slowest scheme in terms of reaction time and is not comparable to a reactive scheme due to the delay introduced by the operator response time. This scheme has application where the operator has been informed of impending loss of generation and can counteract the potential imbalance by shedding load [25].

The application of islanding with respect to the Sasol Synfuels network was explored in chapter 5 applying a case study method.

## 6.11 High-Speed Excitation Systems

Improvements in transient stability can be achieved by rapid temporary increase of generator excitation subsequent to a disturbance. The increased field voltage increases the machine internal voltage which increases synchronising power. The generator terminal voltage is low following a disturbance, and the AVR reacts by increasing the field voltage [2].

The impact of high-speed excitation systems for the improvement of system reliability using controlled-rectifiers fed directly from the generator terminals were identified as early as 1968. Significant improvements have been made in the design of high-speed excitation systems since these initial applications [28].

A high-speed excitation system may have the effect of degrading the damping characteristic of the power system. The excitation system is often supplemented with a PSS to improve system damping.

The Sasol Synfuels generators are equipped with high speed excitation systems.

## 6.12 Discontinuous Excitation Control

A PSS will typically improve first-swing stability by increasing excitation which will increase the rotor synchronising torque. It is possible in the case of both inter-area and local oscillation modes that the excitation may be reduced after the first local-mode peak. This may occur before the highest composite peak. The performance would be improved if the excitation were to remain at ceiling until the composite peak had occurred [2].

Discontinuous Supplementary Excitation (DSE) control can be effectively used to stabilise a synchronous machine with the use of local data. It is not necessary to have a global communication system to stabilise the individual machines [29].

DSE control achieves better performance than a conventional AVR, and is a cost effective and reliable solution to the problem of power system stability [29].

A Transient Stability Excitation Control scheme (TSEC) has been developed that maintains the excitation voltage at its ceiling for the entire first-swing. The TSEC module is built into the PSS and forms part of the excitation feedback loop [2].

The TSEC scheme feedback loop will be activated when the terminal voltage is below a threshold, the field voltage is at its ceiling and the speed is above a setpoint. The scheme is deactivated when the speed drops below a setpoint [2].

Discontinuous excitation control imposes very little stress on the generating-unit shaft and steam supply system. The scheme will, however, cause parts of the system to experience overvoltages. The operation of the discontinuous excitation control system will need to be coordinated with overvoltage protection as well as any differential protection schemes [2].

## 6.13 Power System Stabilisers

A Power System Stabiliser (PSS) is a device which adds supplementary control loops to the AVR system and/or turbine-governor of a generating unit. A PSS is one of the most cost effective methods of improving power system stability.

Work as early as 1968 by Dandeno, *et al*, explored the use of a signal proportional to changes in generator speed to improve dynamic stability limits [27].

Investigations, in 1961, using an analogue computer indicated that the dynamic stability limit of a generator could be significantly improved using a high-speed rectifier exciter and voltage regulator in combination with a supplementary derivative-based control loop. The work illustrated that this method improved dynamic and transient stability limits. The development of this speed-derivative signal is the foundation of the modern PSS [27].

### 6.13.1 PSS Applied to Excitation System

The fundamental principle of the PSS is to recognise that in steady-state conditions the voltage regulator should only be driven by the voltage-error signal $\Delta V$. The purpose of the PSS is to respond to $\Delta V$ oscillations and to add a compensating signal in phase with the change in speed $\Delta\omega$. The principle of a PSS applied to an excitation system is illustrated in the block diagram in figure 6.5 [3].

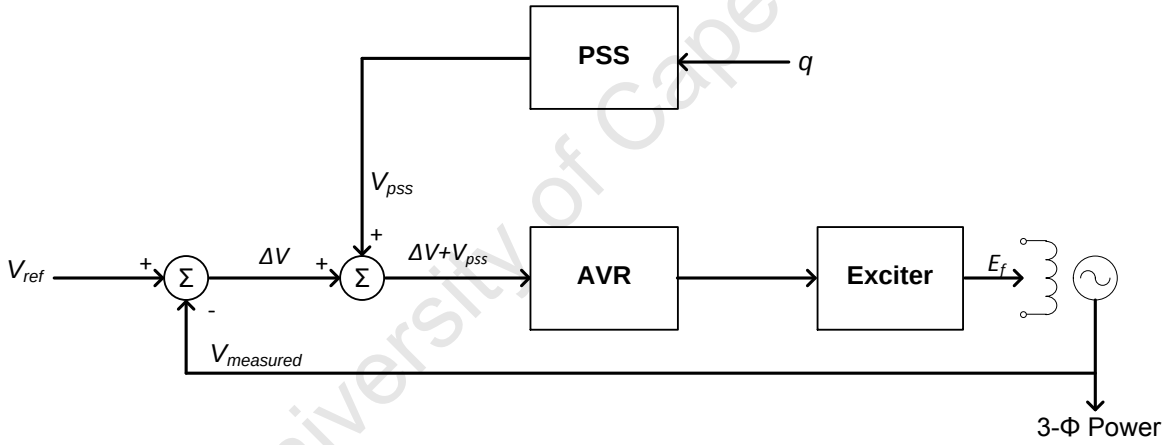


**Figure 6.5:** *PSS Applied to Excitation System*

The measured quantities that may be used as input signals may be the generator active power, the frequency or the rotor speed deviation.

### 6.13.2 PSS Based on Rotor Speed Deviation

The first types of PSS used the speed deviation of the rotor shaft as an input signal. This signal is inherently noisy and needs to be filtered.

The shaft is subject to torsional oscillations and consequently the speed deviation needs to be measure at several points and averaged. This PSS design may also positively influence torsional oscillations.

### 6.13.3 PSS Based on Speed Deviation and Electrical Power

The average rotor sped deviation can be calculated from measured electrical quantities. This eliminates the need to measure the speed deviation at several different points along the shaft. This method calculates the equivalent speed deviation from the integral of accelerating power as shown by equation 6.2.

$$\Delta\omega_{eq} = \frac{1}{M}\int(\Delta P_m - \Delta P_e)dt \quad \ldots \quad (6.2)$$

The change in electrical power is determined from measurements of the electrical power at the generator terminals. The integral of the change in the mechanical power can be determined using equation 6.3.

$$\int \Delta P_m dt = M \cdot \Delta\omega_{measured} + \int \Delta P_e dt \quad \ldots \quad (6.3)$$

The speed-deviation signal is measured at the end of the shaft. The mechanical power changes relatively slowly and consequently the derived integral of mechanical power can be low-pass filtered to remove the torsional frequencies.

### 6.13.4 PSS Effect on Damping

There are damping and synchronising-torque components present in the resultant torque vector. The addition of an AVR means that the excitation will change in response to a disturbance. This may result in a negative damping coefficient which may result in oscillatory instability.

The addition of a PSS results in the addition of a damping component in phase with the speed deviation. This arrangement has favourable synchronising and damping torques. The excitation value is altered by the PSS to reduce oscillations as shown in figure 6.6.

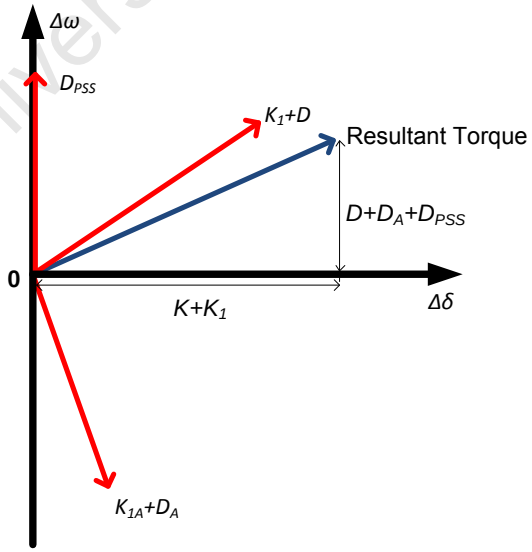


**Figure 6.6:** *Excitation System with AVR and PSS*

## 6.14 Static VAR System (SVS)

SVCs based on conventional thyristor technology have been in use in power systems since the 1970s. This technology was before the widespread use of FACTS devices [3].

The fundamental role of the SVC is to adjust the reactive power compensation according to the system requirements. The ideal SVC offers flexible and continuous operation in both the capacitive and inductive modes [3].

### 6.14.1 Reactive Power Control Elements

1. Thyristor-Controlled Reactor (TCR)
2. Thyristor-Switched Capacitor (TSC)

The voltage-current characteristic of an ideal SVS is shown below in figure 6.7. The SVS should maintain constant voltage, possess unlimited reactive power generating and absorption capability, have no losses and respond instantaneously to system changes [2].

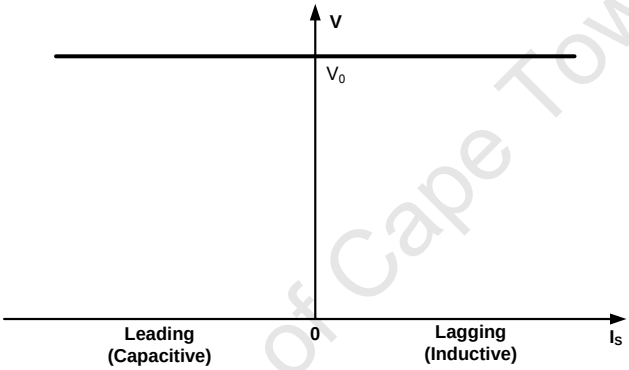


**Figure 6.7:** *Ideal SVS Characteristic*

The operating point of the SVS can be determined by superimposing the system characteristic on the SVS characteristic. This principle is illustrated in figure 6.8 shown below.

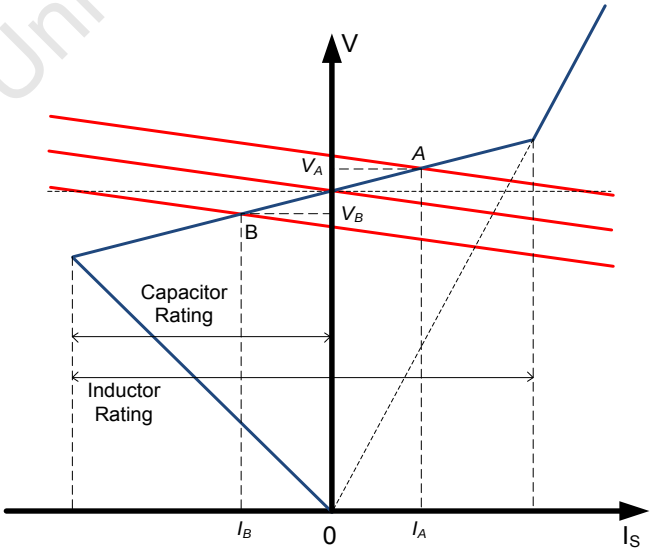


**Figure 6.8:** *Graphical Determination of SVS Operating Point*

The system characteristic is given by equation 6.4 while the SVS characteristic is given by equation 6.5. These equations are equated to find the operating point. The SVS reference voltage is typically the same as the system voltage corresponding to zero SVS reactive current.

$$V_{system} = E_{th} - X_{th}I_s \quad \ldots \quad (6.4)$$

$$V_{SVS} = V_{ref} + X_s I_s \quad \ldots \quad (6.5)$$

In the event of a change in source voltage the SVS will compensate by generating or consuming reactive power, and will effectively become a reactive current source or sink. The change in voltage will, therefore, be less than under the influence of the system characteristic alone.

It can be seen that for large changes in system voltage the SVS control range may be exceeded. This problem can be alleviated by adding banks of capacitors that can be switched.

The SVS should be designed to be able to cope with all normal operating conditions and as far as possible serve to mitigate abnormal conditions. The range should, therefore, be based on all possible operating conditions.

The general principle of an SVS is that of controlled susceptance. The controlled susceptance is either reactive or capacitive. The SVS adjusts the voltage at the point of connection and, in contrast to the synchronous condenser, is not a voltage source.

**Applications of SVCs:**

1. Control of temporary overvoltages
2. Prevention of voltage collapse
3. Transient stability improvement
4. System damping improvement

## 6.15 High Voltage DC Systems

High Voltage DC (HVDC) systems are able to improve power system transient stability. It is possible to rapidly control the power over a HVDC link using power electronics, which has an impact on power system stability [2].

The first commercial HVDC system was installed in Sweden in 1954 between the island of Gotland and the mainland, and was 96 km in length. The ratings of the link are 100 kV, 20MW and 200A. The problems faced by initial HVDC systems were to find reliable switching devices [ABB].

Developments in semiconductor technology allowed high-voltage thyristors to be implemented in HVDC systems, and these thyristors effectively replaced the mercury arc vales from 1967. HVDC technology now allows multiple terminal transmission as well as a range from several MW to above 1 GW [ABB].

Three primary applications of HVDC are listed below:

- Underwater links (> 30 km)
    - Capacitance of cable makes AC transmission impractical
- Asynchronous link between systems
    - Difference in nominal frequencies
    - Stability problems
- Bulk transmission (> 600 km)
    - HVDC is more economical than AC transmission in certain conditions

An HVDC link can be classified as monopolar, bipolar or homopolar. The monopolar link has a single primary conductor while the return path may be via ground or a return conductor. The bipolar link uses two conductors, one of which is positive and the other negative, at the same voltage magnitude. The homopolar category uses two or more, usually negative, conductors of the same polarity. The arrangement for a homopolar HVDC link is illustrated in figure 6.9 [2].

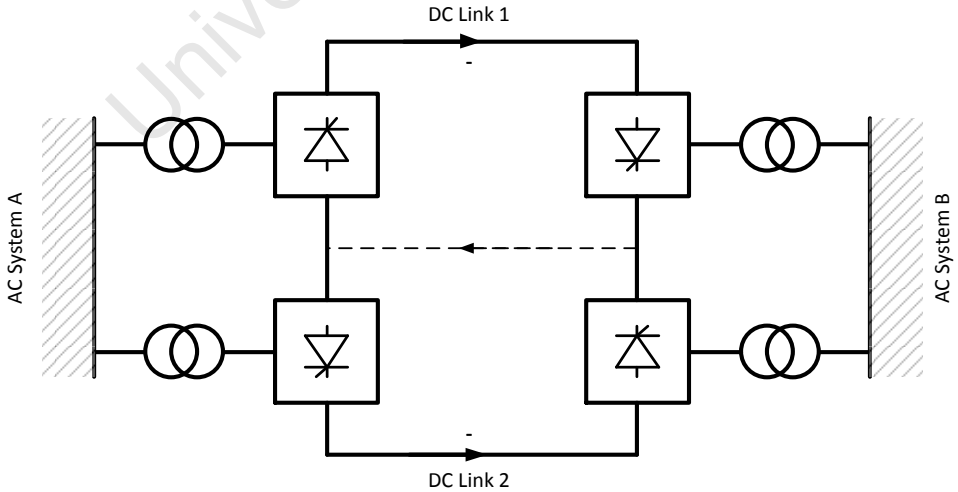


**Figure 6.9:** *Homopolar HVDC Link Arrangement*

The functional diagram of a monopolar HVDC link is illustrated in figure 6.10. The monopolar link is the fundamental building block of the HVDC link categories.

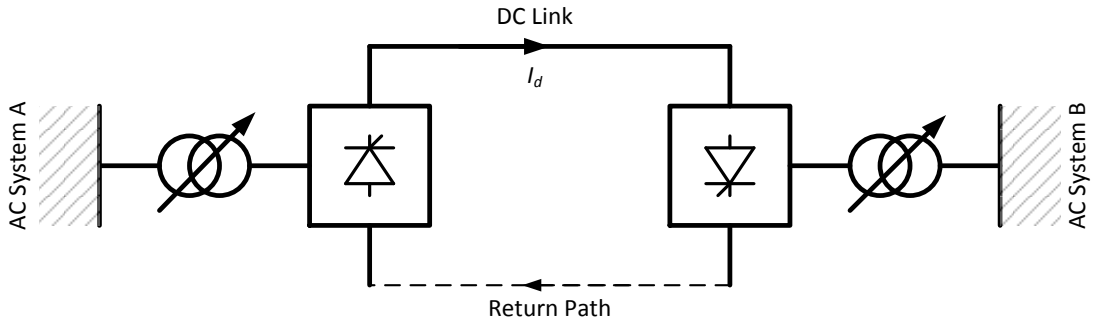


**Figure 6.10:** *Monopolar HVDC Model*

The line current, $I_d$, is given by equation 6.6. It can be noted that the line current can be controlled by both the rectifier and inverter firing angles. The primary control action (~ 10 ms) is typically followed by OLTC action (~ 5 s) to restore the converters to nominal conditions [2].

$$I_d = \frac{V_r \cdot \cos\alpha - V_i \cdot \cos\gamma}{R_r + R_L + R_i} \quad \ldots \quad (6.6)$$

Due to the speed at which the HVDC link can be controlled it is suitable for use in mitigating power swings. The link power can be ramped up or down to reduce a power imbalance and return the system to a stable operating point [2].

It is also possible to apply controllers that allow the HVDC converters to provide reactive power and voltage support during potentially unstable conditions [2].

Conventional HVDC technologies use thyristors as the converter basis. Since the 1990s the trend has been to use IGBTs as the converter basis. IGBT are significantly more controllable than thyristors and consequently make HVDC based on IGBTs a more flexible technology [30].

### 6.15.1 HVDC and Renewable Energy

Renewable energy sources, such as wind-turbines and large-scale hydroelectric stations, are typically in remote areas far from the power system transmission nodes. An example of this is the Cahora Bassa hydroelectric scheme as well as the largely untapped hydroelectric potential in the Democratic Republic of the Congo (DRC). Potential for solar power also exists in the Northern Cape province of South Africa. All of these resources are located at considerable distances from the main power system transmission nodes of the Southern African Power Pool (SAPP).

The transmission technology to be selected is critical for the utilisation of the full potential of these distributed renewable resources. The two fundamental technologies are HVAC and HVDC. The application of an HVDC line from a new resource to an existing node may be preferable to an HVAC link [30].

A general rule is that where a large amount of power is to be transferred over a significant distance, HVDC will typically be more cost-effective than HVAC.

# 7 Conclusions and Recommendations

## 7.1 Sasol Synfuels Power System

Power systems must be designed to maintain stability in the event of severe disturbances, and measures should be implemented to ensure system stability where the problem of power system instability is deemed a risk.

A power angle swing that exceeds 120 degrees is likely to result in instability. It can safely be stated that the approximate transient stability limit is 120 degrees for the machines in this study.

The CCTs were determined for a number of different case studies, including case studies corresponding to planned infrastructure developments.

The CCTs are summarised for all synchronous generators in the Phase 4 configuration in the following chart. A similar chart is presented in chapter 5 for all synchronous motors in the scope.

This chart is a useful tool that has been developed for the presentation of a transient stability assessment.

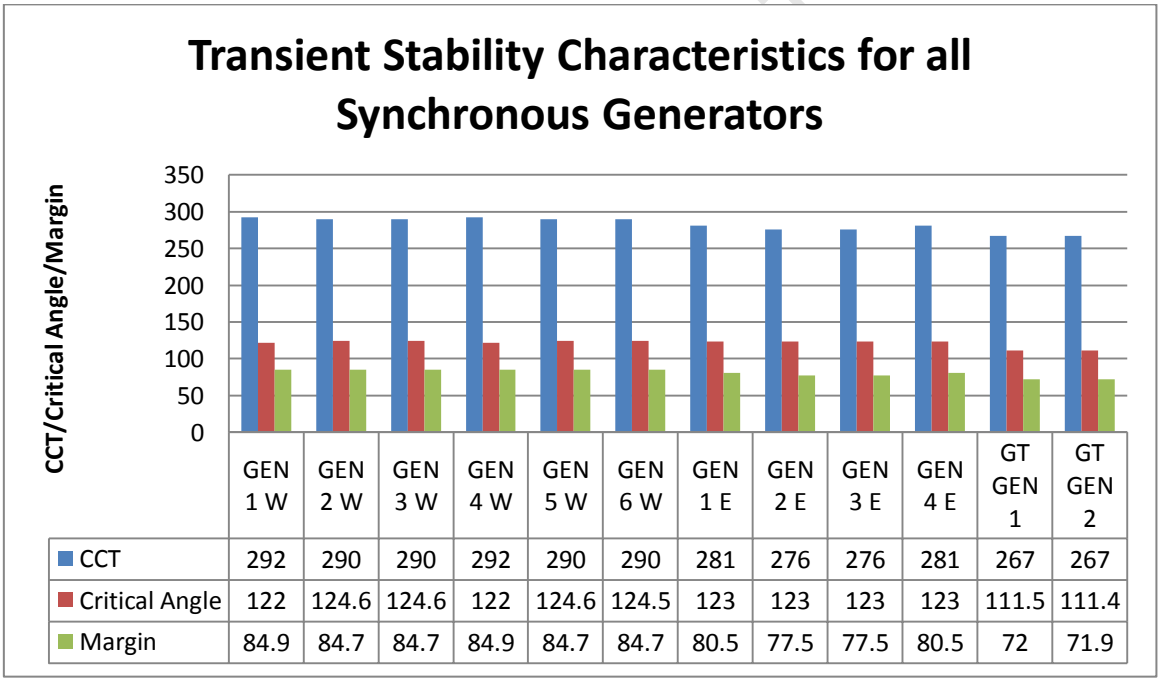


| | GEN 1 W | GEN 2 W | GEN 3 W | GEN 4 W | GEN 5 W | GEN 6 W | GEN 1 E | GEN 2 E | GEN 3 E | GEN 4 E | GT GEN 1 | GT GEN 2 |
|---|---|---|---|---|---|---|---|---|---|---|---|---|
| CCT | 292 | 290 | 290 | 292 | 290 | 290 | 281 | 276 | 276 | 281 | 267 | 267 |
| Critical Angle | 122 | 124.6 | 124.6 | 122 | 124.6 | 124.5 | 123 | 123 | 123 | 123 | 111.5 | 111.4 |
| Margin | 84.9 | 84.7 | 84.7 | 84.9 | 84.7 | 84.7 | 80.5 | 77.5 | 77.5 | 80.5 | 72 | 71.9 |

**Figure 7.1:** *Summary Chart of Synchronous Generator CCTs*

An area of potential concern, highlighted in the background information, was the transient stability margins of the synchronous machines connected to 2H4-SP-02 during N-1 conditions with CLRs installed on the incoming lines.

These results yield the highest variation in the transient stability margin for different configuration. These variations are possible with switched reactors in the projected configuration.

The following chart details the CCTs for the synchronous machines in Phase 2 during N-1 conditions. The lowest CCT is for the BAC motor and is 188 ms during a symmetrical 132 kV bus fault.

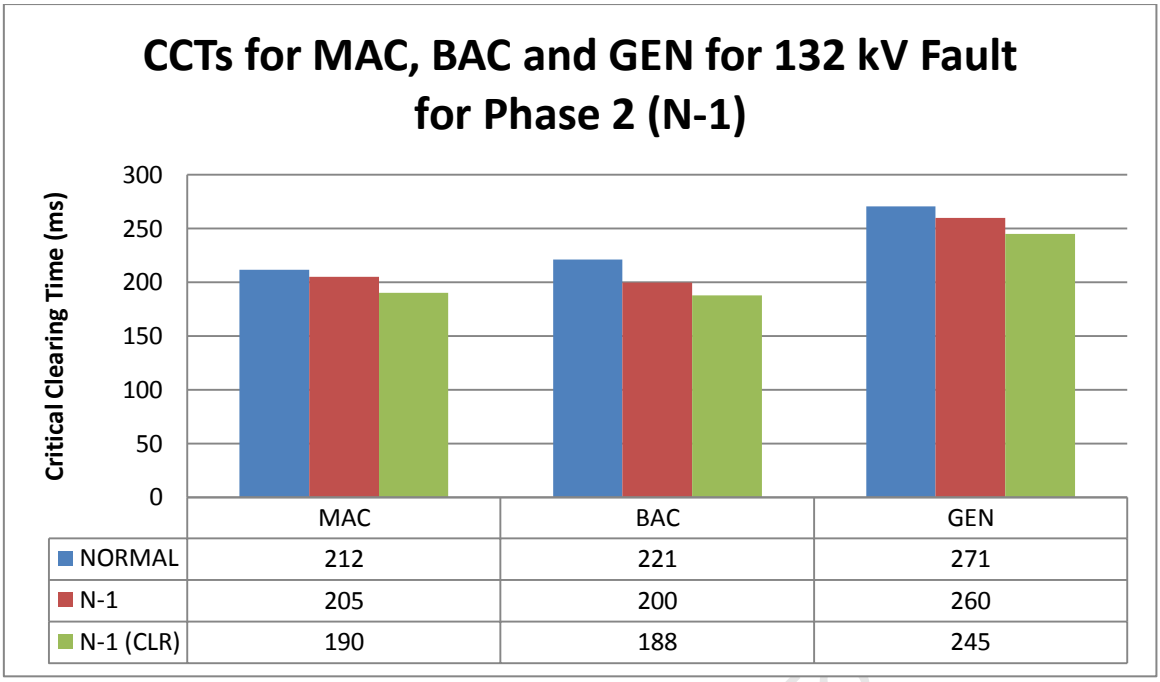


**Figure 7.2:** *Summary Chart for CCTs in Phase 2 N-1 Conditions*

General case studies were undertaken to ascertain the impact of specific parameters on machine transient stability. The results are summarised in table 7.1.

| Factor | Conclusion |
|---|---|
| **System Inertia** | Higher inertia corresponds to improved transient stability but longer post-fault oscillation |
| **Droop Governor** | Complex interaction in terms of speed response that necessitates accurate modelling of the governor. |
| **Voltage Dip** | Ride-through probability is inversely proportional to length and depth of voltage dip |
| **Voltage Impact** | Voltage impact has a more pronounced effect on transient stability than a ramped voltage dip of the same magnitude.<br><br>The magnitude of the power oscillations subsequent to the impact is proportional to the depth of the voltage dip and the inertia of the system |
| **System Fault-Level** | A high system fault-level improves transient stability margins but has an adverse impact on equipment sizing. |
| **Fault Type** | The most severe fault which causes transient instability is a symmetrical short-circuit at the 132 kV bus. |
| **Fault Clearing Time** | A shorter clearing time improves the chances of retaining transient stability. |
| **N-1 Supply Contingency** | The N-1 supply contingency has the effect of reducing the system fault-level.<br><br>The reduced system fault-level negatively impacts on the transient stability margins. |

**Table 7.1:** *General Conclusions from Case Studies*

## 7.2 Power System Stability Improvement

The following technologies were investigated in the context of the improvement of the transient stability of the Sasol Synfuels power system:

- High-Speed Fault Clearing

  This is desirable for all aspects of power system design. As new technologies become available, including new circuit breakers and IEDs, they will be assessed and evaluated on a case by case basis.

- Reduction of Transmission System Reactance

  Due to the high fault levels already an area of concern this option is not feasible. The reduction of system reactance would increase the fault levels which would then improve the transient stability margins. The negative impact of the CLRs on the transient stability margins may be offset by switching the CLRs out of the network during N-1 conditions. This could be implemented provided the fault levels remain within system ratings at all times.

- Regulated Shunt Compensation

  The installation of SVCs at the 132 kV level warrants further investigation. The improved voltage profile during disturbed conditions would improve transient stability margins.

- Dynamic Braking

  This option may be feasible for new generation projects but not for integration into an existing system due to the high cost and complex nature of the installation.

- Reactor Switching

  This option has the same disadvantage in terms of cost and complexity as dynamic braking. The added disadvantage of continuous inherent energy losses, when a primary mandate for new installations is energy efficiency, is a significant barrier to entry for this technology.

- Independent-Pole Breaker Operation

  This technology is typically applicable to the transmission network above 400 kV and not industrial power systems. The same applies for single-pole switching.

- Power System Stabilisers

  This technology has limited impact on small generators connected in parallel in an industrial power system. The transient stability improvement would not be justified by the cost of retrofitting this technology.

- HVDC Lines

  As distributed renewable generation becomes feasible it may be desirable to use HVDC lines to integrate these power plants with the Sasol Synfuels network. This is evaluated on a case by case basis.

## 7.3 Applications of Methodology

The methodology applied in this study can be applied across the spectrum of heavy industry where there are synchronous machines interconnected with the utility supply.

The binary search method can be applied without any prior knowledge of the transient response of the machine being analysed. The CCTs for all synchronous machines in the power network can be calculated provided an adequately detailed model is available.

It is important that the sub-transient parameters are used for the synchronous machines being analysed. If these parameters are not available it is possible to use the typical parameters, which may be calculated by the software package, provided that the risk of reduced accuracy is acceptable. The transient or equivalent models should not be used for modelling of the synchronous machine. The equivalent model in particular provides very poor results compared to the realistic sub-transient parameters.

The existence of a detailed network model for an industrial power system is an invaluable tool. This tool is essential for a wide range of network analyses.

It is important that the complete system (as far as practical) be modelled when doing power system stability studies. There are complex interactions between the different types of loads and generators that should not be neglected.

Particular attention should be paid to the accurate modelling of large induction motors since these elements have a significant impact on the transient stability of nearby synchronous machines.

# 8 References

[1] Glover, J.D., Sarma, M.S., Overbye, T.J., "Power System Analysis and Design", Fourth Edition, Thomson Learning, 2008

[2] "Power System Stability and Control", Kundur, P., Electric Power Research institute, McGraw-Hill, 1994

[3] "Power System Dynamics: Stability and Control", Machowski, J., Bialek, J.W., Bumby, J.R., 2008

[4] "Electric Power Systems", Michel Crappe, Faculté Polytechnique, Mons, Belgium, Wiley-ISTE, June 2008

[5] "Definition and Classification of Power System Stability", IEEE Transactions on Power Systems, Vol. 19, No. 2, May 2004, pp. 1387-1401.

[6] "Motor Behaviour through Power System Disturbances", Bottrell, G. W, 1980, IEEE Transactions on Industry Applications

[7] "Out-of-step protection fundamentals and advancements", Tziouvaras D.A., 2003

[8] "Generalisation of the equal-area criterion for synchronous machines", Willems, J.L., 1969

[9] "Power System Stability: Volume II: Power Circuit Breakers and Protective Relays", Kimbark, E.W., 1950

[10] "Industrial Power System Stability", de Kock, J.A., University of Stellenbosch, 1987

[11] "Definition and Classification of Power System Stability", Kundur, P., IEEE Transactions on Power Systems, Vol. 19, No. 2, May 2004

[12] "Load Shedding for Utility and Industrial Power System Reliability", Basler Technical Paper

[13] "Power Control and Stability of Electric Generating Stations", Steinmetz, C.P., AIEE, 1920

[14] "Electrical Power Systems Quality", Dugan, R.C., Second Edition

[15] "Out-of-Step Protection for Generators", Berdy, J., General Electric Company, Schenectady, New York, 1975

[16] "Loss-of-Excitation Protection for Modern Synchronous Generators", Berdy, J., General Electric Company, Schenectady, New York, 1978

[17] "Investigation of the Influence of Series Compensation in AC Transmission Systems on Bus Connected Parallel Generating Units with Respect to Subsynchronous Resonance", Kumar, R., IEEE Bologna PowerTech Conference, 2003

[18] "Effects of Unified Power Flow Controllers on Transient Stability", Limyingcharoen, S., IEEE Proceedings – Generation, Transmission and Distribution, 1998

[19] "Optimal Switching of Dynamic Braking Resistor, Reactor or Capacitor for Transient Stability of Power Systems", Rahim, A., IEEE Proceedings, 1991

[20] "Turbine Fast Valving to aid System Stability: Benefits and other Considerations", Edwards, L., IEEE Transactions on Power Systems, 1986

[21] "Improved Transient Stability using Generator Tripping based on Tracking Rotor-Angle", Karady, G., IEEE Proceedings, 2002

[22] "Single Pole Switching for Stability and Reliability", Mittelstadt, W., IEEE Transactions on Power Systems, 1986

[23] "Single-Pole Switching: A Study of System Transients with Transposed and Untransposed Lines", Basler, S., IEEE PES Winter Meeting, 1973

[24] "Fast Turbine Valving and Independent Pole Tripping Breaker Applications for Plant Stability", Balu, N., IEEE Transactions on Power Apparatus and Systems, 1980

[25] "Optimisation of a Load Shedding Scheme", Grewal, G., IEEE Industry Applications Magazine, July 1998

[26] "Improvement of Reliability in Active Networks with Intentional Islanding", Pilo, F., IEEE International Conference on Electric Utility Deregulation, Restructuring and Power Technologies, 2004

[27] "Effect of High-Speed Rectifier Excitation Systems on Generator Stability Limits", Dandeno, P., IEEE Transactions on Power Apparatus and Systems, 1968

[28] "Experience with High-Speed Excitation Systems", McClymont, K., IEEE Transactions on Power Apparatus and Systems, 1968

[29] "The Transient Stabilisation of a Synchronous Machine by Discontinuous Supplementary Excitation Control", Harley, R., IEEE Transactions on Power Apparatus and Systems, 1985

[30] "HVDC – A Key Solution in Future Transmission Systems", Heyman, O., ABB Sweden, ABB Technical Library

[31] "Siemens Siprotec 7UM622 Technical Manual", Siemens Website Download Page, February 2011

[32] "Siemens Application Note – Protection of Medium Sized and Large Generators with SIPROTEC 7UM6", Siemens Website Download Page, February 2011

# 9 Appendices

## 9.1 ETAP Models

The method used for load flow studies is the **Newton-Raphson** method with a maximum iteration of 10 and a precision of 0.0001. The load flow method takes account of transformer phase-shift and transformer LTCs. The initial bus voltages are calculated.

The method used for fault-level studies is the **IEC** standard using a c factor of 1.1.

The method used for transient stability studies is the **Accelerated Gauss-Seidel** method with a maximum iteration of 9999 and a precision of 0.00001. The acceleration factor used is 1.45. This method was checked for accuracy against the Newton-Raphson method.

The following ETAP models were used in the investigation.

### 9.1.1 Phase 1 Model

The Phase 1 model comprises two composite models, namely **16 O2 T** and **GT Generators**.

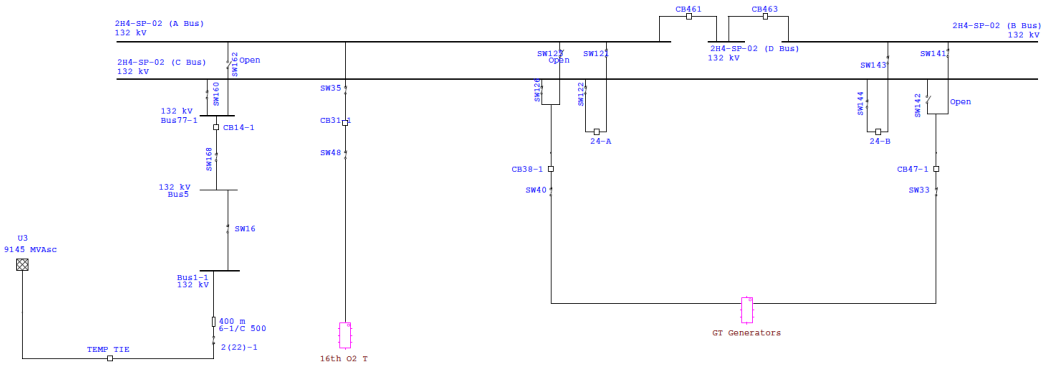


**Figure 9.1:** *Phase 1 Network Model*

### 9.1.2 Phase 2 Model

Phase 2 involves a study of three different network configurations. The models for the network configuration are covered in this appendix.

The Phase 2 model includes two additional composite models, namely **Additional DS 1** and **Additional DS 2**.

**Configuration 1**

Configuration 1 is described in the body of the work and is the high fault-level case implemented with a ring bus.

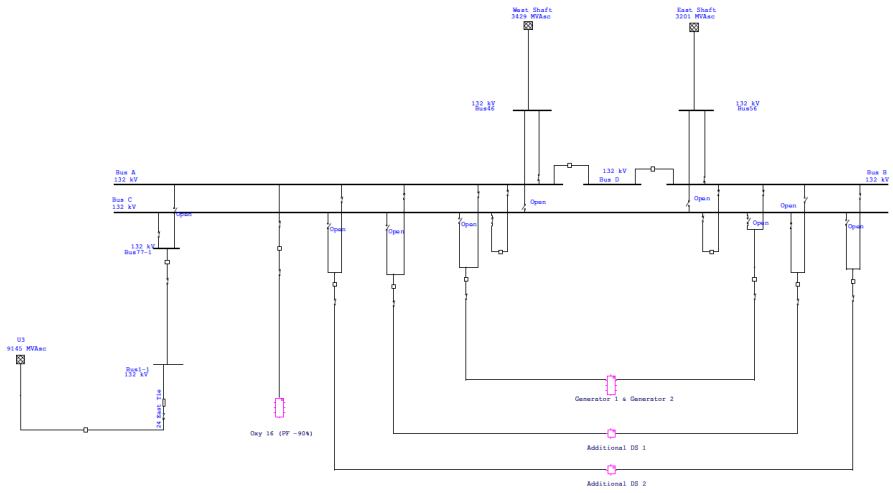


**Figure 9.2:** *Phase 2 Network Model – Configuration 1*

**Configuration 2**

Configuration 2 is described in the body of the work and is the normal fault-level case implemented with a split ring bus.

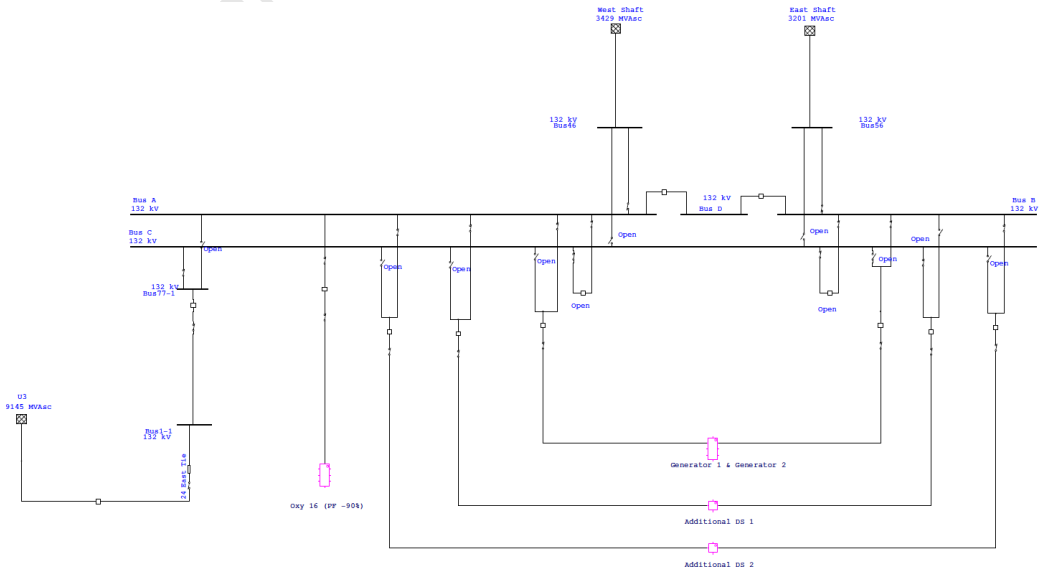


**Figure 9.3:** *Phase 2 Network Model – Configuration 2*

**Configuration 3**

Configuration 3 is described in the body of the work and is the reduced fault-level case implemented with a split ring bus and CLRs on two of the incomers.

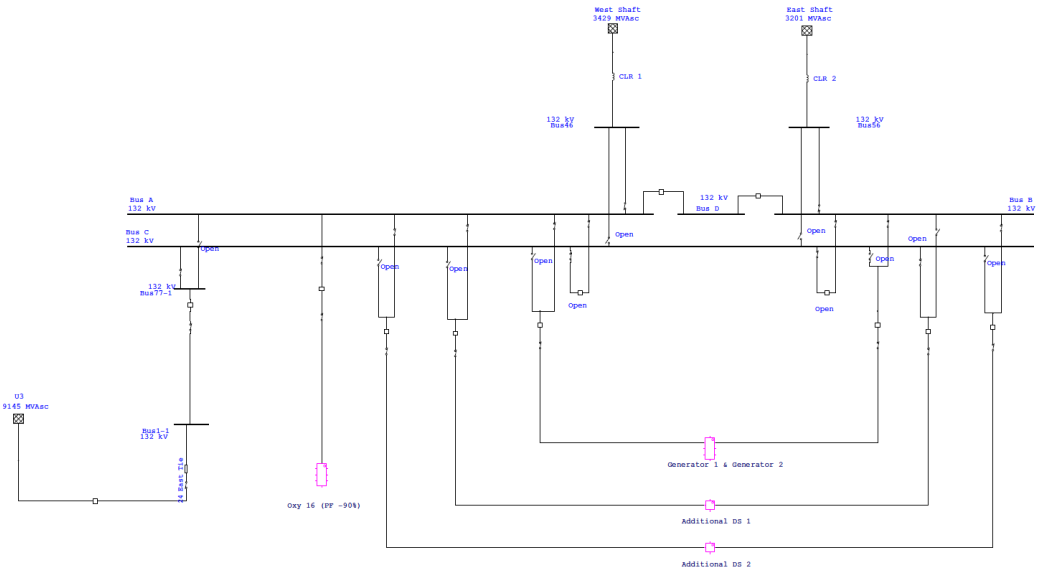


**Figure 9.4:** *Phase 2 Network Model – Configuration 3*

### 9.1.3 Phase 3/4 Model

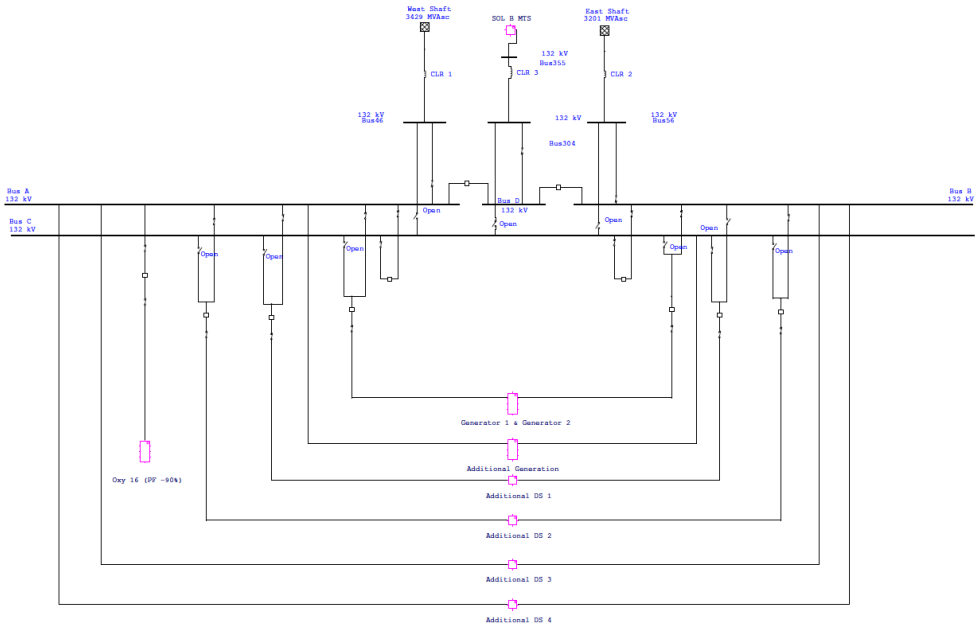


**Figure 9.5:** *Phase 3 Network Model*